ELECTRON PARAMAGNETIC RESONANCE INVESTIGATION OF IRRADIATED LITHIUM ACETATE DIHYDRATE AND MERCURIC ACETATE SINGLE CRYSTALS

Clinton James Coneway

United States
Naval Postgraduate School

THESIS

ELECTRON PARAMAGNETIC RESONANCE
INVESTIGATION OF IRRADIATED LITHIUM
ACETATE DIHYDRATE AND
MERCURIC ACETATE SINGLE CRYSTALS

by

Clinton James Coneway

June 1971

Approved for public release; distribution unlimited.

Electron Paramagnetic Resonance Investigation of Irradiated Lithium Acetate Dihydrate and Mercuric Acetate Single Crystals

by

Clinton James Coneway
Lieutenant, United States Navy
B.S., The University of Texas, 1966

Submitted in partial fulfillment of the
requirements for the degree of

MASTER OF SCIENCE IN PHYSICS

from the

NAVAL POSTGRADUATE SCHOOL
June 1971

ABSTRACT

An electron paramagnetic resonance study of x-ray irradiated single crystals of lithium acetate dihydrate and mercuric acetate has been made. The $\cdot CH_2CO_2^-$ radical has been identified in lithium acetate dihydrate irradiated at liquid nitrogen temperature. The HCH angle was found to be $118.^{\circ}2 \pm 2.0^{\circ}$. The principal elements of the hyperfine tensor and the g tensor were calculated. Mercuric acetate irradiated at liquid nitrogen temperature showed the presence of two CO_2^- species. Spectra at $-80^{\circ}C$ showed the presence of two $\cdot CH_2CO_2^-$ radicals. The principal values of the hyperfine tensor for the two magnetically distinct sites were obtained.

TABLE OF CONTENTS

LIST OF TABLES

LIST OF ILLUSTRATIONS

Figure

Figure

ACKNOWLEDGEMENT

The author expresses his sincere appreciation to Dr. William M. Tolles of the Naval Postgraduate School, Monterey, California, for his assistance and interest in this research project. Also, appreciation is expressed to Mr. Robert Sanders of the Naval Postgraduate School for his assistance in any of the technical problems encountered.

I. INTRODUCTION TO ELECTRON PARAMAGNETIC RESONANCE

A. BACKGROUND ON EPR SPECTRA OF TRAPPED ORGANIC RADICALS IN SINGLE CRYSTALS

Since its discovery in 1945 by Zavoisky, electron paramagnetic resonance has become one of the most powerful tools in physical research, and many different systems have been studied. Of particular interest in recent years has been the study of single crystals which have been irradiated to form organic radicals within the crystal lattice [1]. Single crystals have been used as host for organic radicals because in polycrystalline solids the radicals are highly anisotropic. This anisotropy causes broadened hyperfine resonance lines which make interpretation of the spectra difficult and cause the weaker signals to be obscured.

Gisch [2] gives an excellent background on EPR studies of trapped organic radicals in single crystals beginning with some of the earliest work and continuing through 1968. The studies made on single crystals of saturated carboxylic acids and their salts, the simpler amino acids, and certain unsaturated acids, when irradiated with x-rays, gamma rays, or high energy electrons were summarized. Since 1968 work has continued with EPR investigations of the radicals formed in these single crystalline hosts. Improvements in the art of growing single crystals have allowed researchers to examine even the most complex amino acids. Box, Freund, and Budzinski have studied one of the 10 essential amino acids, valine, and by use of EPR have determined the effects of irradiation of a single

crystal of this acid. They were able to identify the radical formed in valine following irradiation at liquid nitrogen temperature as $(CH_3)_2$ CHCH· C00H and found that the unpaired electron was on the β carbon. By proper temperature control individual phases in the radiation damage process were isolated [3]. Shields, Marsh, and Hamrick [4] have studied the irradiation damage of five amino acids and by correlation with optical spectra have used EPR to identify trapped radicals of the form $R_1R_2\dot{C}C00H$ in the amino acids glycine, alanine, and aspartic acid. Valine and leucine were found to have no optical absorption which verified earlier findings that the unpaired electron was on the β carbon and a π system does not exist in these acids [3].

B. BACKGROUND ON EPR INVESTIGATIONS OF METALLIC ACETATES

Analysis of the spectra from radiation damaged crystals of metallic acetates has been primarily concerned with the identification of the trapped radical (s) by interpreting the hyperfine proton interaction. Kispert and Rogers [8] investigated the EPR spectra of single crystals of sodium acetate trihydrate irradiated and observed at liquid nitrogen temperatures. Four lines with intensity ratios of 1:3:3:1 and proton hyperfine splitting of 22.5G were observed. In addition, each of the four lines had two satellite lines which were observed only at high microwave power. The four lines were identified as the methyl radical, $\cdot CH_3$, and the satellite lines were attributed to spin flip transitions

arising when there is a simultaneous change in the spin state of the odd electron on the methyl radical and of the neighboring protons of the water of crystallization. Tolles, Crawford, and Valenti [9] noted the presence of the methyl radical in single crystals of zinc acetate dihydrate irradiated at 77°K. Decay of the methyl radical was found to correspond to an increase in the $\cdot CH_2CO_2^-$ radical. The proposed mechanism was hydrogen abstraction by the methyl radical from a neighboring acetate ion.

$$\cdot CH_3 + CH_3CO_2^- \longrightarrow CH_4 + \cdot CH_2CO_2^-$$

They supported this hypothesis by synthesizing $Zn(CH_2DCO_2)_2 \cdot 2H_2O$ and showed that the decay and growth of this species exhibited an isotope effect. The barrier to internal rotation of the $CH_2\cdot$ about the C-C bond was calculated to be $5.0 \frac{Kcal}{Mole}$. Tolles, Sanders and Gisch [10] found that single crystals of strontium acetate hemihydrate irradiated at liquid nitrogen temperatures produced the radical $CH_3\dot{C}O_2^{2-}$ and not the methyl radical as in other acetates. Upon warming the irradiated strontium acetate crystal it was found that $CH_3\dot{C}O_2^{2-}$ was replaced by two distinct $\cdot CH_2CO_2^-$ radicals. Apaydin and Clough [11] investigated the irradiation damage in single crystals of cupric acetate monohydrate which had been irradiated at room temperature. In this crystal the Cu^{2+} ions form exchange coupled ion pairs and the conversion of one member of a pair to diamagnetic Cu^+ ion. Morton-Blake [12] investigated single crystals of cupric acetate monohydrate following irradiation at

liquid nitrogen temperatures. He found a prominent spectrum of an S= 1/2 species and attributed this paramagnetic change to electron transfer and pairing to one of the electrons in the Cu-Cu pair. Morton-Blake [13] found a similar S=1/2 species in irradiated single crystals of nickel acetate. The presence of the spin 1/2 species indicated that one of the electrons in Ni^{2+} ion had paired with a free electron created in the crystal following irradiation.

EPR studies of the above mentioned acetates are the only known published reports. It, therefore, becomes the purpose of this report to investigate with EPR irradiated single crystal acetates not previously reported in literature. The two crystals selected were lithium acetate dihydrate and mercuric acetate. This work will: (1) report possible radical species present following x-ray irradiation at both room and liquid nitrogen temperature, (2) obtain best principal values of the A and g tensors of the radicals formed, (3) study temperature dependence of radical formation, and (4) make recommendations for future studies of these acetate crystals.

C. SPIN HAMILTONIAN OF TRAPPED RADICALS IN SINGLE CRYSTALS

Using the notation of Slichter [16] the spin Hamiltonian for a free radical in which a single unpaired electron may interact with several nuclei may be written:

$$\mathcal{H}_{SPIN} = \beta \bar{H} \cdot \bar{\bar{g}} \cdot \bar{S} - \sum_i \gamma_i \hbar \bar{H} \cdot \bar{I}_i + \sum_i \bar{S} \cdot \bar{\bar{A}} \cdot \bar{I}_i$$

The first term represents the Zeeman energy, or the energy of interaction between the electron spin moment with the external magnetic field. The second term represents the enrgy of interaction between the i^{th} nucleus and the external magnetic field. The third term represents the summation of the energy of the hyperfine interaction between the electron spin and the spin of the i^{th} nucleus, I_i. $\overline{\overline{A}}_i$ is the hyperfine coupling tensor. This third term is also known as the sum of the isotropic Fermi contact interaction and the anisotropic dipolar action.

The elctron Zeeman term can be written:

$$\mathcal{H}' = \beta(H_x H_y H_z)\begin{pmatrix} g_{xx} & g_{xy} & g_{xz} \\ g_{yx} & g_{yy} & g_{yz} \\ g_{zx} & g_{zy} & g_{zz} \end{pmatrix}\begin{pmatrix} S_x \\ S_y \\ S_z \end{pmatrix}$$

The g tensor is anisotropic only if there is spin orbit coupling, i.e. if the electron possesses both spin and orbital angular momentum. An anisotropic g tensor means that the electron spin is not oriented exactly along the magnetic field tensor and; therefore, $\bar{S}$ does not represent the true spin of the electron. The true form of the Hamiltonian for an anisotropic g tensor may be written:

$$\mathcal{H} = \beta \bar{H} \cdot \bar{\bar{g}} \cdot \bar{\hat{S}}$$

where $\hat{\bar{S}}$ is a fictitious spin. In the presence of a magnetic field there will be an interaction between H and the orbital angular momentum, of the electron. Thus, the true Hamiltonian for the magnetic interaction can be written:

$$\mathcal{H} = \beta \bar{H} \cdot \bar{L} + g_e \beta \bar{H} \cdot \bar{S}$$

Carrington and McLachlan [14] show that the two forms for the true spin Hamiltonian are equivalent. By writing the matrix representation of the two Hamiltonians in the same basis the following equations are derived:

$$g_{xx} = g_e - 2\rho \sum_n \frac{\langle 0|L_x|n\rangle\langle n|L_x|0\rangle}{\Delta E_n}$$

$$g_{yy} = g_e - 2\rho \sum_n \frac{\langle 0|L_y|n\rangle\langle n|L_y|0\rangle}{\Delta E_n}$$

$$g_{zz} = g_e - 2\rho \sum_n \frac{\langle 0|L_z|n\rangle\langle n|L_z|0\rangle}{\Delta E_n}$$

where ρ represents the spin orbit coupling constants which can be found from atomic spectra. ΔE_n can be derived from electronic spectra and is the difference in energies from the ground state to the n^{th} electronic level. Reference 17 points out that most g tensors of

organic free radicals are within 1% of the free electron value of 2.002319.

Morton [18] has an excellent description of the hyperfine interaction between the electron spin S and the nuclear spin I. Since g is nearly isotropic the hyperfine tensor A will be a symmetrical 3 x 3 matrix which can be diagonalized and resolved into isotropic and anisotropic components. Together the two components form an effective Hamiltonian given by:

$$\mathcal{H}' = \left(\frac{8\pi g_e \beta \gamma_N}{3}\right) \psi^2(0)\, \bar{S} \cdot \bar{I}$$

$$- g\beta\gamma_N \left[\bar{S}\bar{I} r^{-3} - 3(\bar{S}\cdot\bar{r})(\bar{I}\cdot\bar{r}) r^{-5}\right]$$

The first term is the isotropic interaction and is usually called the Fermi-contact interaction. This term will be non-zero only if the $\psi^2(0)$ term is non-zero; that is, if the orbital of the unpaired electron has S character. It is possible to estimate the S-character of the orbital by comparing the experimentally determined $\bar{\bar{A}}$ with a parameter $\bar{\bar{A}}_o$ calculated as if the electron were entirely in the S orbital of the atom concerned.

The second term of the equation is the anisotropic or dipole-dipole interaction of the electron and the nuclei. The anisotropic term gives the p character of the orbital and is a traceless tensor.

II. EXPERIMENTAL WORK

A. OBTAINING DATA

The primary work of the EPR spectroscopist is to obtain information about the $\bar{\bar{A}}$ and $\bar{\bar{g}}$ tensors of the spin Hamiltonian. To get this information, experimental measurements must be made on single crystals which for this work have been irradiated to form the radical(s). From the outward appearances of the crystal, a set of orthogonal (xyz) axes can be chosen. Any convenient axes may be used but it is important to pick a set which can be assigned similarly to different crystals of the same material. Once a set of axes is chosen, the crystal can be rotated with knowledge of the position of the external magnetic field with respect to these axes. Then by orienting the crystal at different values of θ and ϕ, a coupling constant (s) is obtained for each orientation. The crystal rotation, ϕ, and the rod rotation θ are shown in Figure 1.

The $\bar{\bar{g}}$ tensor was obtained by rotating the crystal through θ and ϕ as above for the $\bar{\bar{A}}$ tensor and comparing the location of the resonance line(s) relative to that of 2,2 diphenyl-1-picrylhydrazyl (DPPH). The g tensor for DPPH is known from literature and is 2.0036. The position of the resonance line for DPPH was marked in the recorder relative to the resonance spectra for a solid mixture of 0.1% $MnCl_2$ in MgO. The EPR spectra for 0.1% $MnCl_2$ in MgO consists of a single line, each 86.84 gauss independent of orientation. The DPPH displayed a single

line at 3263.97 gauss. This line for DPPH was located between the 3214.57 gauss and 3301.41 gauss lines of 0.1% $MnCl_2$ in MgO. Since the g values for most single crystals are near the free electron value, the lines for the $\overline{\overline{g}}$ tensors of lithium acetate dihydrate and mercuric acetate were expected to lie near the line for DPPH. The reading of 3263.97 gauss for the g value of DPPH was set equal to 2.0036. The DPPH was removed from the glass rod and the irradiated single crystal was placed on the rod. By use of the formula for resonance and assuming constant energy, one can write for the DPPH:

$$h\nu = \beta g_{DPPH} H_{DPPH}$$

which then equals the unknown term $g_{unk}\ \beta\ H_{unk}$:

$$g_{unk}\ \beta\ H_{unk} = \beta\ (2.0036)(3263.97)$$

and

$$g_{unk} = \frac{6539.69}{H_{unk}}$$

Thus, by measuring the value of the magnetic field at the point of resonance for the sample, the value of g_{unk} can be calculated.

Values for both the $\overline{\overline{A}}$ and $\overline{\overline{g}}$ tensors were calibrated by comparison of the linear recorder values with those of a variable frequency proton resonance probe.

B. EQUIPMENT UTILIZED

All the EPR spectra were obtained with a Varian V - 4502 - 06 X band EPR spectrometer utilizing 100^{Kc}/sec modulation with a nine inch magnet and field dial regulation. The cavity was a conventional reflection type cavity, equipped with a Varian variable temperature control unit. The temperatures were additionally monitored with a copper-constantan thermocouple.

Single crystals were exposed to x-ray radiation using a copper target at 40KV and 40 mA. .For irradiation at room temperature, exposures were for 1 hour, while at liquid nitrogen temperatures, irradiation was for 2 hours. Gisch [2] reported that precooling of strontium acetate hemihydrate was required to prevent shattering of the crystals when first exposed to liquid nitrogen temperatures. This precooling was found to be unnecessary for any of the crystals investigated in this work.

Crystals were aligned on a glass rod by the use of a Baush and Lomb microscope. Only the angle $\emptyset$ needed to be aligned with the microscope since the crystal was rotated in the cavity about the angle θ. The method of crystal orientation at room temperature is described by Crawford [19]. At liquid nitrogen temperatures the crystals were aligned without warmup by keeping the crystals in a liquid nitrogen bath under the microscope and orienting the crystal about the angle $\emptyset$

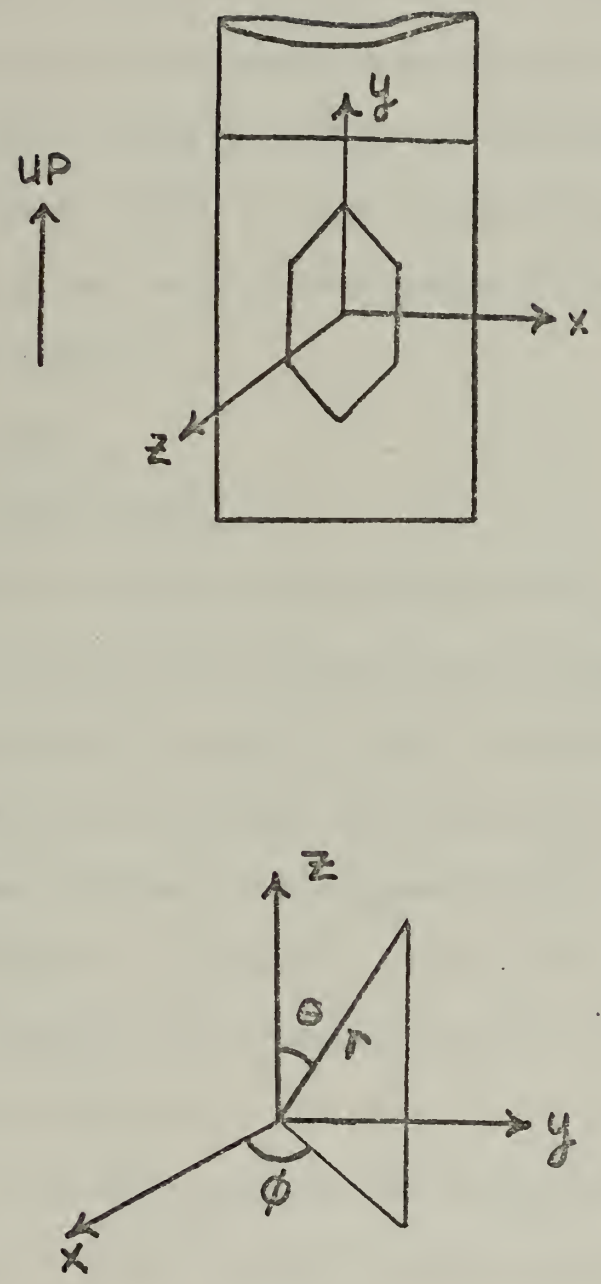

Figure 1. The orthogonal axis system (x,y,z) utilized to orient crystal relative to the magnetic field (top). The rotations θ and ø ($\frac{\theta}{\phi}$) (bottom).

The quartz rods on which the crystals were mounted had two flats ground parallel to each other on both ends of the rod. The end opposite the mounted crystal was clipped to an angle indicator positioned over the center of the spectrometer cavity. It was estimated that the angular position of the crystal (θ) could be measured accurately within $\pm 1^{\circ}$ with this apparatus [19, 20]. The angle ϕ could be determined within $\pm 1^{\circ}$ when oriented at room temperature and within $\pm 3^{\circ}$ when oriented at liquid nitrogen temperatures.

C. CRYSTAL GROWING

1. Lithium Acetate Dihydrate

Single crystals of lithium acetate dihydrate were grown by slow evaporation of a saturated aqueous solution at room temperature. Lithium acetate dihydrate from the J.T. Baker Chemical Company, Phillipsburg, New Jersey, was utilized with no further test for purity. By mixing 25 grams of lithium acetate dihydrate with 100 ml of distilled water a saturated solution was obtained. A modified Petri dish 9 centimeters in diameter and 2 centimeters deep was filled half full with the solution and then covered. The amount of the dish covered had a large influence on the size and quality of the crystals grown. About 90 percent coverage was found to produce the best crystals. The lithium acetate dihydrate crystal crystallized as shown in Figure 2. The choice of the crystal axes is shown.

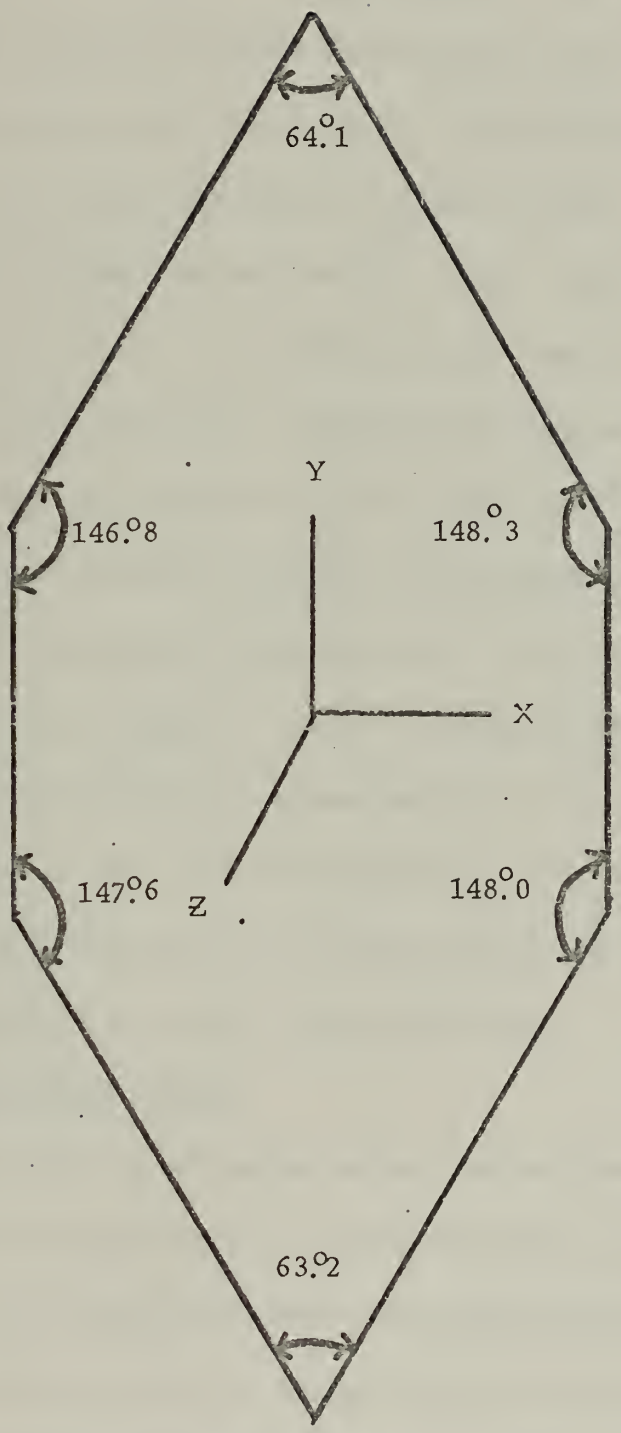

Figure 2. A single crystal of lithium acetate dihydrate with the external axis system.

2. Mercuric Acetate

Single crystals of mercuric acetate were grown under the same conditions as those for lithium acetate dihydrate. It was found that single crystals of mercuric acetate could be grown every time by mixing 32 grams of mercuric acetate from the J.T. Baker Chemical Company, Phillipsburg, New Jersey, with 100 ml of distilled water. About 80% coverage of the dish gave the best results. Three or four hours after mixing the solution, the bottom of the Petri dish would be covered with a thin layer of yellow precipitate. No study was made on the precipitate. Within a few hours following the formation of this precipitate the crystals of mercuric acetate would form. The presence of the precipitate was always necessary for crystal growth. The crystals had the external form shown in Figure 3. When the mercuric acetate crystals were removed from the dish the crystals were clear but after a few hours they turned orange. EPR runs were made before and after the color change with no difference noted in the spectra and, therefore, no further importance was placed on the color change.

3. Other Acetate Crystals

Single crystals of magnesium acetate tetrahydrate and barium acetate hydrate were grown under the same conditions as above. Twenty-five grams of salt combined with 100 ml of distilled water gave good results. The addition of 10 ml of acetic acid to the solution gave even a higher probability of getting good single crystals.

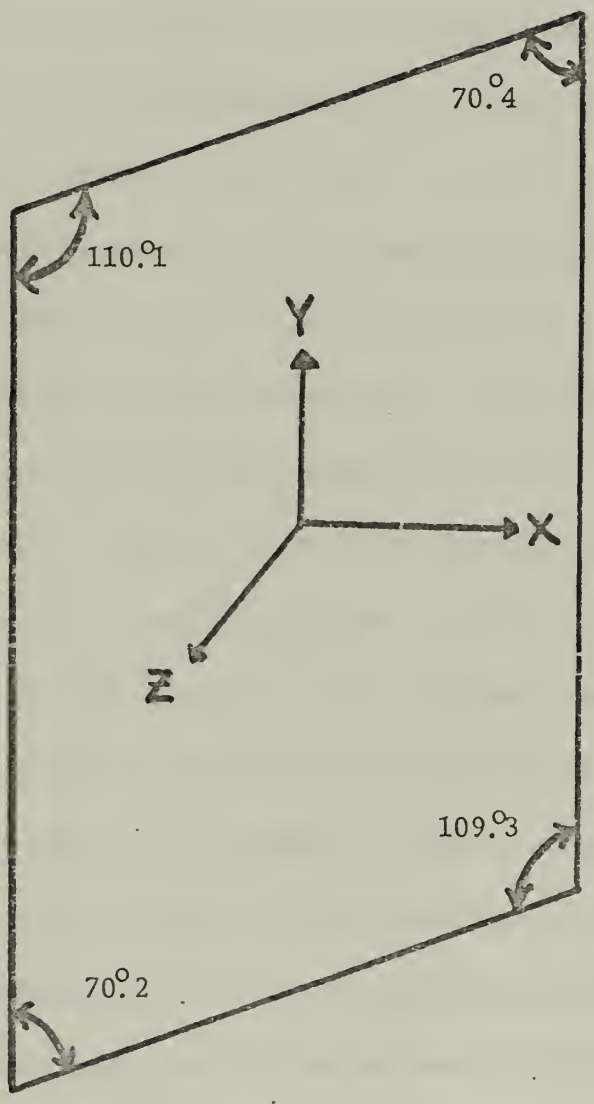

Figure 3. The external appearance of mercuric acetate with the orthogonal crystal axis system.

C. CATALOGUING THE DATA

After obtaining the coupling constants and/or the g tensors at the different orientations desired, it becomes necessary to locate the orientation of the principal (radical(s)) axes system relative to the crystal axes system. The method chosen to do this is the interpretation of a stereographic projection. Each θ and ϕ on the net corresponds to one orientation of the crystal relative to the magnetic field. Once the values of the coupling constants are plotted on the net a reasonable estimate of the principal values can be made. Tolles [21] presents an excellent method to solve the stereographic projection to obtain approximate principal values. Once the approximate principal values have been obtained from the net, a computer program exists [22] which performs a least square fit of the parameters. The principal values are fed into the computer to give a reasonable starting point to locate the least squared best values. It is possible to derive values of the elements of the A and/or g tensor in terms of the crystalline set of orthogonal axes (xyz) as explained in Ref. 14. The transformation which diagonalizes this tensor will then define the relative orientation of the x,y,z system with respect to the radical principal orthogonal axes (X Y Z). If the crystal structure of the molecule is known and it is assumed that the orientation of the atoms in the radical does not differ with that of the undamaged molecule, then these principal axes can be assigned. Thus, the direction cosines which are obtained from diagonalizing the A and/or g tensor are the same as the direction cosines of the radical

principal axes with respect to the crystal axis system. The principal values of the A tensor will be along the principal axes in the radical [19]. The computer program listed in Appendix I will least square the input data and then diagonalize the A and/or g tensors, printing out the principal values and direction cosines with deviation from the calculated values.

III. EXPERIMENTAL RESULTS

A. LITHIUM ACETATE DIHYDRATE

1. Spectra of Radicals Formed

EPR spectra obtained from x-ray damaged single crystals of lithium acetate dihydrate were found to depend on the temperature of the crystal during irradiation, the magnetic field orientation relative to the crystal axes, and the temperature of the crystal at the time of observation. Figure 4 shows the spectra of two crystals, both irradiated at liquid nitrogen temperatures and observed at room temperature and at 173°K. The resonance lines shows a 1:2:1 intensity in the room temperature spectrum while the 173°K spectrum shows the splitting of the center line into two lines. Figure 5 shows the spectrum of a crystal irradiated at room temperature for one hour and observed at 173°K. The broadening of the center line is evident and analysis of the spectrum would be difficult. Figure 6 shows the spectra of a crystal irradiated and observed at room temperature 2 hours and 24 hours following irradiation. The decay of the 1:2:1 lines is evident and the intensity

of the other lines is unchanged. Figure 7 shows the same crystal at a different ($\begin{matrix}\theta \\ \phi\end{matrix}$) orientation as observed 2 hours and 25 hours following irradiation.

After examination of the spectra of both room and liquid nitrogen temperature irradiation, it was decided that the room temperature irradiated crystal observed at 173°K provided little information. Therefore, the lithium acetate crystal was studied at 173°K following irradiation at liquid nitrogen temperatures, and at room temperature following irradiation at room temperatures.

2. Liquid Nitrogen Temperature Irradiation

EPR spectra of single crystals of lithium acetate dihydrate following irradiation at liquid nitrogen temperature shows the formation of only one species at any observation temperature. This species with a 1:2:1 intensity has been identified by Crawford [19] and Valenti [20] as the $\cdot CH_2CO_2^-$ radical. To obtain coupling constants for this radical the temperature of observation was varied until the best splitting of the center line occurred. This optimum splitting was obtained at 173°K. Figure 4 shows this splitting of the center line.

Using various magnetic field orientations ($\begin{matrix}\theta \\ \phi\end{matrix}$), the coupling constants for the two protons of the $\cdot CH_2CO_2^-$ radical were obtained. The values were plotted on a stereographic projection and the best estimates for the principal values were obtained. By use of the computer program in Appendix I, these values were further refined by a least

of the other lines is unchanged. Figure 7 shows the same crystal at a different (θ / ϕ) orientation as observed 2 hours and 25 hours following irradiation.

After examination of the spectra of both room and liquid nitrogen temperature irradiation, it was decided that the room temperature irradiated crystal observed at 173°K provided little information. Therefore, the lithium acetate crystal was studied at 173°K following irradiation at liquid nitrogen temperatures, and at room temperature following irradiation at room temperatures.

2. Liquid Nitrogen Temperature Irradiation

EPR spectra of single crystals of lithium acetate dihydrate following irradiation at liquid nitrogen temperature shows the formation of only one species at any observation temperature. This species with a 1:2:1 intensity has been identified by Crawford [19] and Valenti [20] as the $\cdot CH_2CO_2^-$ radical. To obtain coupling constants for this radical the temperature of observation was varied until the best splitting of the center line occurred. This optimum splitting was obtained at 173°K. Figure 4 shows this splitting of the center line.

Using various magnetic field orientations (θ / ϕ), the coupling constants for the two protons of the $\cdot CH_2CO_2^-$ radical were obtained. The values were plotted on a stereographic projection and the best estimates for the principal values were obtained. By use of the computer program in Appendix I, these values were further refined by a least

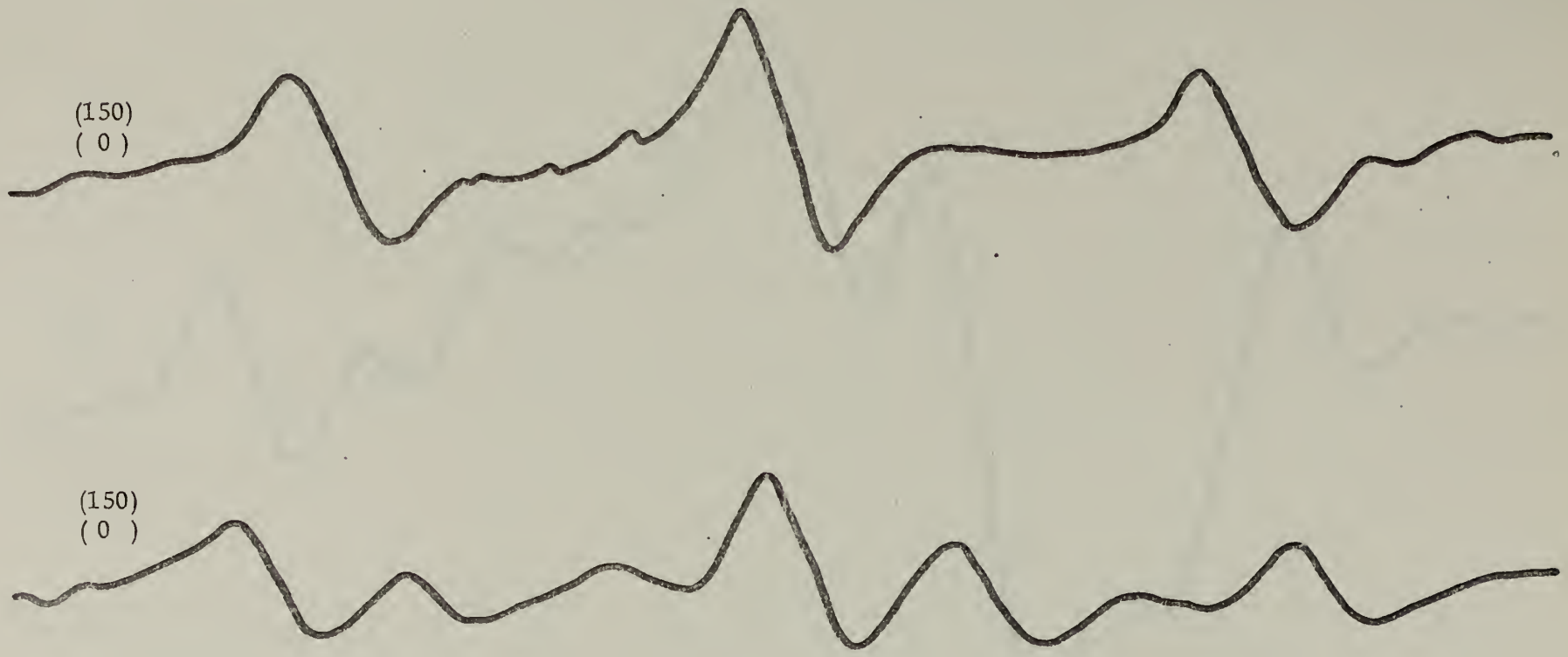

Figure 4. Two spectra of liquid nitrogen temperature irradiated lithium acetate dihydrate (top) observed at room temperature and (bottom) observed at -100°C.

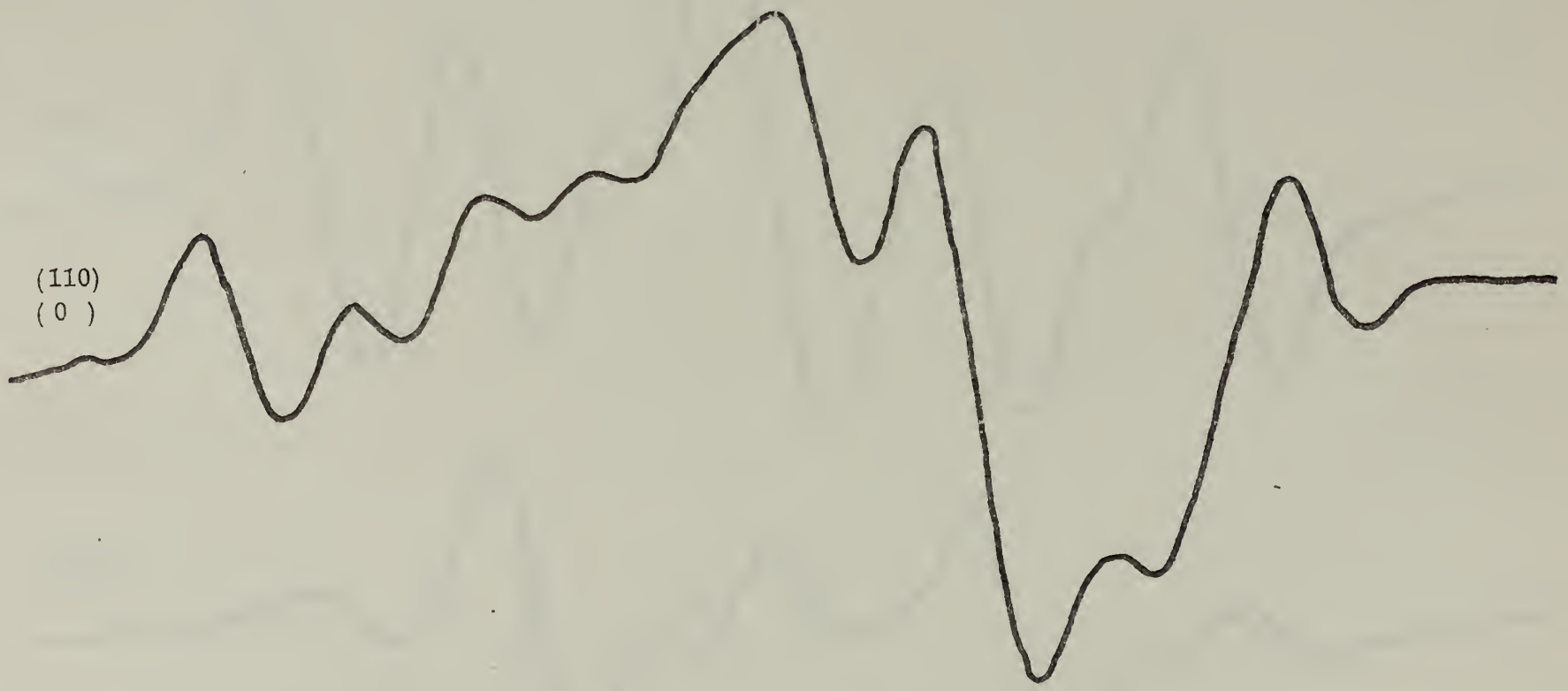

Figure 5. Spectrum of a single crystal of lithium acetate dihydrate irradiated for an hour at room temperature and observed at 173°K.

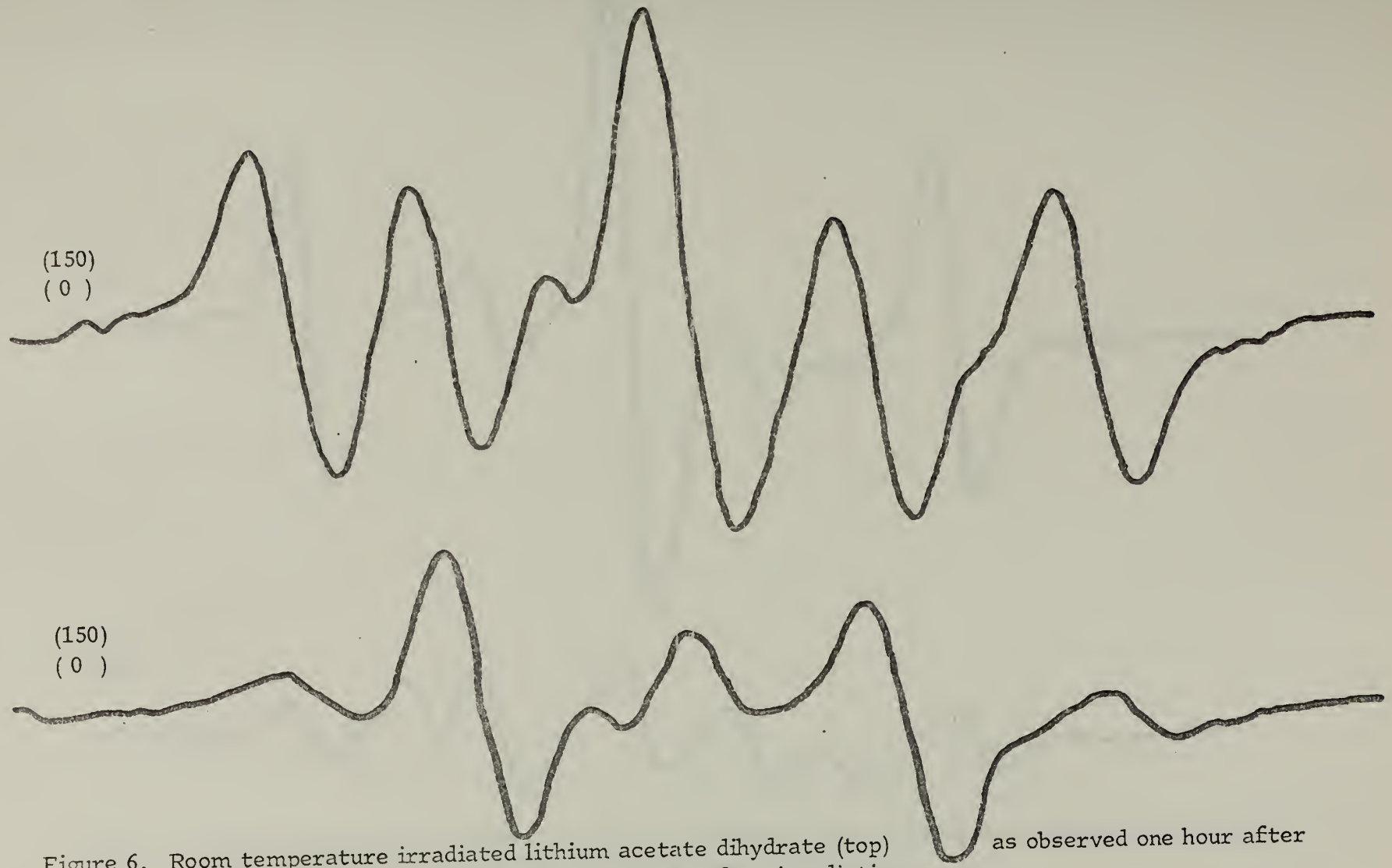

Figure 6. Room temperature irradiated lithium acetate dihydrate (top) as observed one hour after irradiation and (bottom) as observed one day after irradiation.

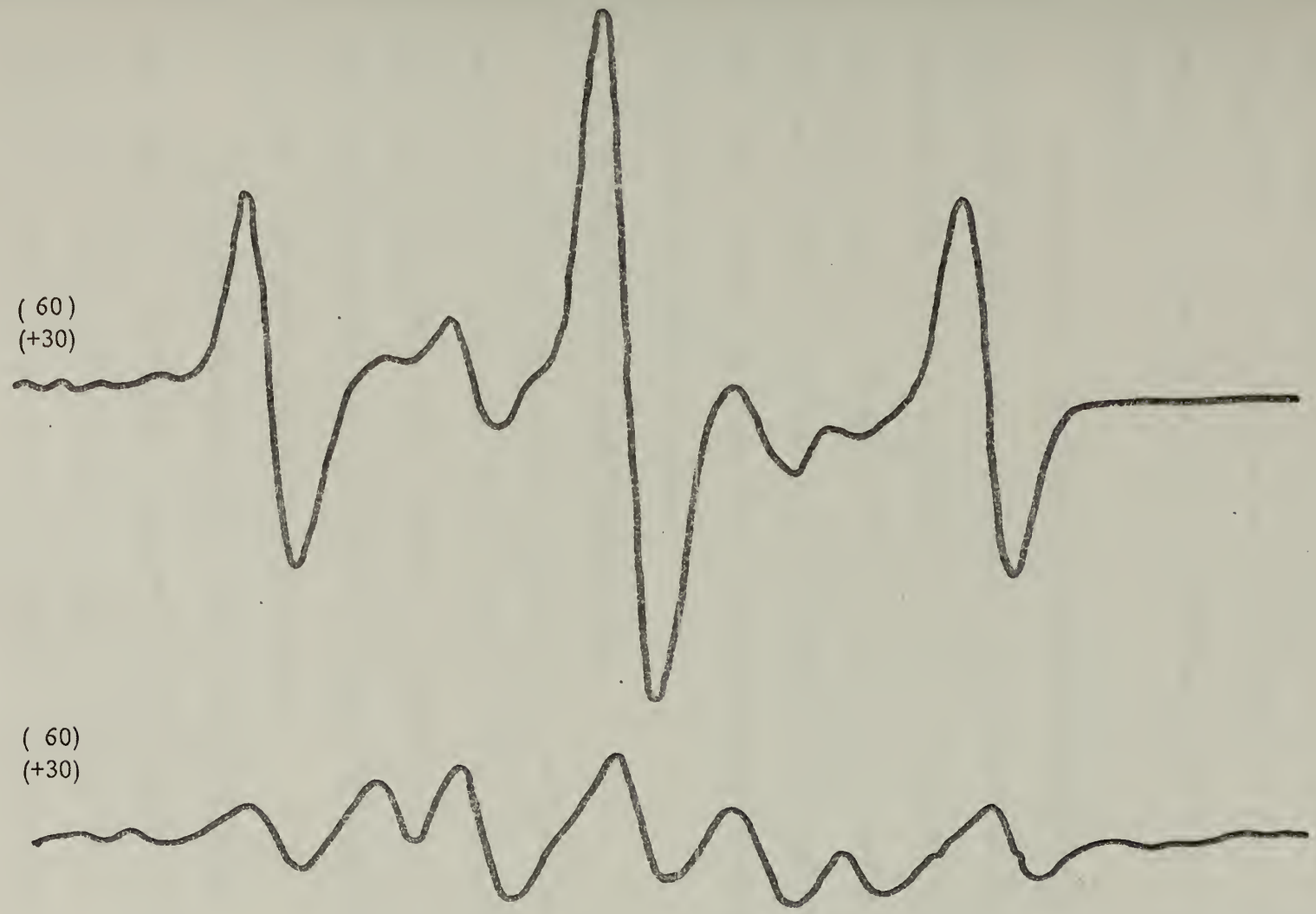

Figure 7. Room temperature irradiation spectra of lithium acetate dihydrate observed (top) 2 hours after irradiation and (bottom) 25 hours after irradiation.

square fit. The experimental (observed) and calculated values for the coupling constants are shown in Figure 8. The agreement is excellent with the largest difference found at the maximum and minimum coupling constant values where the field vector is perpendicular to the C-H bond and along the C-H bond respectively. The HCH angle was calculated to be $118.2^{o} \pm 2^{o}.0$.

The g tensor was obtained by the method mentioned earlier. The g tensor principal values were found to lie as expected for the symmetry of the lithium acetate dihydrate crystal. The three principal values were found to lie along the π orbital, half way between the HCH bond parallel to the C-C bond, and perpendicular to the HCH plane. Table I lists the principal values of the coupling constants for the two protons with their direction cosines.

3. Correlation with Crystallographic Data

Crawford [19] found that he could explain his results if he assumed a planar configuration for the $\cdot CH_2CO_2^-$ radical. Since Valenti [20] could not explain his results using the perpendicular model, the planar model was decided upon for the lithium acetate dihydrate radical $\cdot CH_2CO_2^-$. This planar model is shown in Figure 9.

The expected orientation of a $\cdot CH_2CO_2^-$ radical in lithium acetate dihydrate was calculated using the information given by Galigne, et. al. [23]. The crystal structure in lithium acetate dihydrate orthorombic with space group Cmmm and the unit cell dimensions are a=6.82Å, 6=10.88Å and c=6.62Å. The coordinates of the atoms

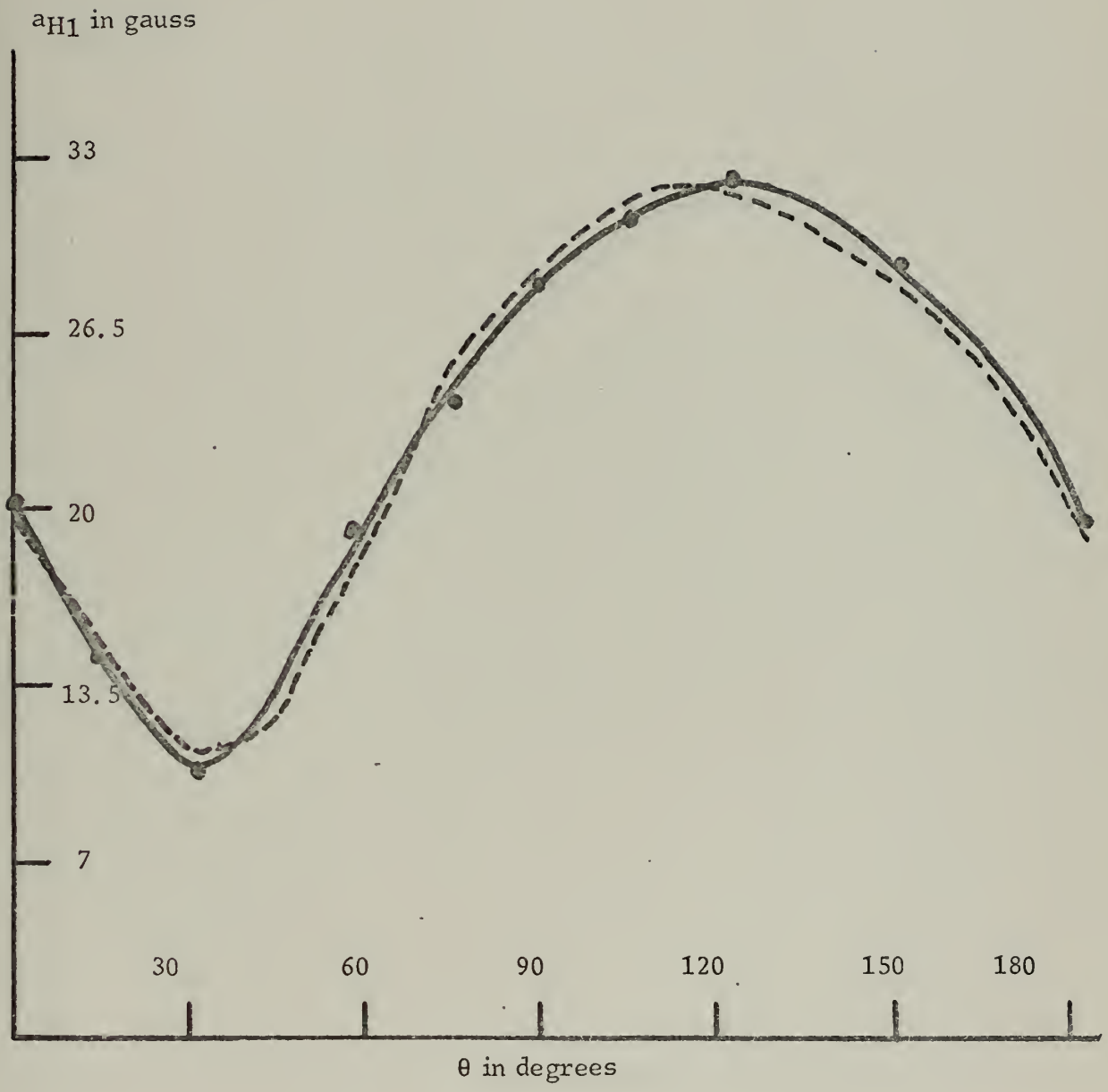

Figure 8A. H_1 atom coupling constant versus orientation of magnetic field in XYZ axis system for lithium acetate dihydrate. Dashed line is calculated value. $\phi = 90^\circ$

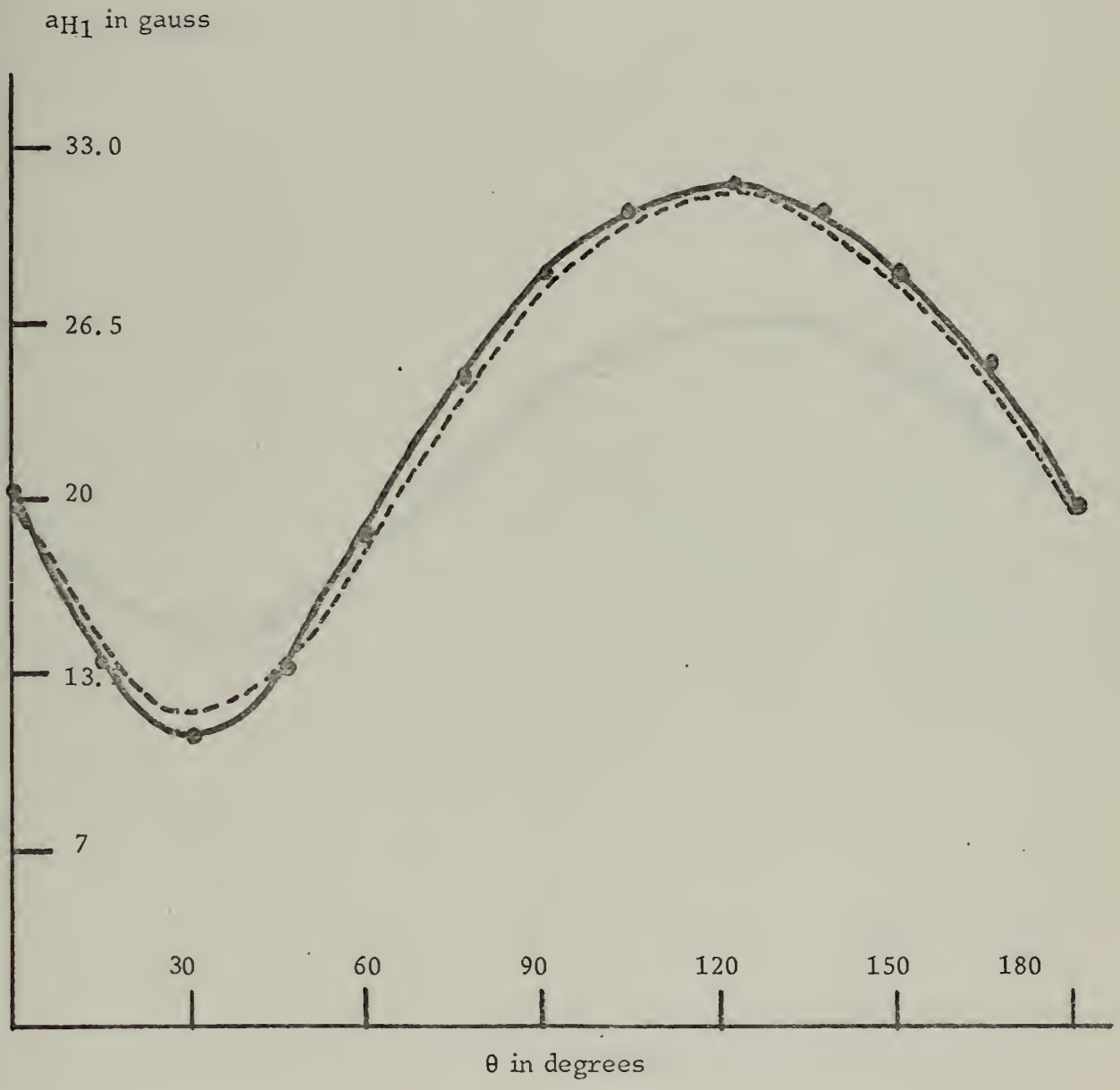

Figure 8B Ø = + 60

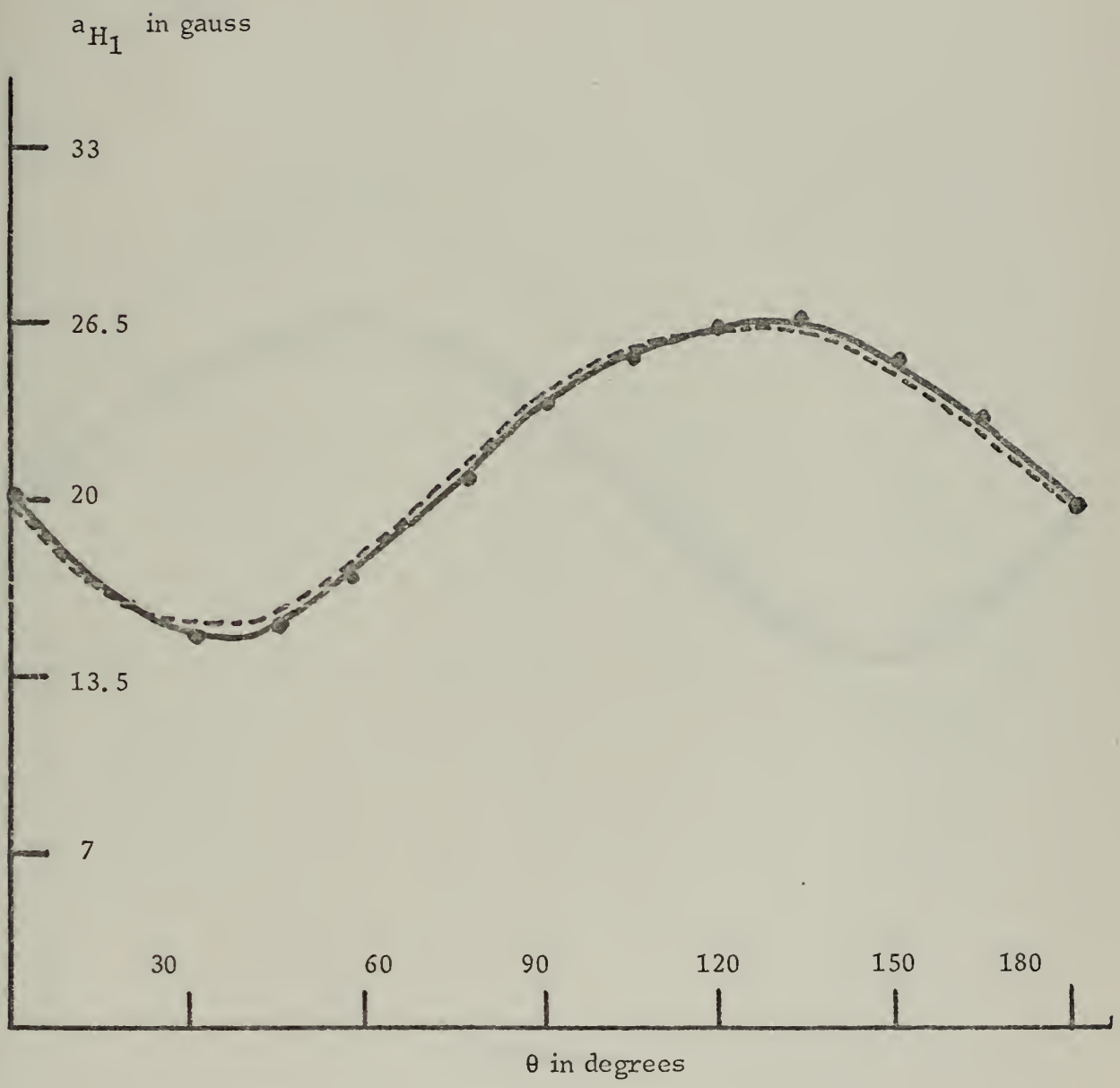

Figure 8C Ø = +30

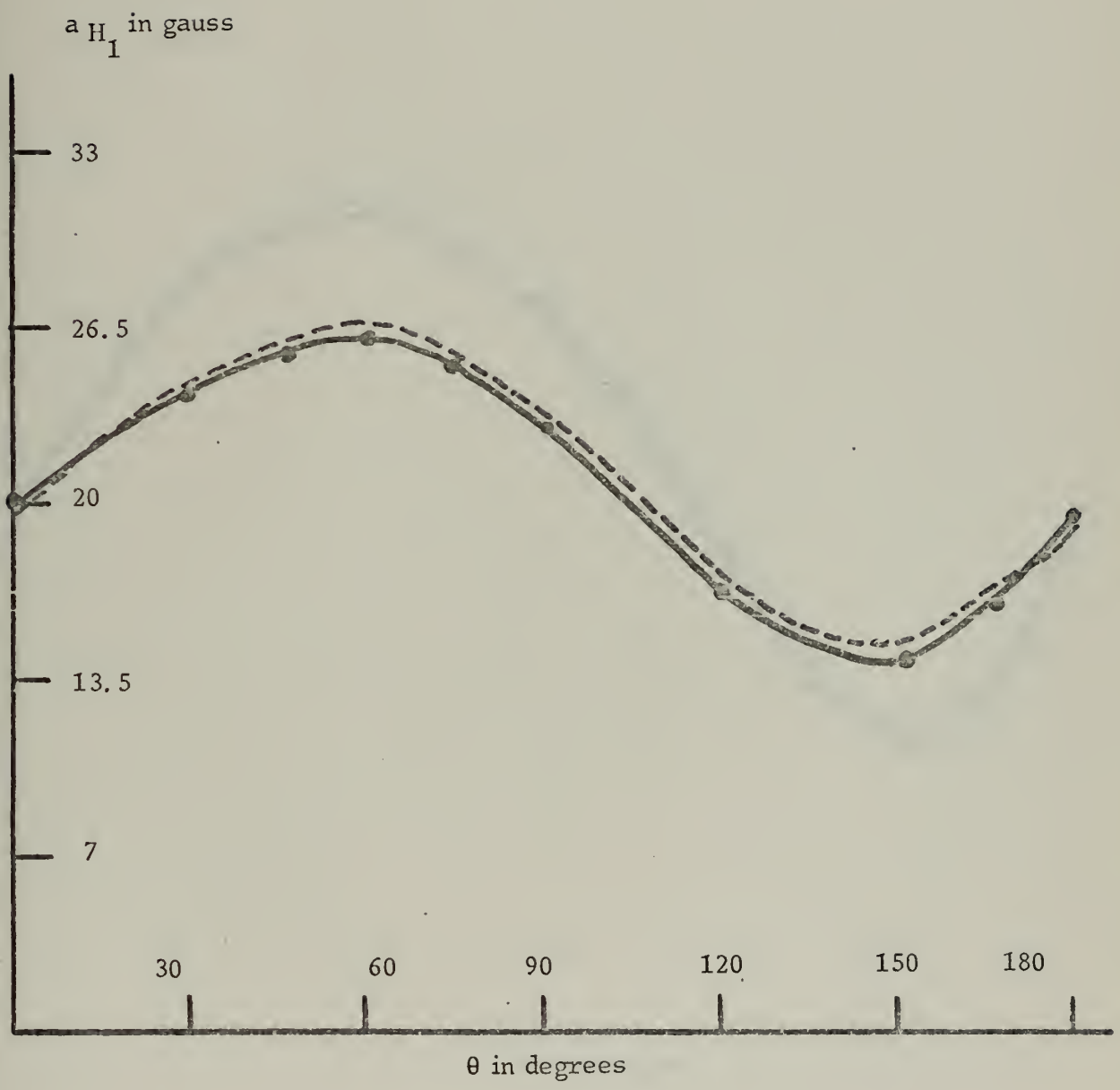

Figure 8D $\phi = -30^{\circ}$

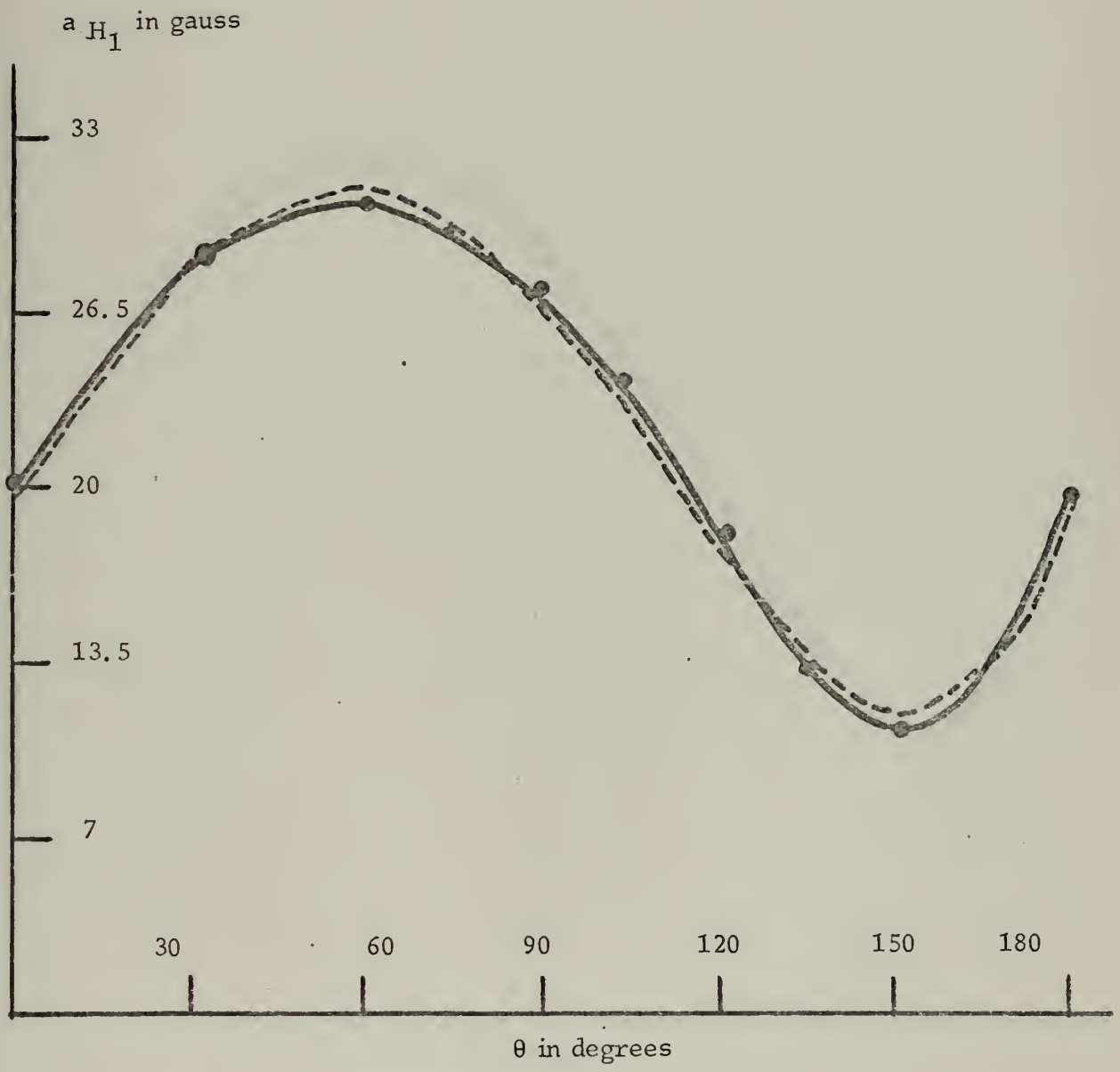

Figure 8E $\phi = -60^{\circ}$

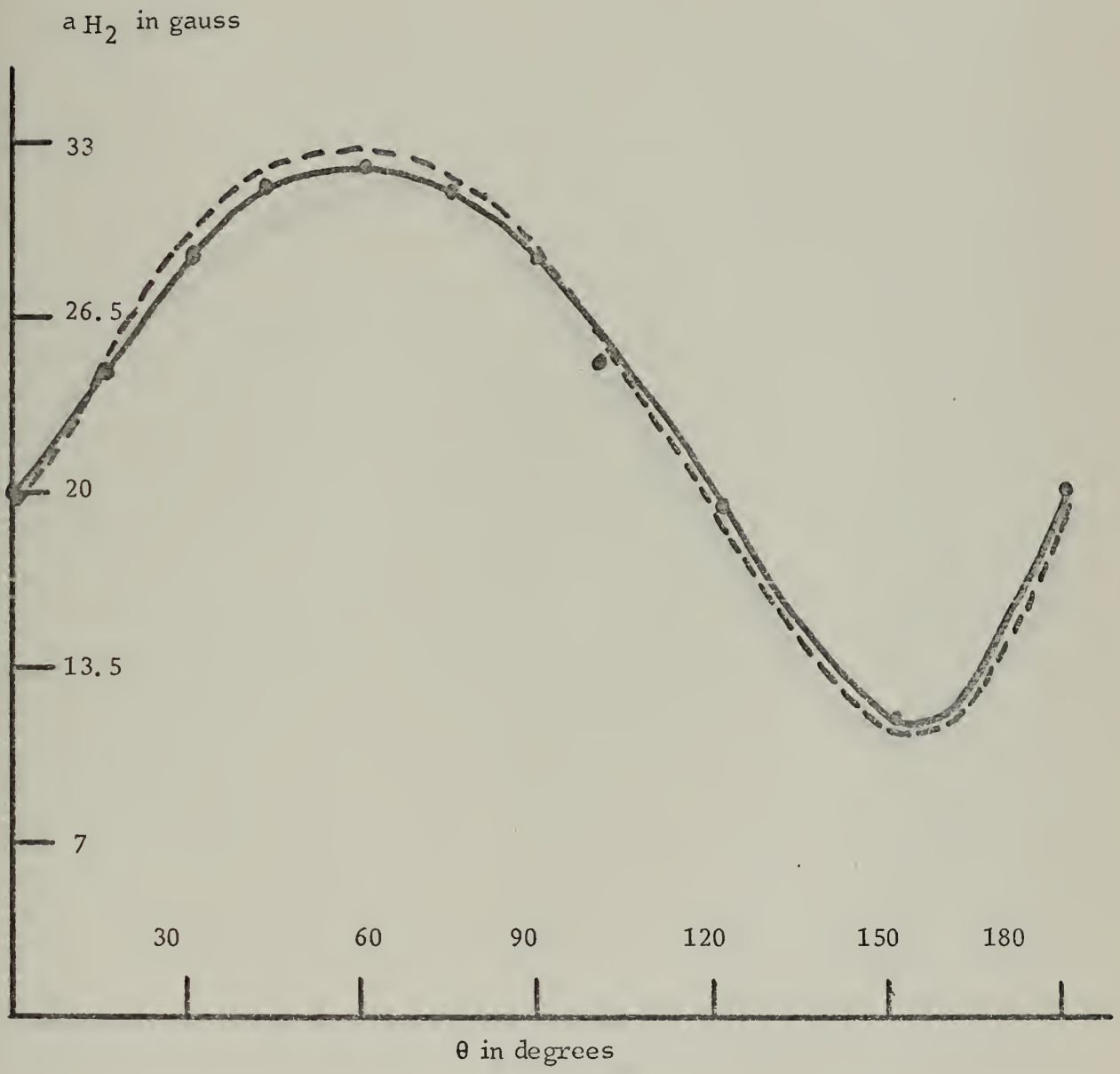

Figure 8F H_2 atom coupling constant versus orientation of magnetic field in XYZ axis system for lithium acetate dihydrate $\phi = 90$. Dashed line is calculated value.

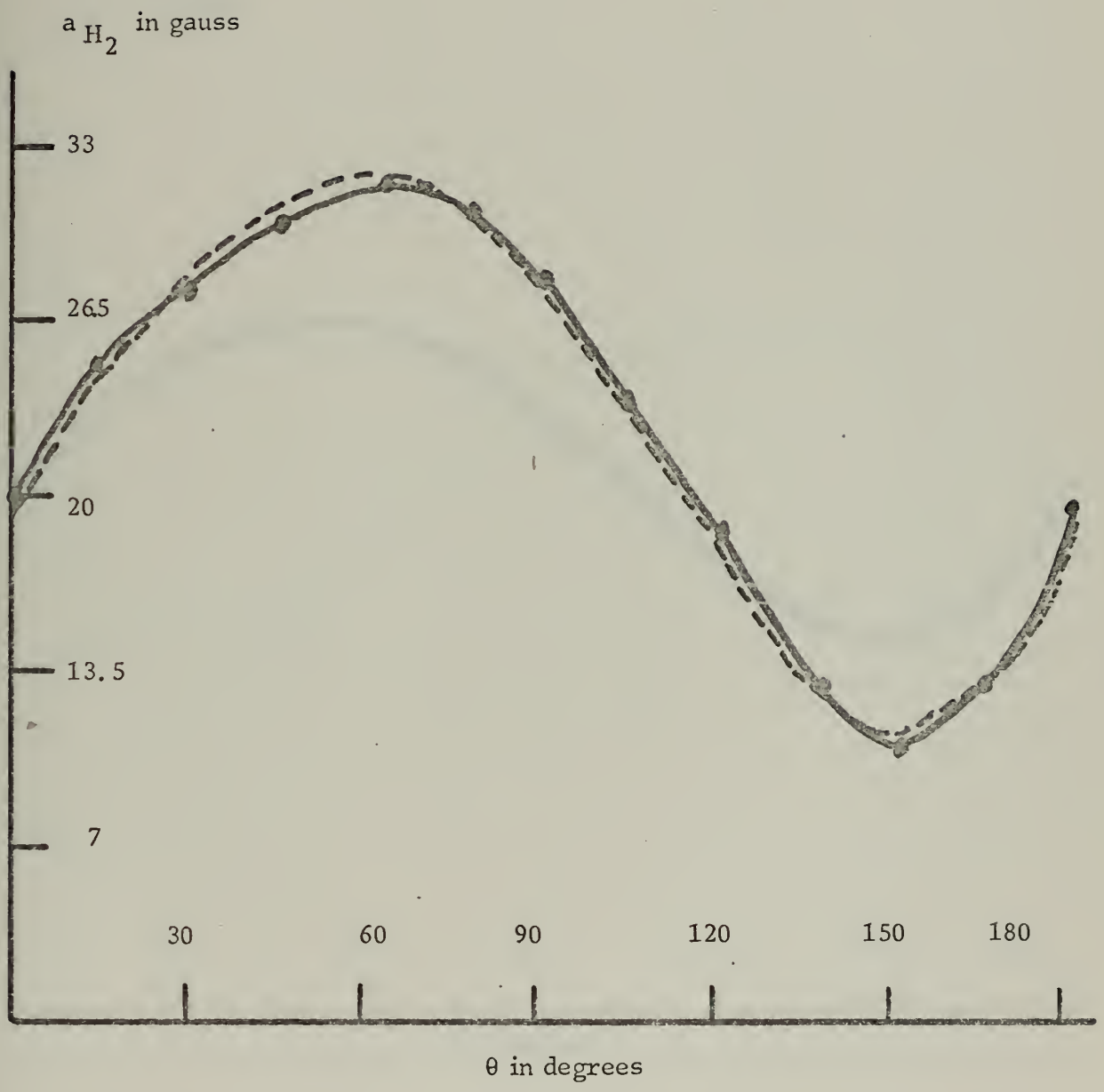

Figure 8G $\phi = 60$

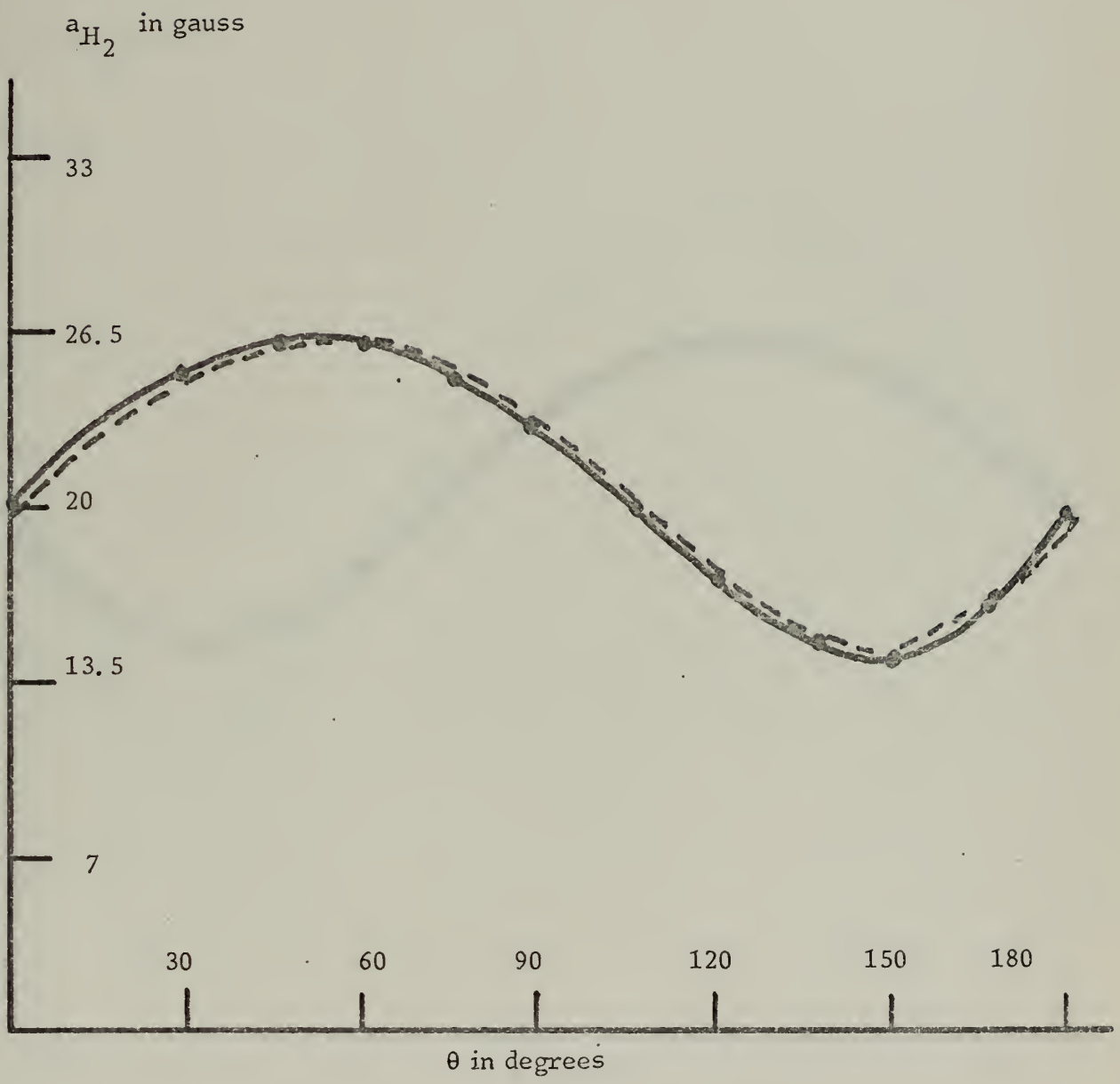

Figure 8H Ø = 30

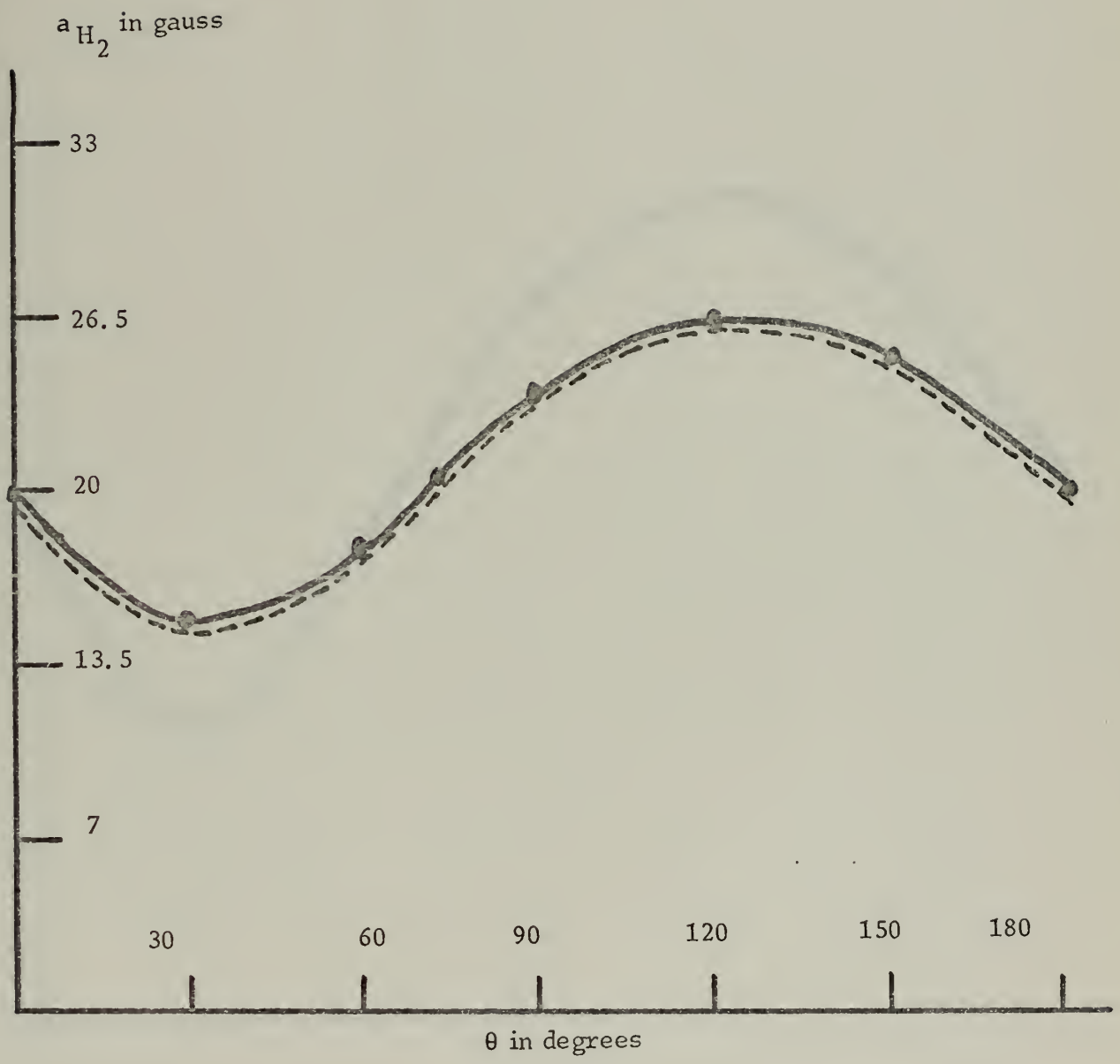

Figure 8I $\phi = -30$

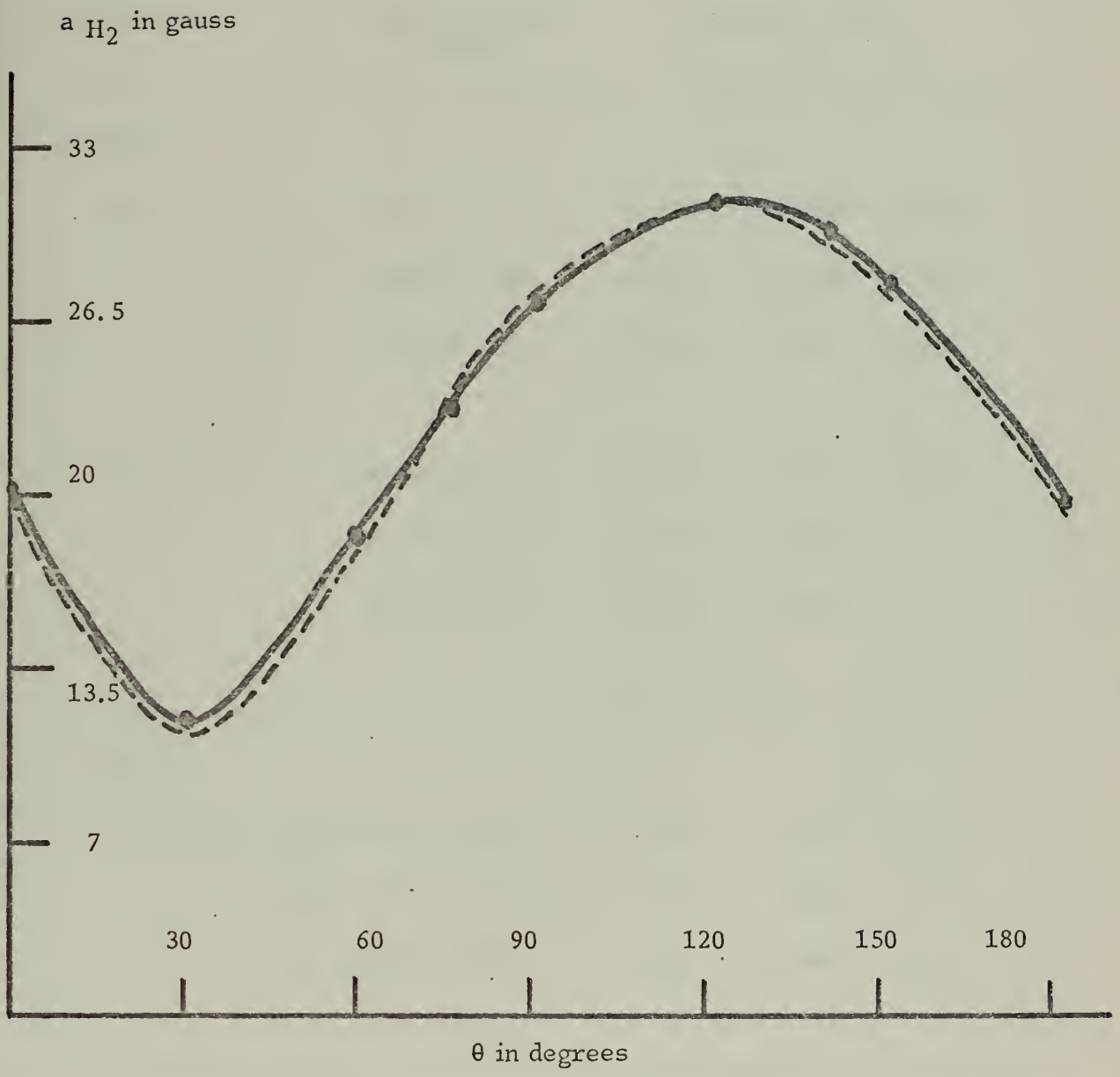

Figure 8J ∅ = -60

TABLE I

Species	Principal Values (MHZ)	Direction Cosine X	Y	Z
$\cdot CH_2CO_2^-$				
H_1	$-59.16 \pm .76$	0.999	-0.011	0.016
	$-94.47 \pm .39$	0.018	0.859	-0.512
	$-29.90 \pm .53$	0.007	-0.512	-0.859
H_2	$-59.04 \pm .78$	0.999	-0.018	0.022
	$-93.82 \pm .39$	0.005	0.859	0.512
	$-30.01 \pm .59$	-0.028	-0.512	0.859
$\cdot CH_2CO_2^-$				
g Tensor	$g_{xx}=2.0035 \pm 0.0002$	0.930	0.331	-0.161
	$g_{yy}=2.0038 \pm 0.0002$	-0.342	0.939	-0.041
	$g_{zz}=2.0027 \pm 0.0001$	0.138	0.093	0.986

Principal values for the coupling constants and g tensor for the $\cdot CH_2CO_2^-$ radical in liquid nitrogen temperature irradiated lithium acetate dihydrate observed at 173°K.

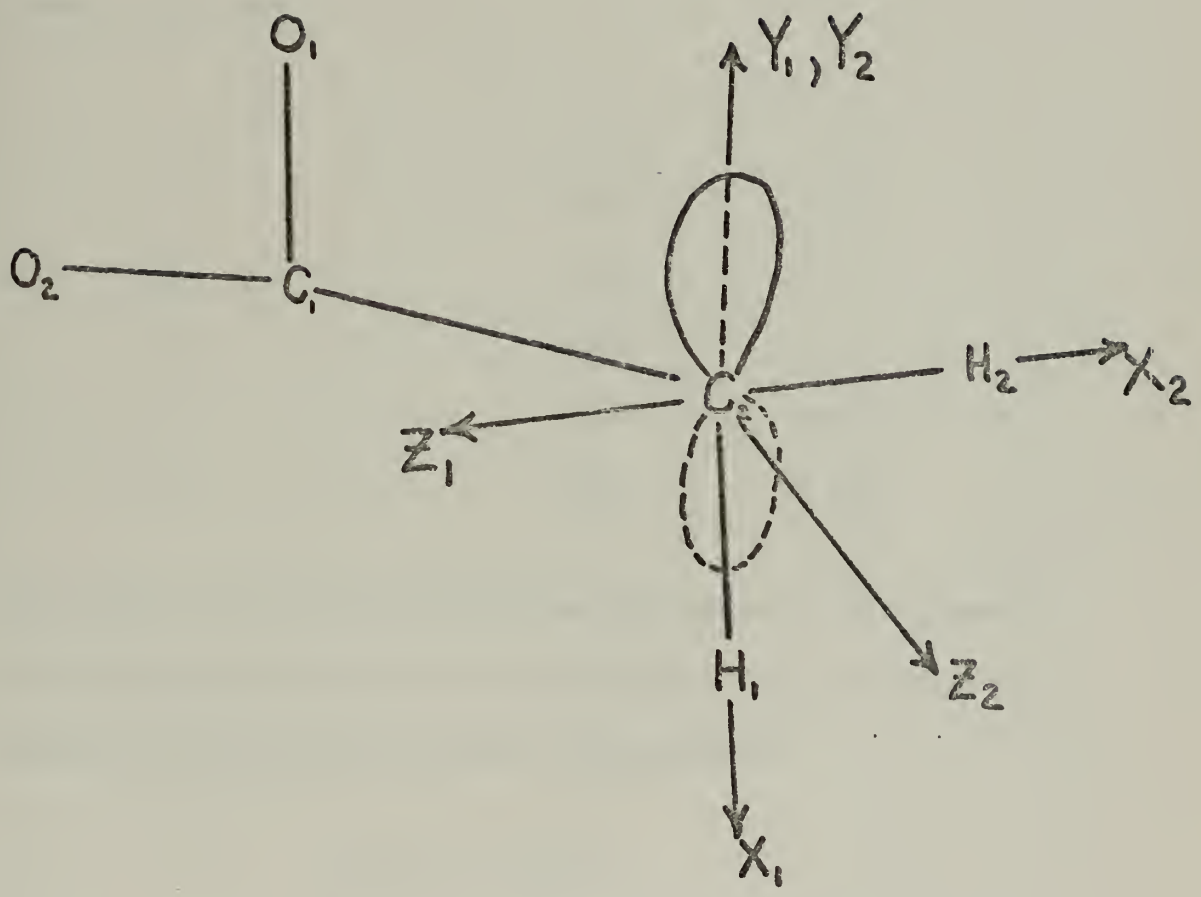

Figure 9. Locations of the hyperfine axes in the $\cdot CH_2CO_2^-$ radical (planar configuration) [Ref. 19]

in terms of the x,y,z system were calculated by using the simple transformations expressed as:

$$a = x$$

$$b = y$$

$$c = z$$

These results are:

	x	y	z
L_i	0	5.440	1.873
C_1	0	3.139	0
C_2	0	1.616	0
O_1	0	2.025	3.310
O_2	0	3.707	1.108

The vectors for the distances between the appropriate atoms were calculated and normalized to give the direction cosines of the vectors relative to the crystal axis system. For example:

$$\bar{V}_{c_1c_2} = (0, -1, 0)$$

$$\bar{V}_{o_1o_2} = (0, .6088, -.7970)$$

The angle between the C_1-C_2 bond and the CO_2 plane was calculated from the above atom locations to be 0^o and; therefore, the planar model for the $\cdot CH_2CO_2^-$ radical is valid. This assumes that the carbons do not

change positions following irradiation. A vector which is perpendicular to both the CO_2^- and the CH_2 planes can be expressed as:

$$\bar{V} = \bar{V}o_1o_2 \times \bar{V}c_1c_2 = (-1, 0, 0)$$

By assuming that the HCH angle was 120^o the direction cosines for the C-H bonds were calculated:

$$\bar{V}p = \bar{V}c_1c_2 \times \bar{V} = (0, 0, -1)$$

$$\bar{V}c_1h_1 = .5\bar{V}c_1c_1 + \frac{\sqrt{3}}{2}\bar{V}p = (0, -.5000, .8660)$$

$$\bar{V}c_1h_2 = -.5\bar{V}c_1c_2 - \frac{\sqrt{3}}{2}\bar{V}p = (0, .5000, -.8660)$$

4. Room Temperature Irradiation of Lithium Acetate Dihydrate

Following irradiation at room temperature a single crystal of $Li(CH_3CO0) \cdot 2H_20$ still showed the 1:2:1 spectrum for the $\cdot CH_2CO_2^-$ radical; however, the presence of at least one more species was found. Figures 5 and 6 show these additional lines. The $\cdot CH_2CO_2^-$ radical present in the liquid nitrogen temperature irradiated lithium acetate crystal was found to be present in room temperature irradiations. The analysis of the additional lines seen in the room temperature irradiated crystal was attempted but no positive results were obtained. Initial attempts at interpreting the spectra as due to a single hydrogen atom interaction proved to be incorrect. By waiting for the $\cdot CH_2CO_2^-$ radical to decay it was hoped that the spectrum for the new species would become easier to interpret, but this approach was also unsuccessful. No further attempts were made to determine the identity of this species.

B. MERCURIC ACETATE

1. Spectra of Radicals Formed

Single crystals of mercuric acetate were irradiated at both liquid nitrogen and room temperatures. The results of irradiation at liquid nitrogen temperatures for 2 hours and observation at -170°C are shown in Figure 10. The presence of two inequivalent sites was seen by rotation of the crystal about θ and observing the splitting of the line. Figure 11 shows two spectra seen following liquid nitrogen irradiation and warmed to -80°C. The decay of the two species observed at -170°C is seen. Figure 14 shows two spectra of room temperature irradiated mercuric acetate crystals. One spectrum shows the familiar 1:2:1 intensity while the other which is rotated 30° about θ shows a splitting of the outer two lines.

2. Liquid Nitrogen Temperature Irradiation of Mercuric Acetate

Following two hours of liquid nitrogen temperature irradiation mercuric acetate crystals were found to be extremely brittle. Great care was needed to prevent the crystals from breaking into tiny slivers which were useless for EPR studies. Future studies of this crystal at low temperatures will require some type of permanent mounting which will give no EPR signal following irradiation.

The spectrum observed at -170°C was very intense and completely covered any other lines (Figure 10). The spectrum seen at -170°C decayed rapidly when warmed to -80°C and when lowered again to -170°C was not seen. This showed the irreversible nature of the species.

Since previous researchers had found the presence of the $\cdot CH_2CO_2^-$ radical and also this radical was seen in lithium acetate dihydrate it was hypothesized that the two intense spectral lines seen at -170°C were due to $\cdot CO_2^-$. The g tensor for $\cdot CO_2^-$ is well known and so by comparison it was hoped to show that these lines in mercuric acetate were also $\cdot CO_2^-$. By the use of DPPH, as previously described, the g tensors for the two species were obtained. Table II lists the g tensor principal values along with their direction cosines. The accepted values from Ref. 14 are also listed for comparison. The experimental values for the g tensors compare favorably with accepted values and therefore, $\cdot CO_2^-$ radicals are believed to be present at -170°C.

Upon warming the crystal to -80°C the spectra in Figure 11 were seen. The decay of the $\cdot CO_2^-$ is evident and the presence of two $\cdot CH_2CO_2^-$ radicals can tentatively be made. Figure 11 shows the eight expected lines for two inequivalent $\cdot CH_2CO_2^-$ radicals. After orienting the crystal at various magnetic field positions the coupling constants were obtained. Due to superposition and crossing over of the lines, interpretation was quite difficult. Many plots of θ verses coupling constants at constant Ø's were made in an attempt to get smooth sinusoidal curves. The final coupling constants assigned to each of the four protons for the two $\cdot CH_2CO_2^-$ radicals are shown in Figures 12 and 13. The curves show the calculated values and the experimental values.

Calculating the HCH angles for the two radicals gave $100.^{\circ}5 \pm 2.0$ and $113.^{\circ}7 \pm 2.0$. These values are to be compared with those expected

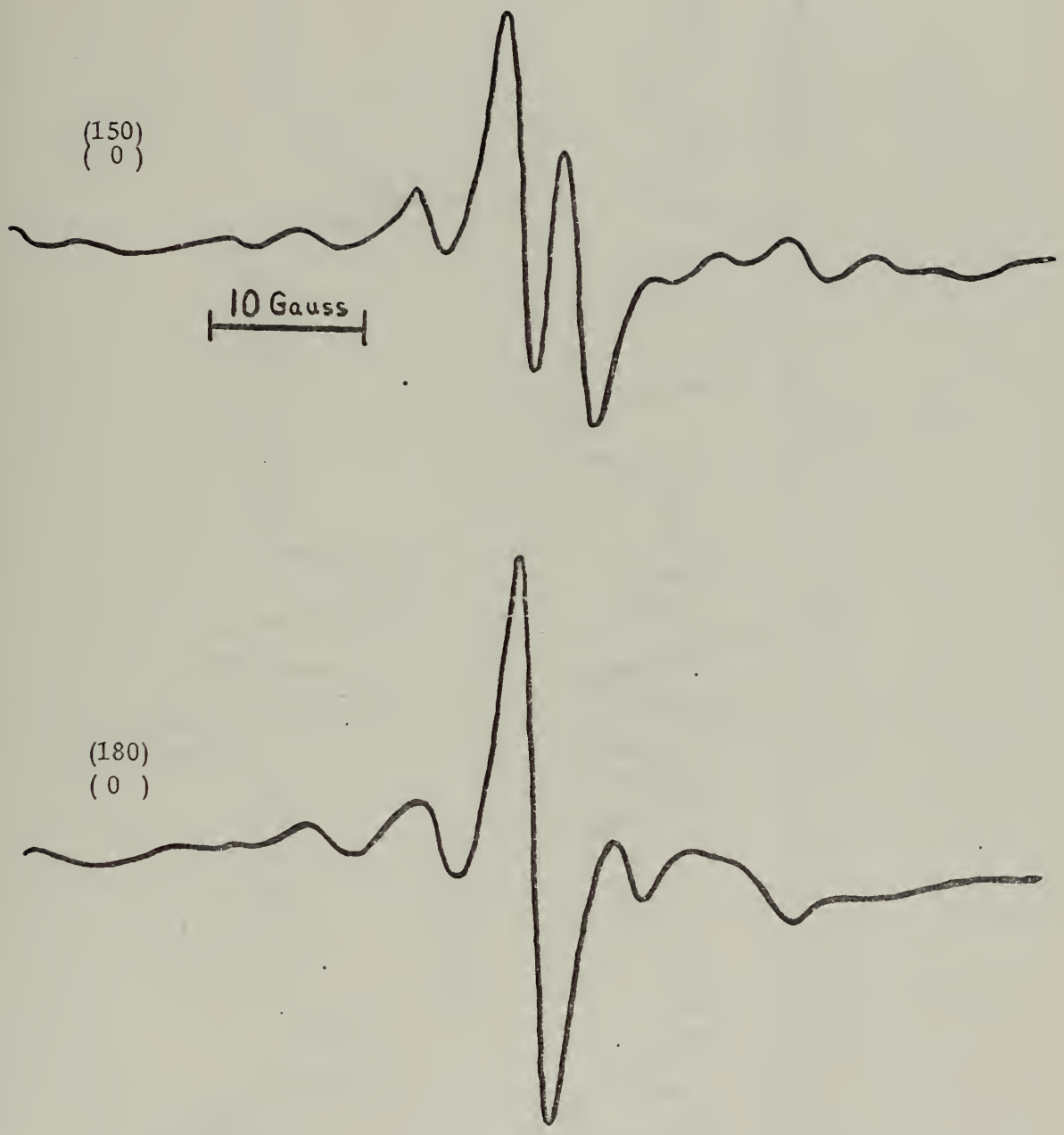

Figure 10. Spectra of liquid nitrogen temperature irradiated mercuric acetate observed at -170°C. Top spectrum is at $(150)_0$ and bottom is at $(180)_0$.

Figure 11. Two spectra of liquid nitrogen temperature irradiated mercuric acetate observed at -80°C. Top is at $\binom{0}{0}$ and bottom is at $\binom{30}{+30}$

TABLE II

Species	Principal Values	Direction Cosines		
		X	Y	Z
g_1	g_{xx} -2.00166 $\pm$ .00003	0.9286	-0.2568	-0.2677
	g_{yy} -1.999608 $\pm$ .00003	0.3522	0.8368	0.4192
	g_{zz} -2.00040 $\pm$ .00002	0.1164	-0.4836	0.8675
g_2	g_{xx} -2.00194 $\pm$ .00004	.9689	-.2693	.2462
	g_{yy} -1.99582 $\pm$ 0.00003	.1987	-.5087	-.8377
	g_{zz} -2.00040 $\pm$ 0.00003	.1478	.8605	-.4875
gCO_2^-	g_{xx} =2.0032			
	g_{yy} =1.9975			
	g_{zz} =2.0014			

g Tensors for the species present in liquid nitrogen temperature irradiated mercuric acetate observed at -170°C. Accepted values for g tensor of CO_2^- from Ref. 14 are included.

of 120°. No attempt was made to explain the differences other than experimental error. No crystallographic data has been published for mercuric acetate and this would be a necessary step to completely understand the angle differences if they are not due to experimental error. Table III lists the principal values of the four coupling constants along with their respective direction cosines.

3. Room Temperature Irradiation of Mercuric Acetate

Room temperature irradiation and observation of mercuric acetate showed a different spectrum from liquid nitrogen irradiation as seen in Figure 14. At some orientations the 1:2:1 intensity spectrum indicative of the $\cdot CH_2CO_2$ radical was seen. By simple θ rotations, however, the outer two lines would split indicating the presence of two species. The center line would not split at room temperature and so no coupling constants were obtained at this temperature. The interesting fact about room temperature irradiation of mercuric acetate was that upon lowering the temperature of the crystal to -80°C the same spectrum was obtained as for a liquid nitrogen irradiated crystal warmed to -80°C. This indicated a reversible behavior. Upon lowering the room temperature of the irradiated crystal to -170°C the intense CO_2^- lines were not seen. This seemed to indicate that the two CO_2^- species decayed away at warmer temperatures.

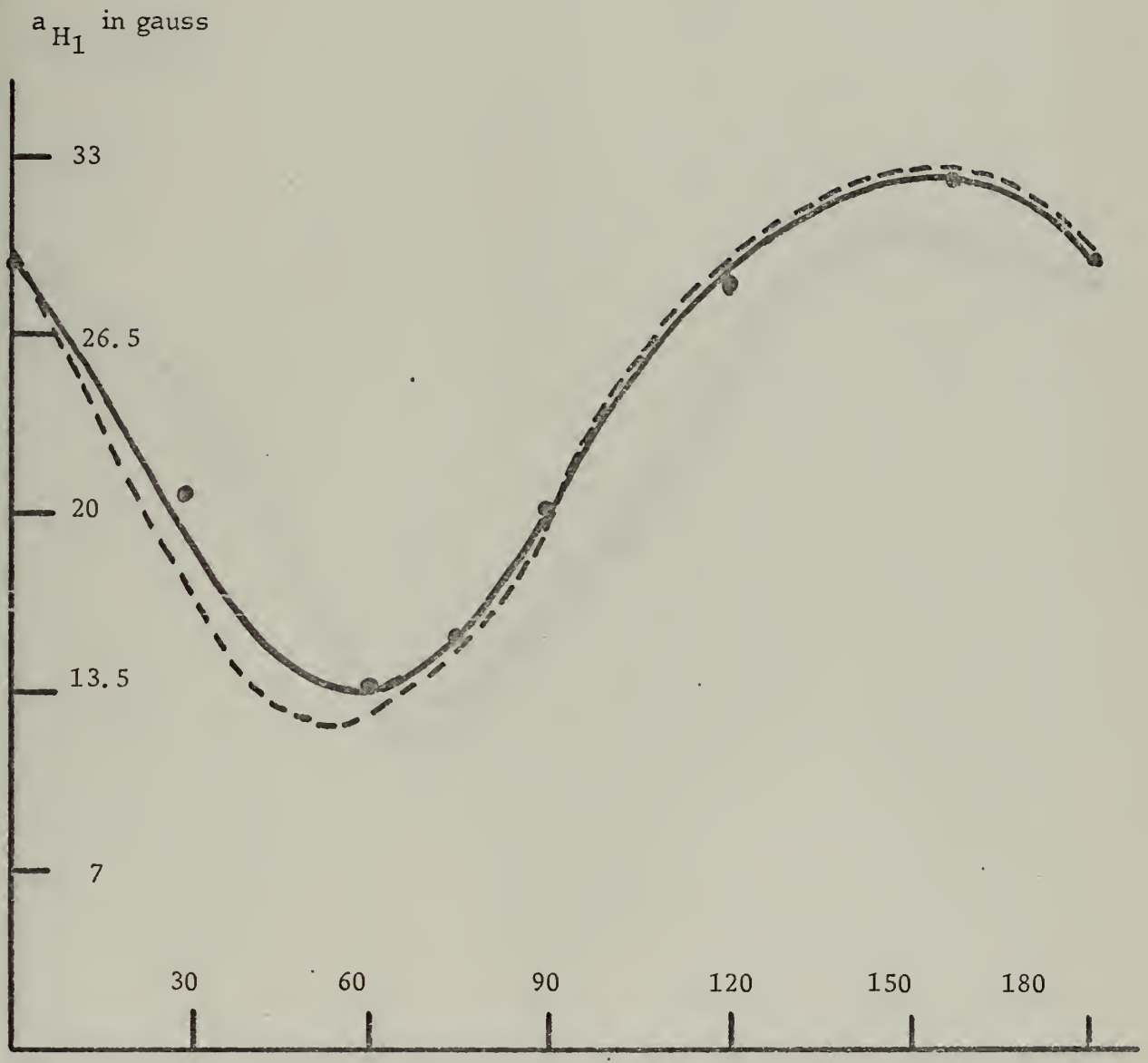

Figure 12A H_1 atom coupling constants versus orientation of magnetic field in XYZ axis systems for mercuric acetate. $\phi = 90$ Dashed line = calculated values.

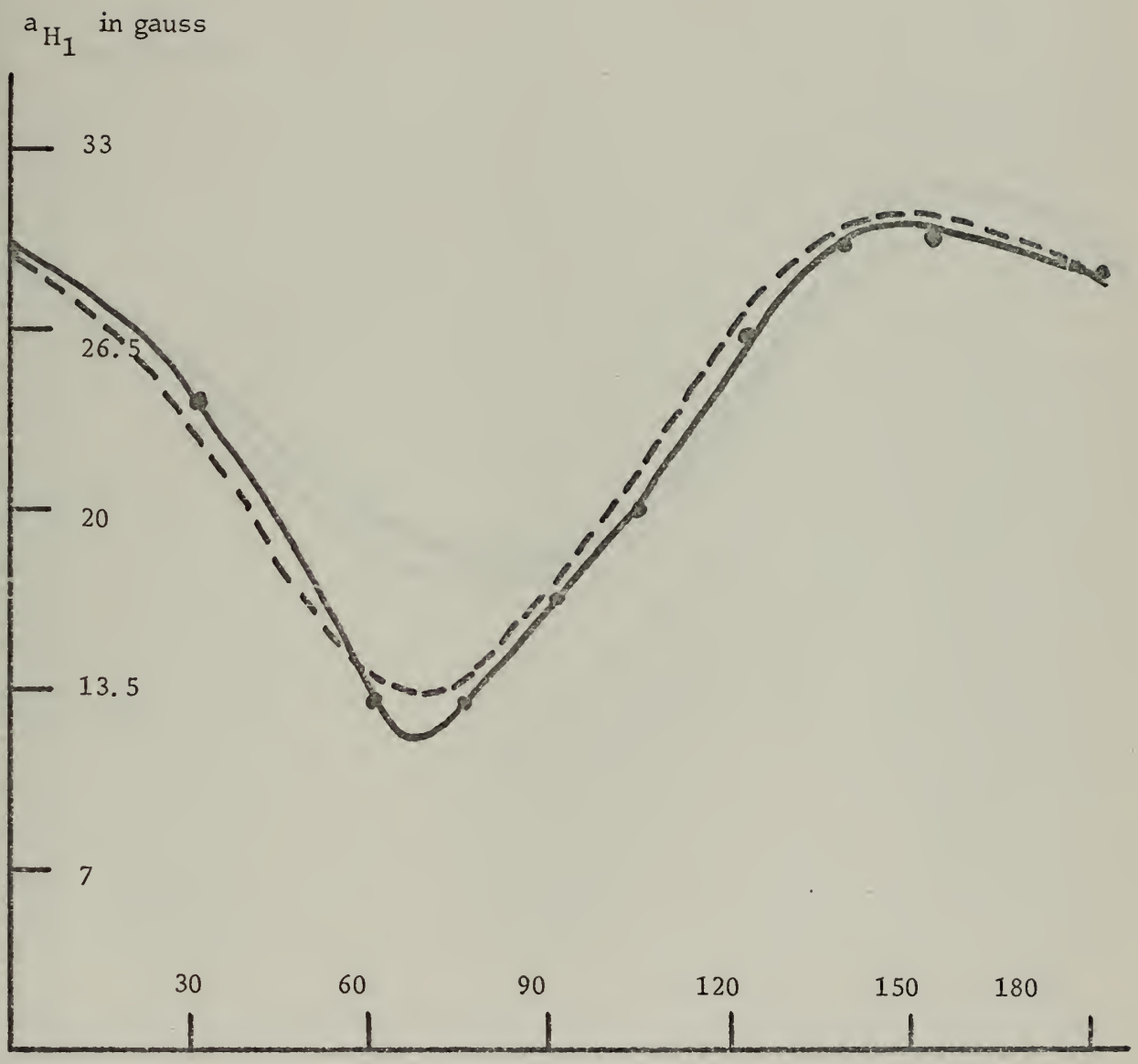

Figure 12B $\phi = 60$

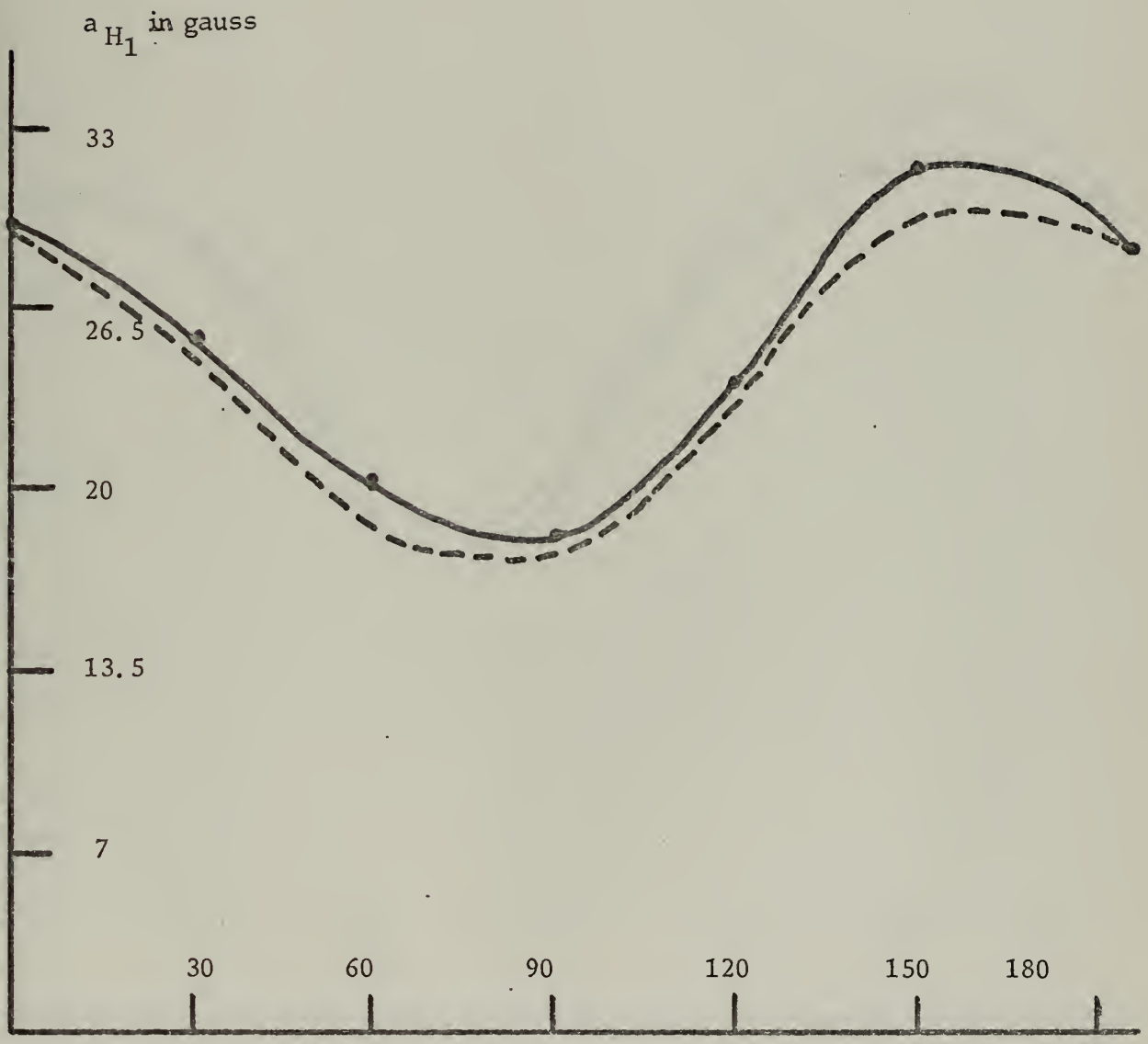

Figure 12C $\theta = 30$

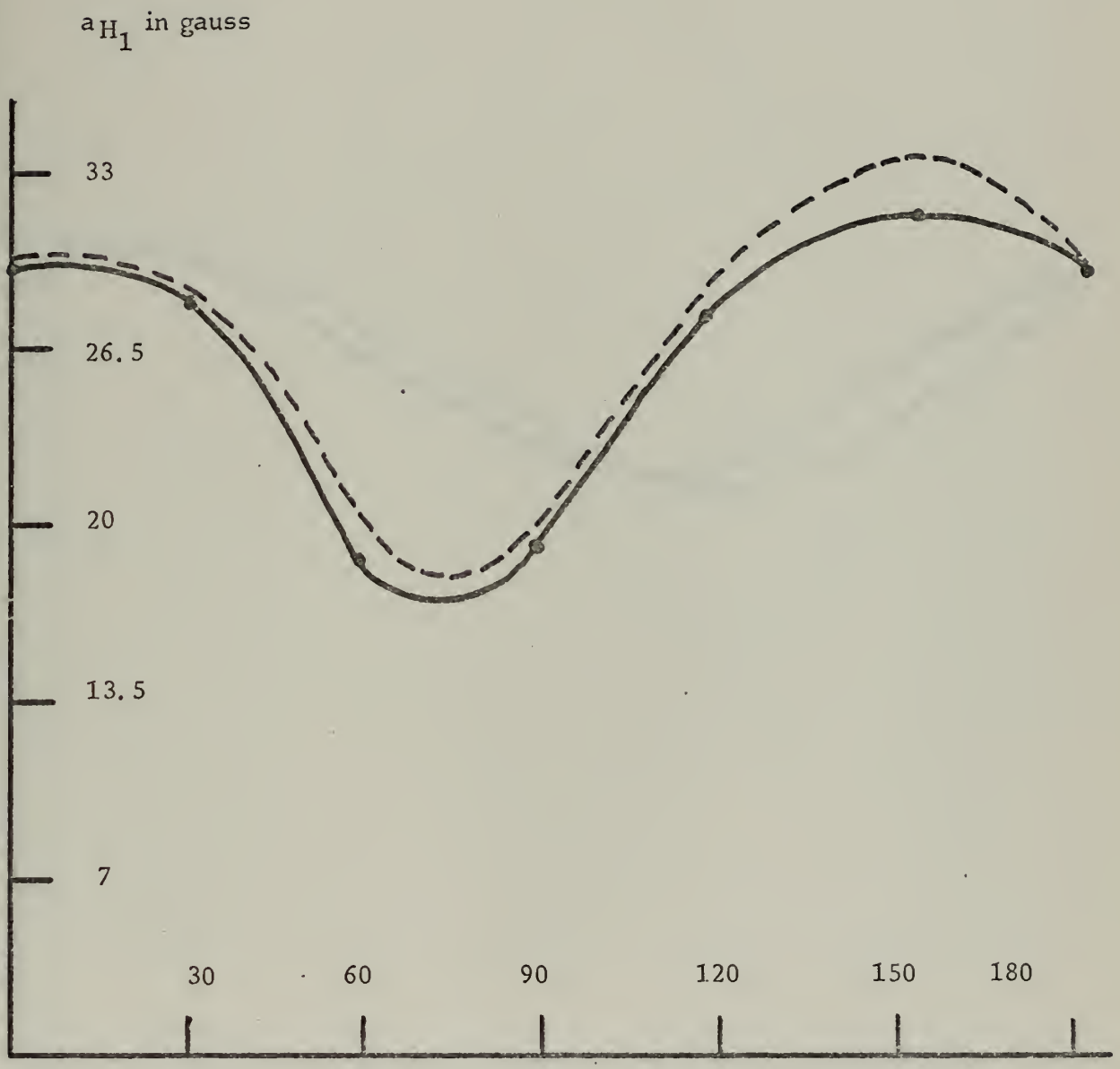

Figure 12D $\phi = 0$

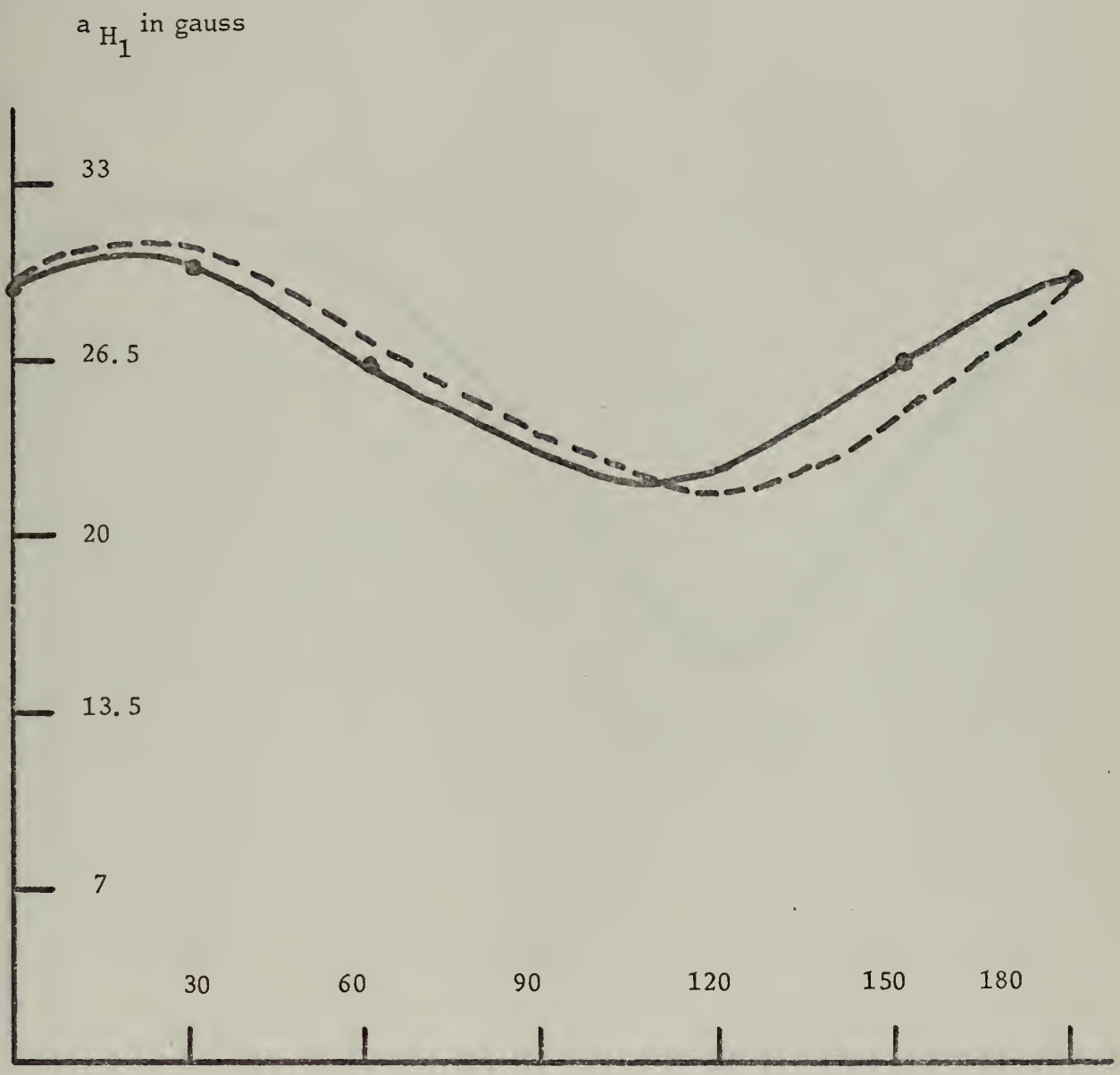

Figure 12E $\phi = -30$

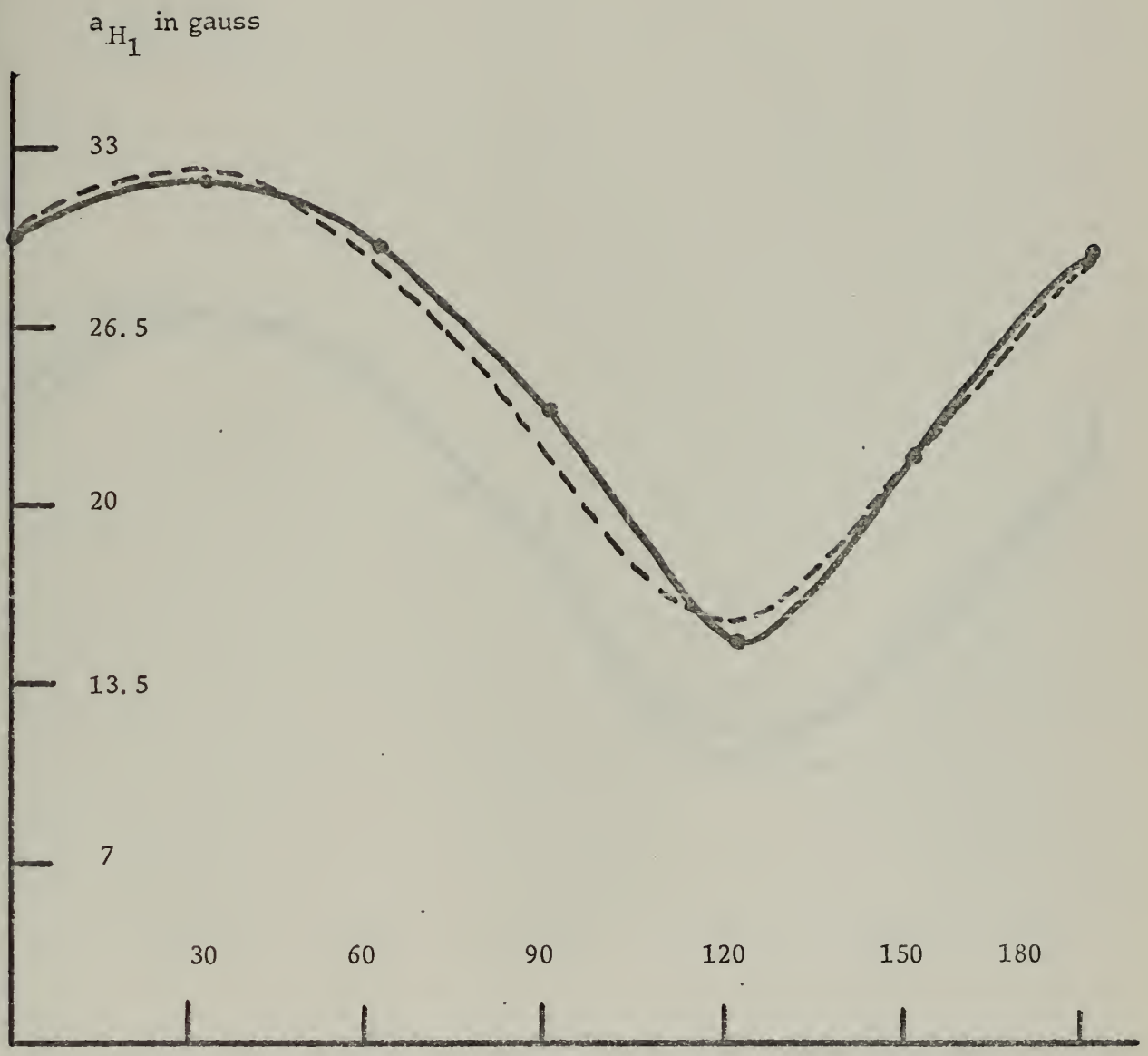

Figure 12F $\phi = -60$

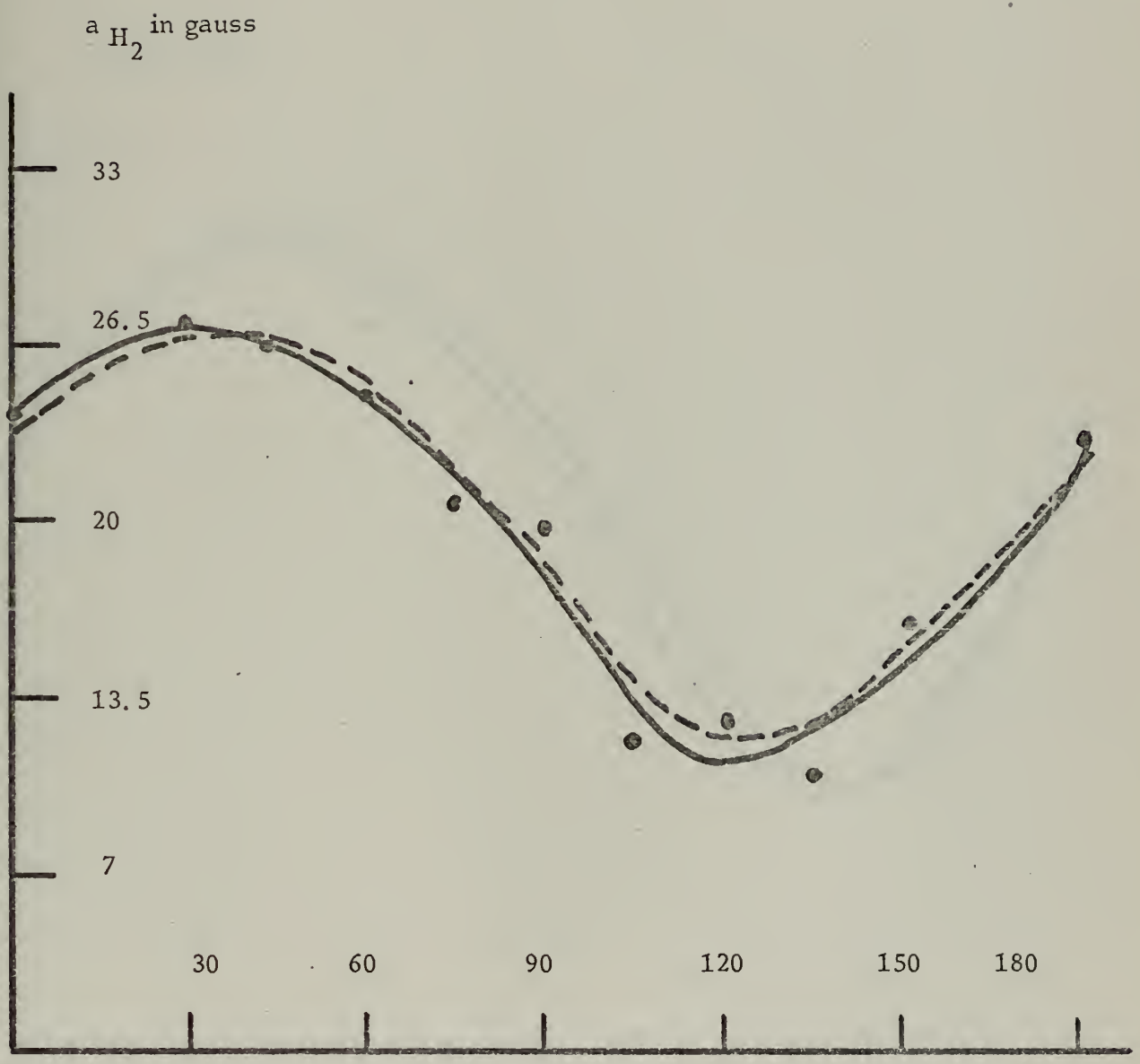

Figure 12G H_2 atom coupling constants versus magnetic field orientation in XYZ axis system. $\emptyset$ = 90. Dashed line = calculated value.

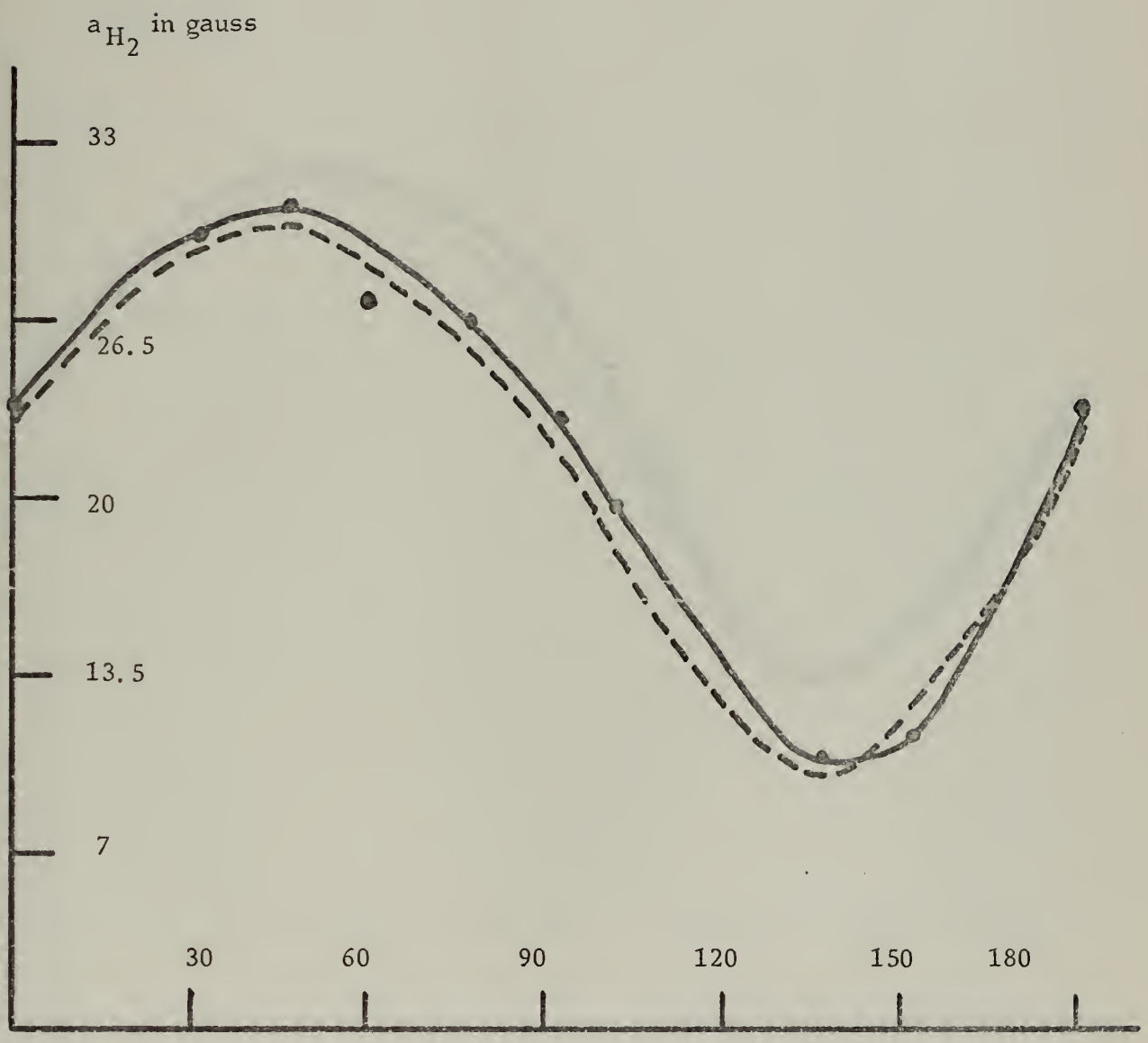

Figure 12H $\phi = 60$

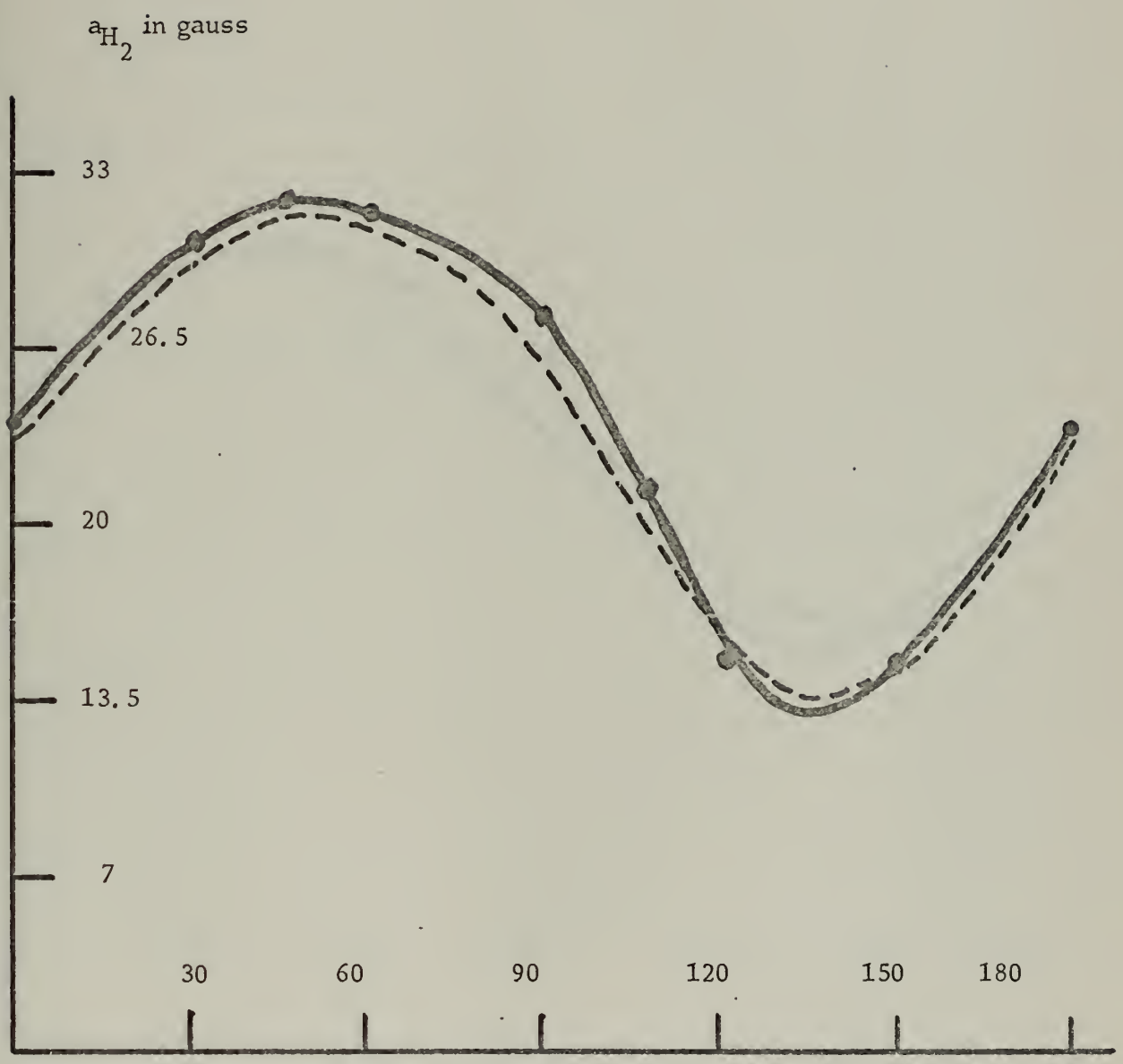

Figure 12I Ø = 30

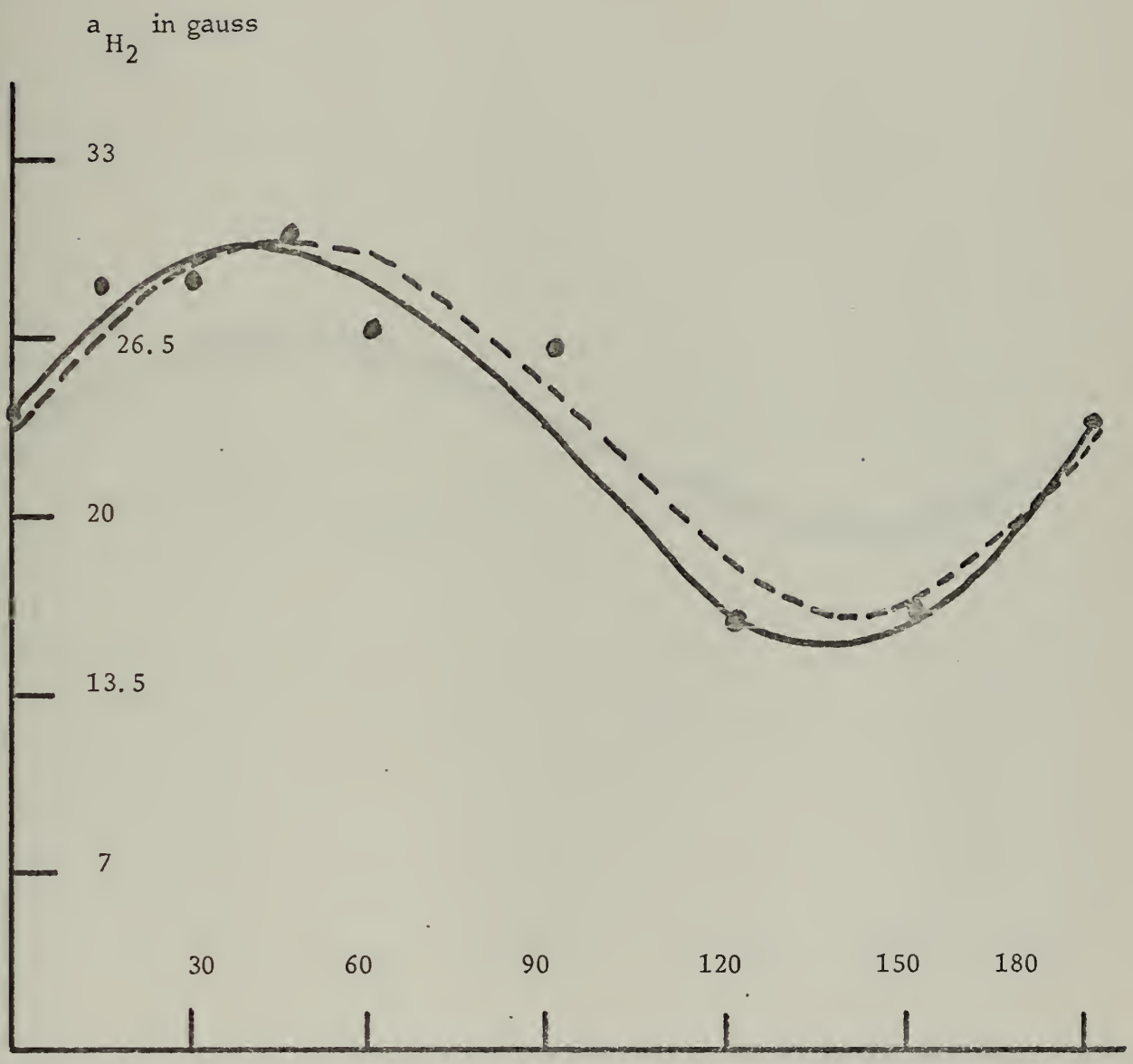

Figure 12J $\phi = 0$

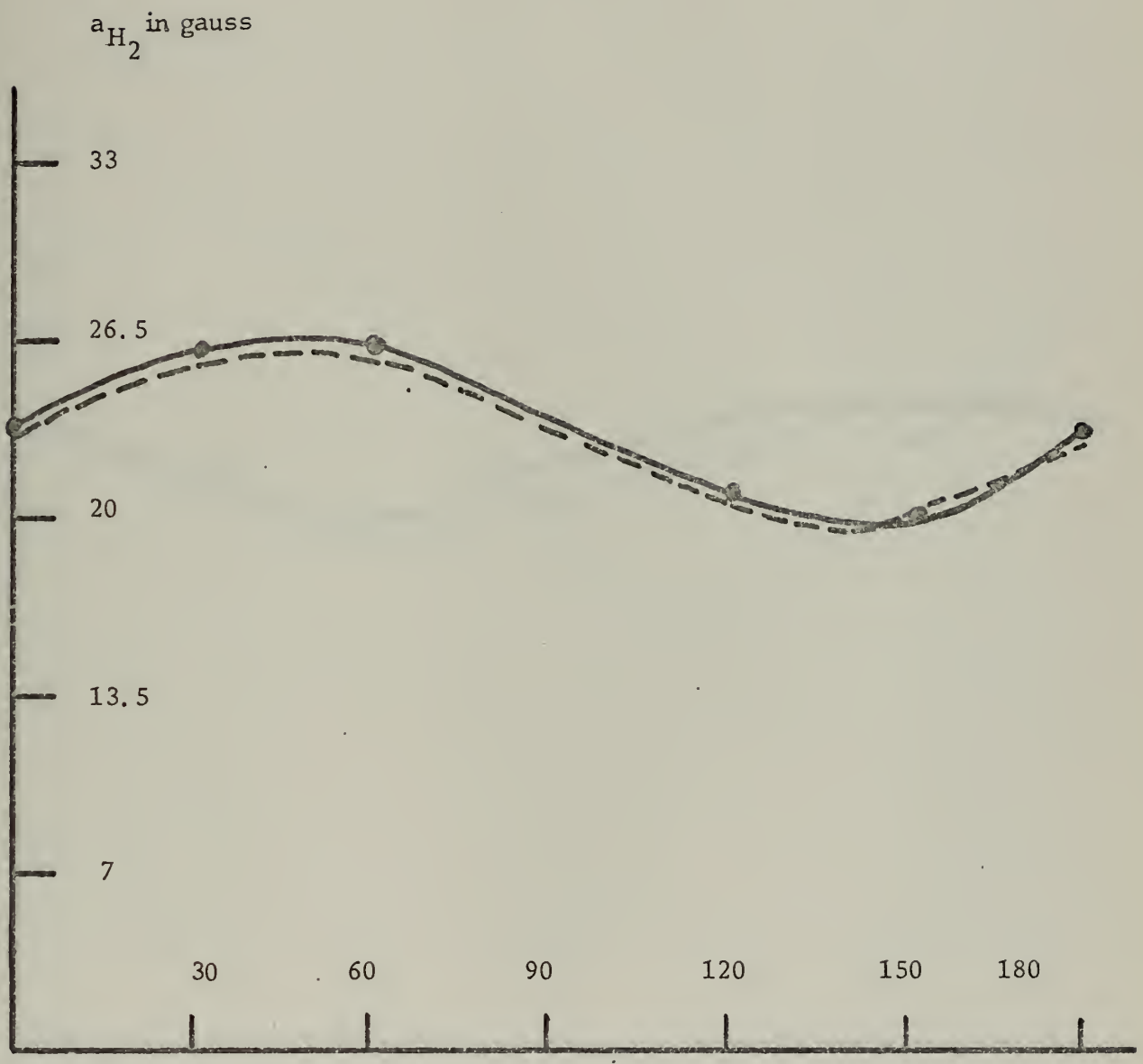

Figure 12K $\phi = -30$

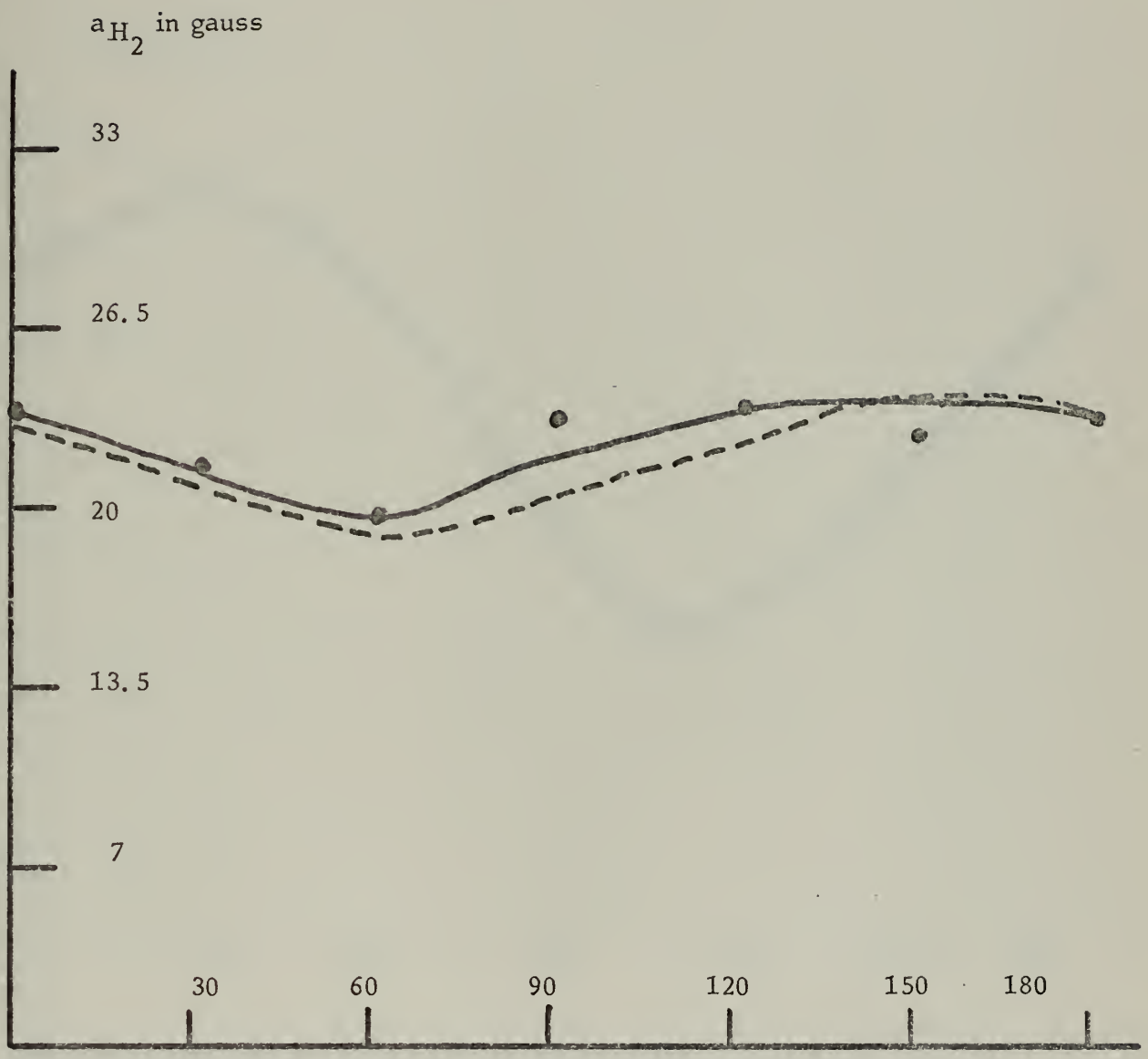

Figure 12L $\emptyset = -60$

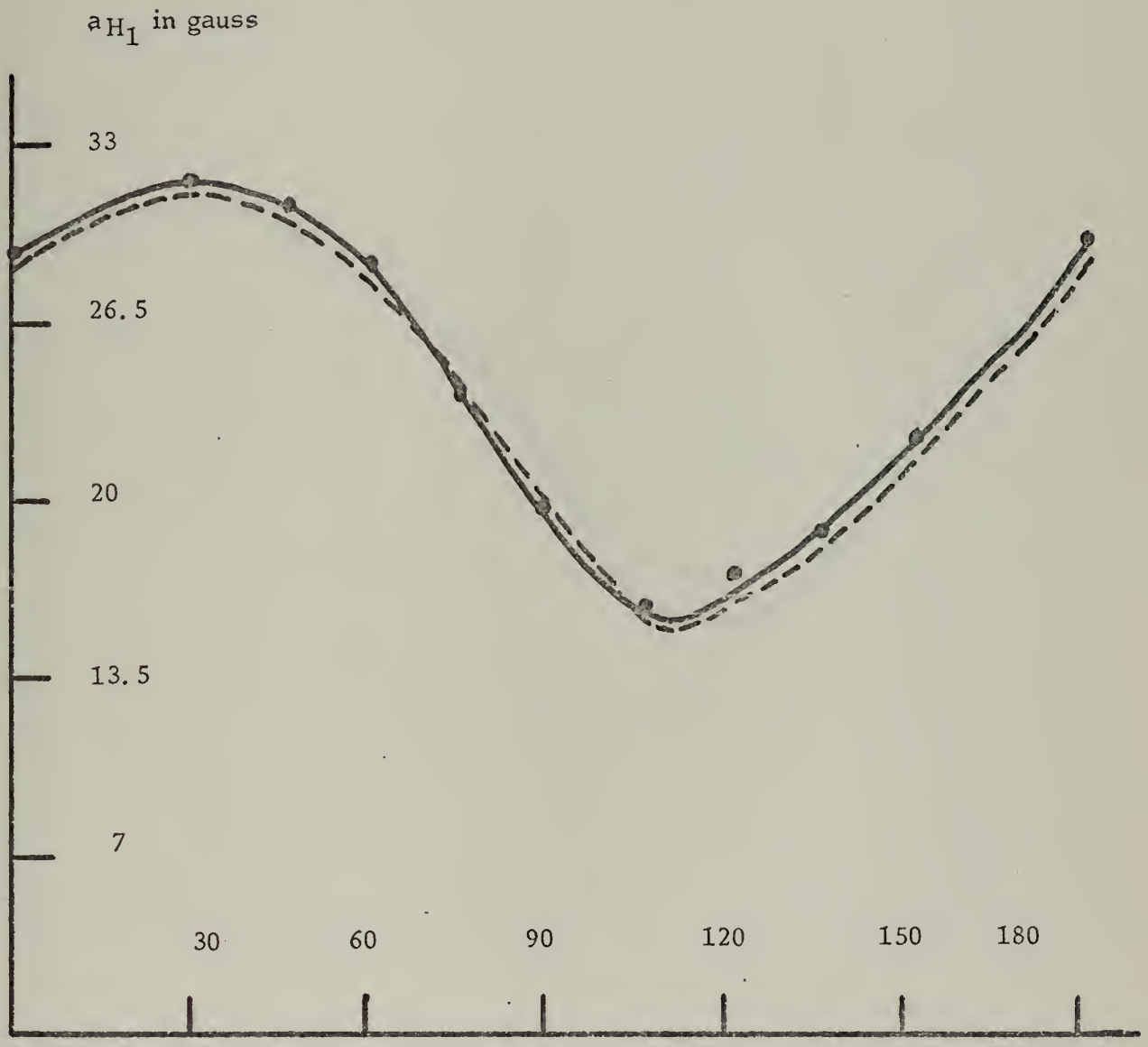

Figure 13A H_1 atom coupling constants versus magnetic field orientation in XYZ azis system. $\emptyset = 90$
Dashed line = calculated value

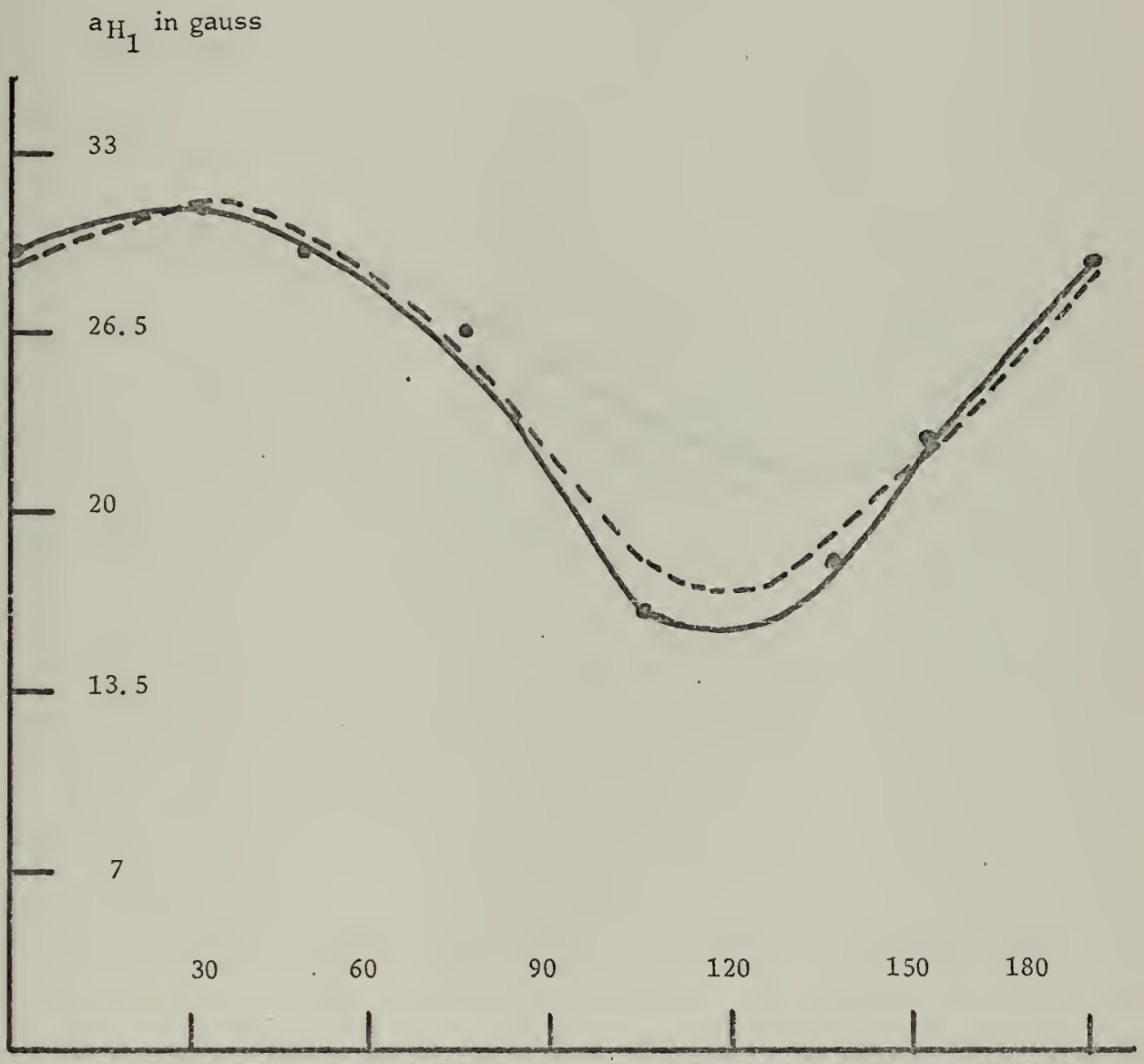

Figure 13B $\emptyset = 60$

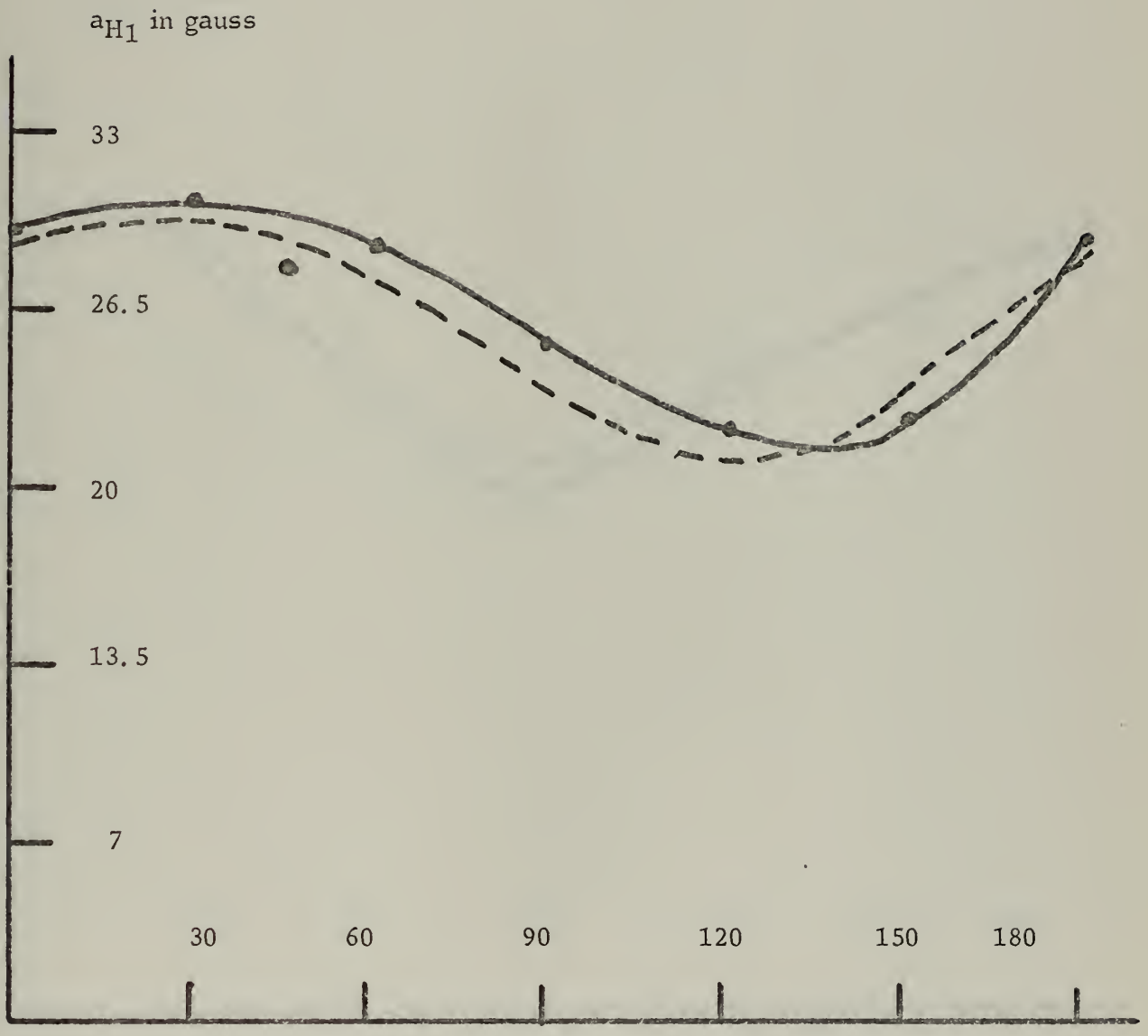

Figure 13C $\emptyset$ = 30

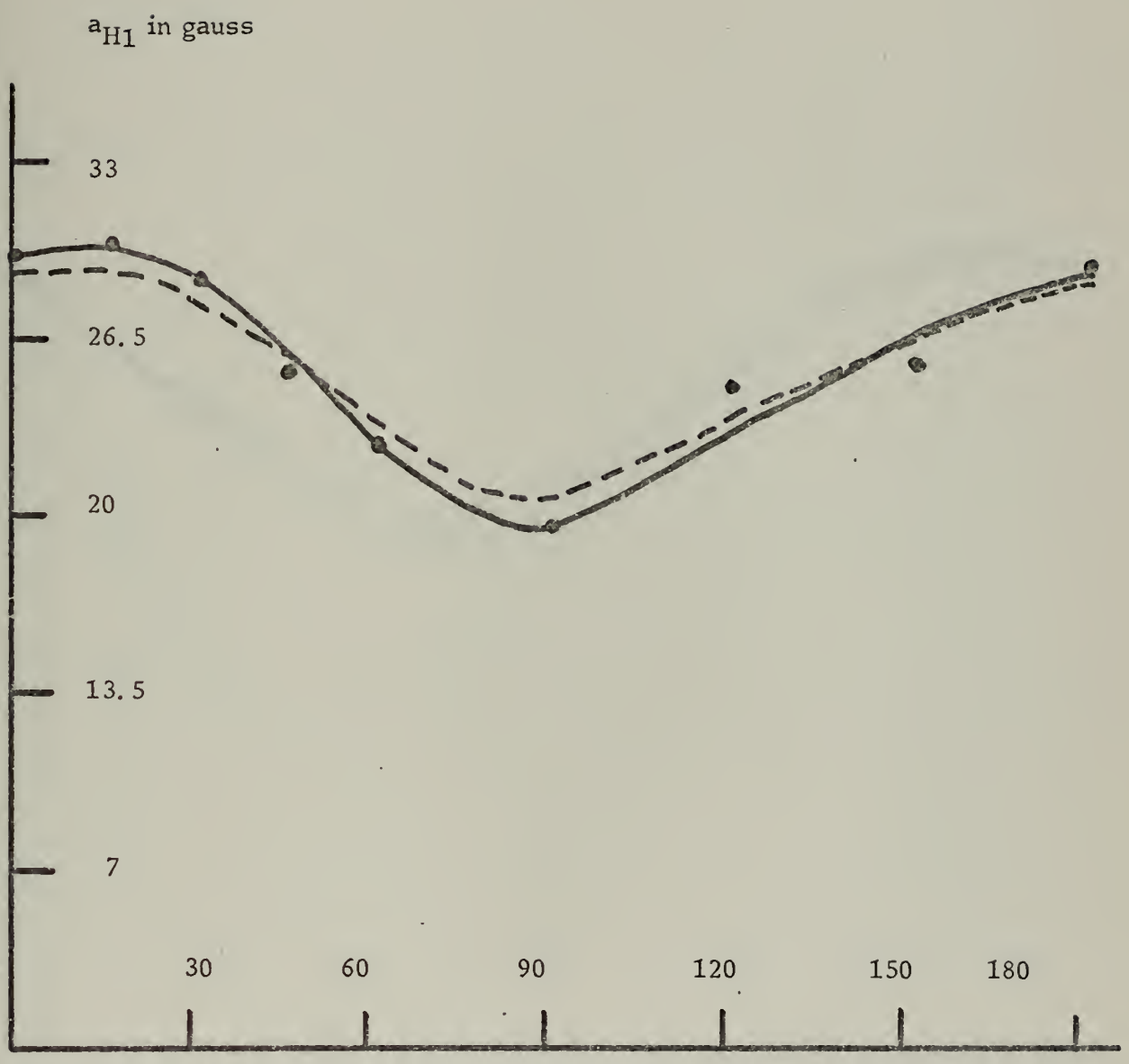

Figure 13D $\emptyset = 0$

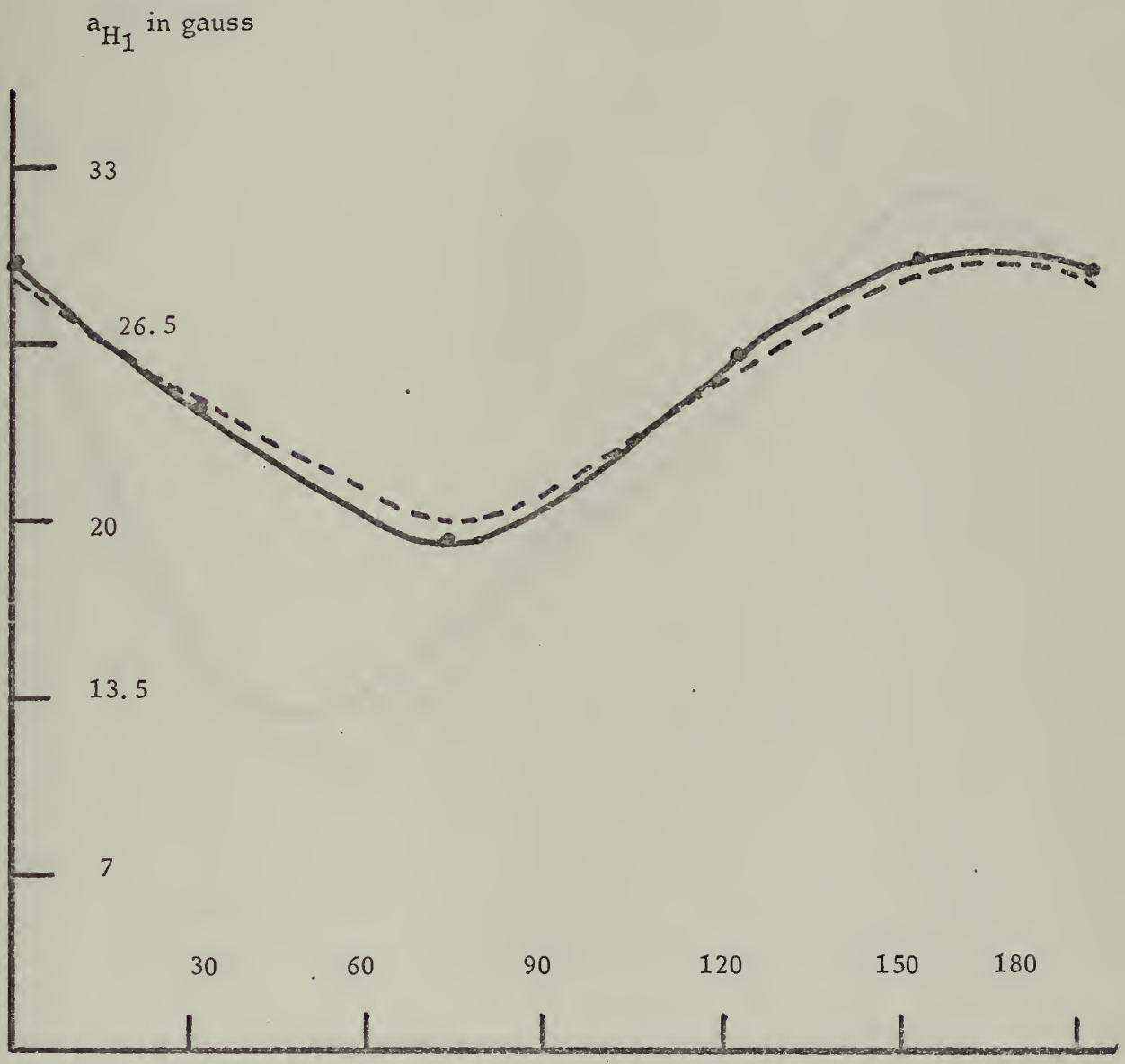

Figure 13E $\phi = -30$

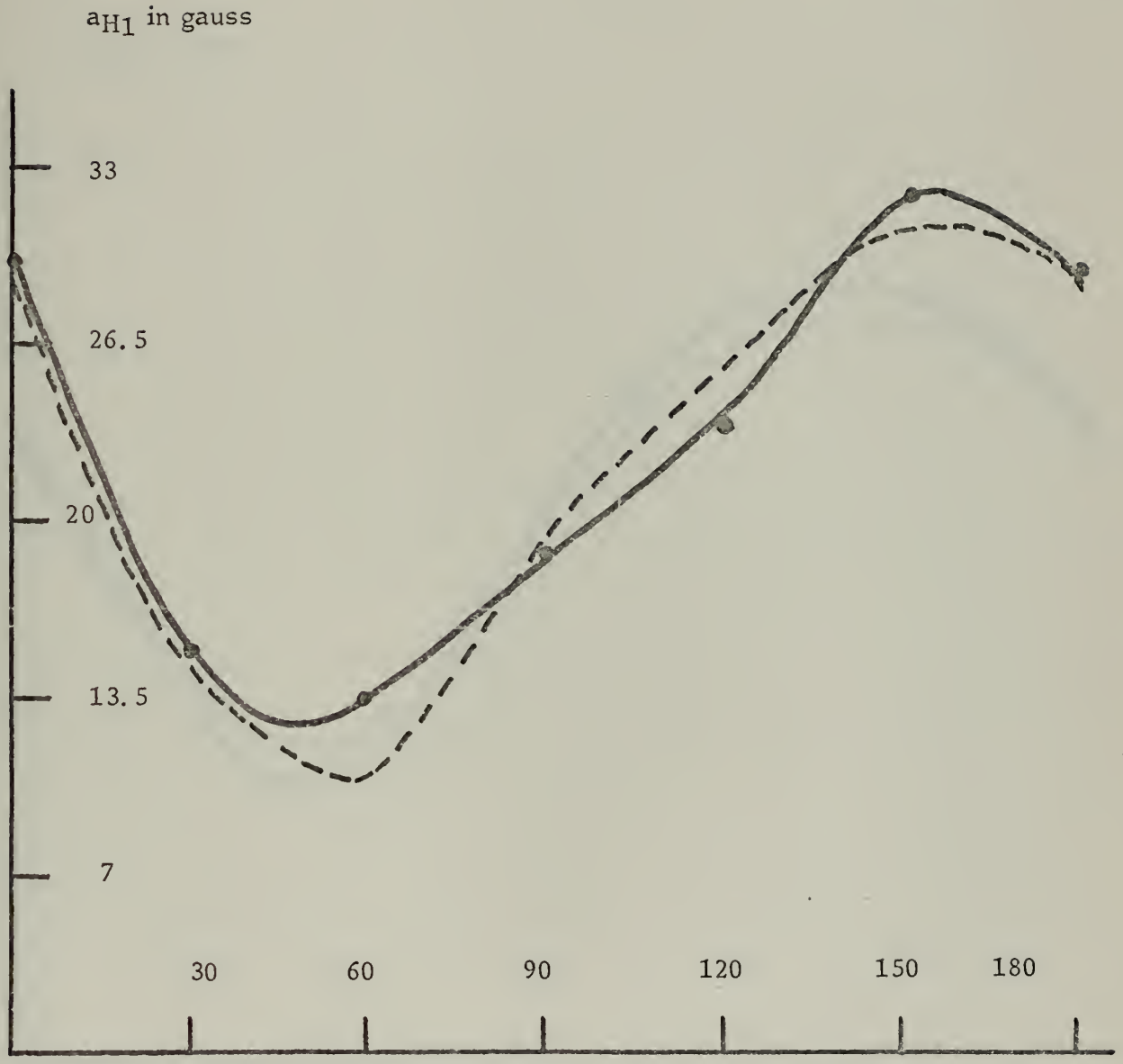

Figure 13F $\emptyset = -60$

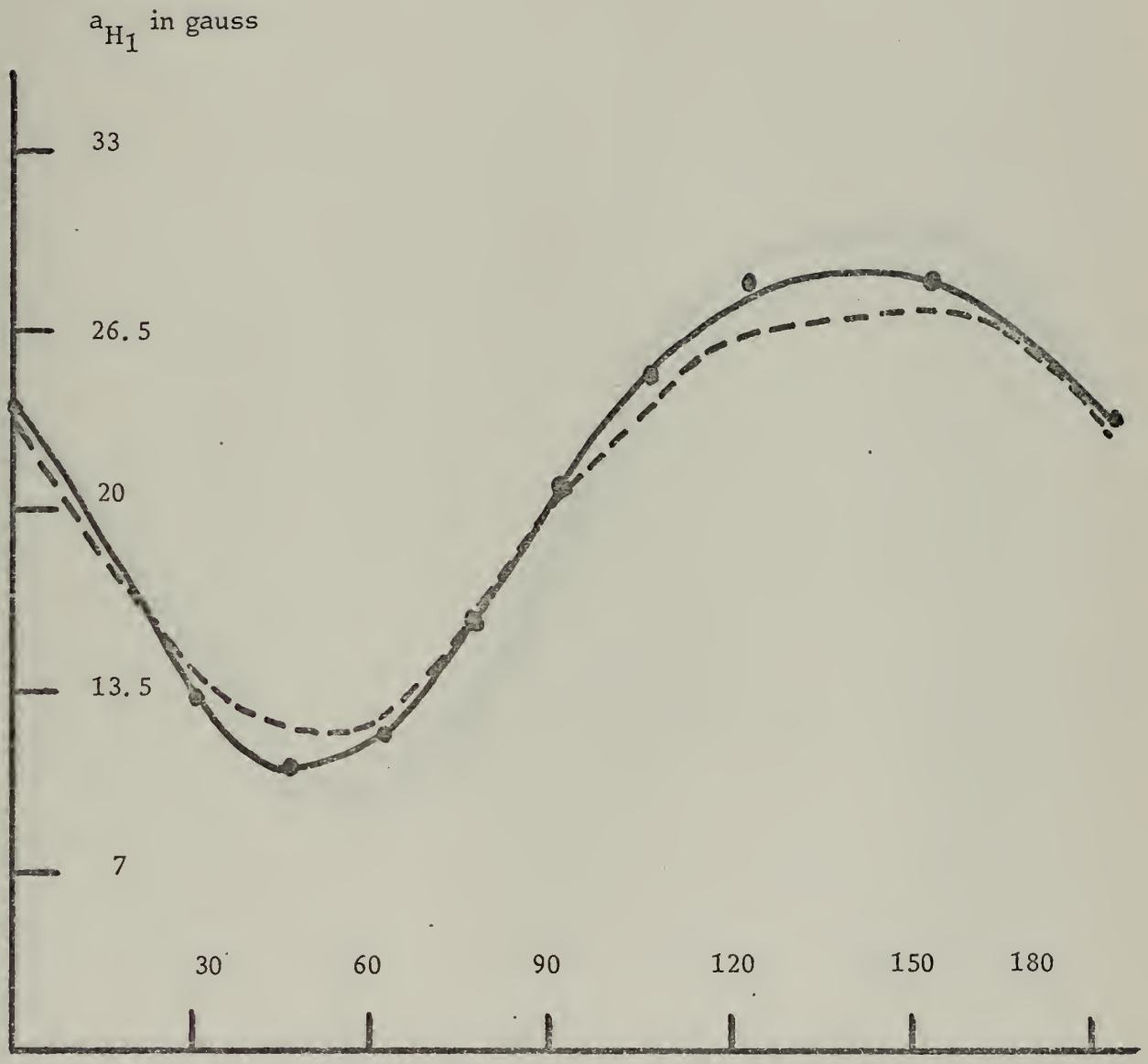

Figure 13G H_2 atom coupling constant versus magnetic field orientation in XYZ axis system $\phi = 90$
Dashed line = calculated value

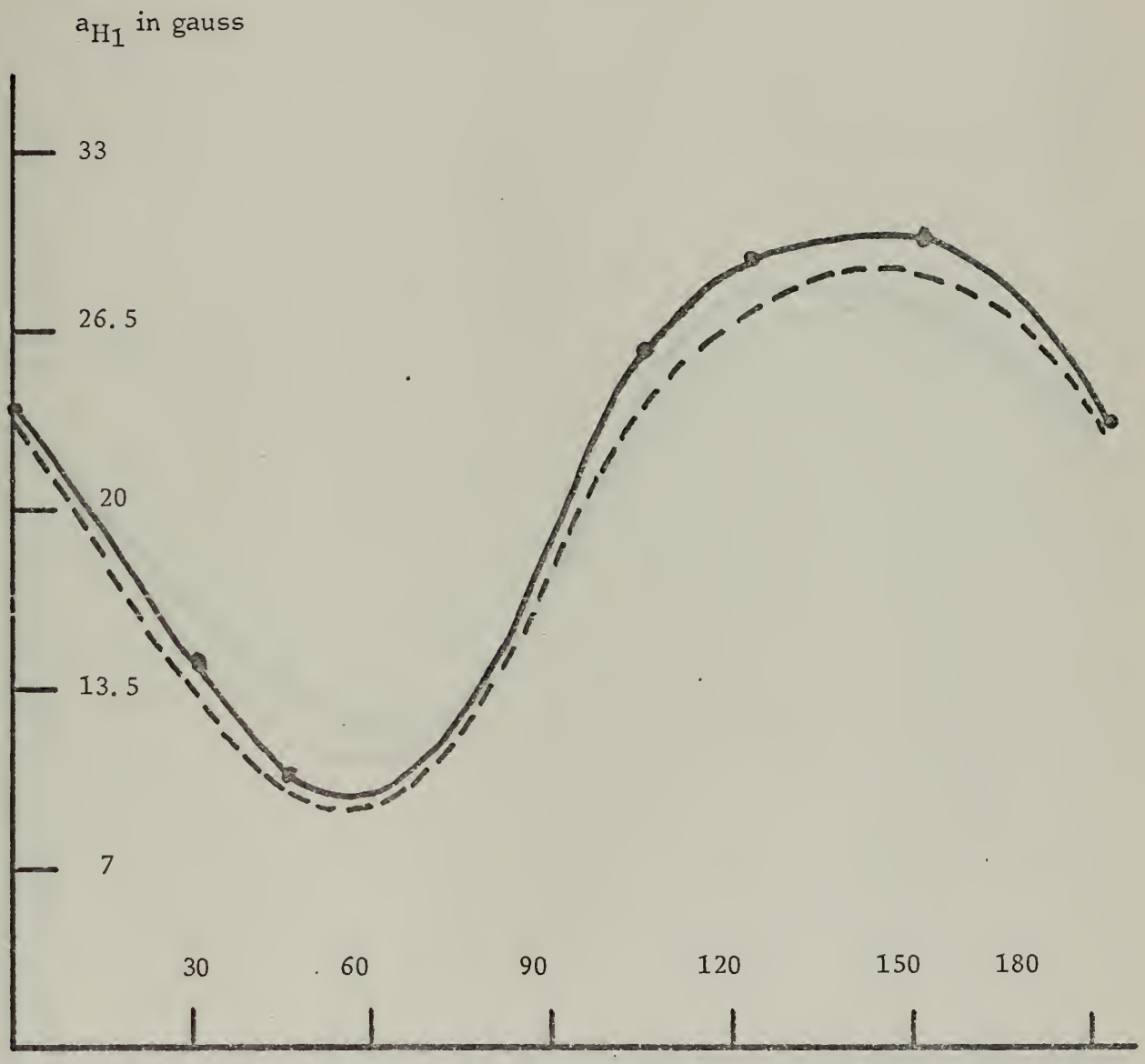

Figure 13H $\emptyset = 60$

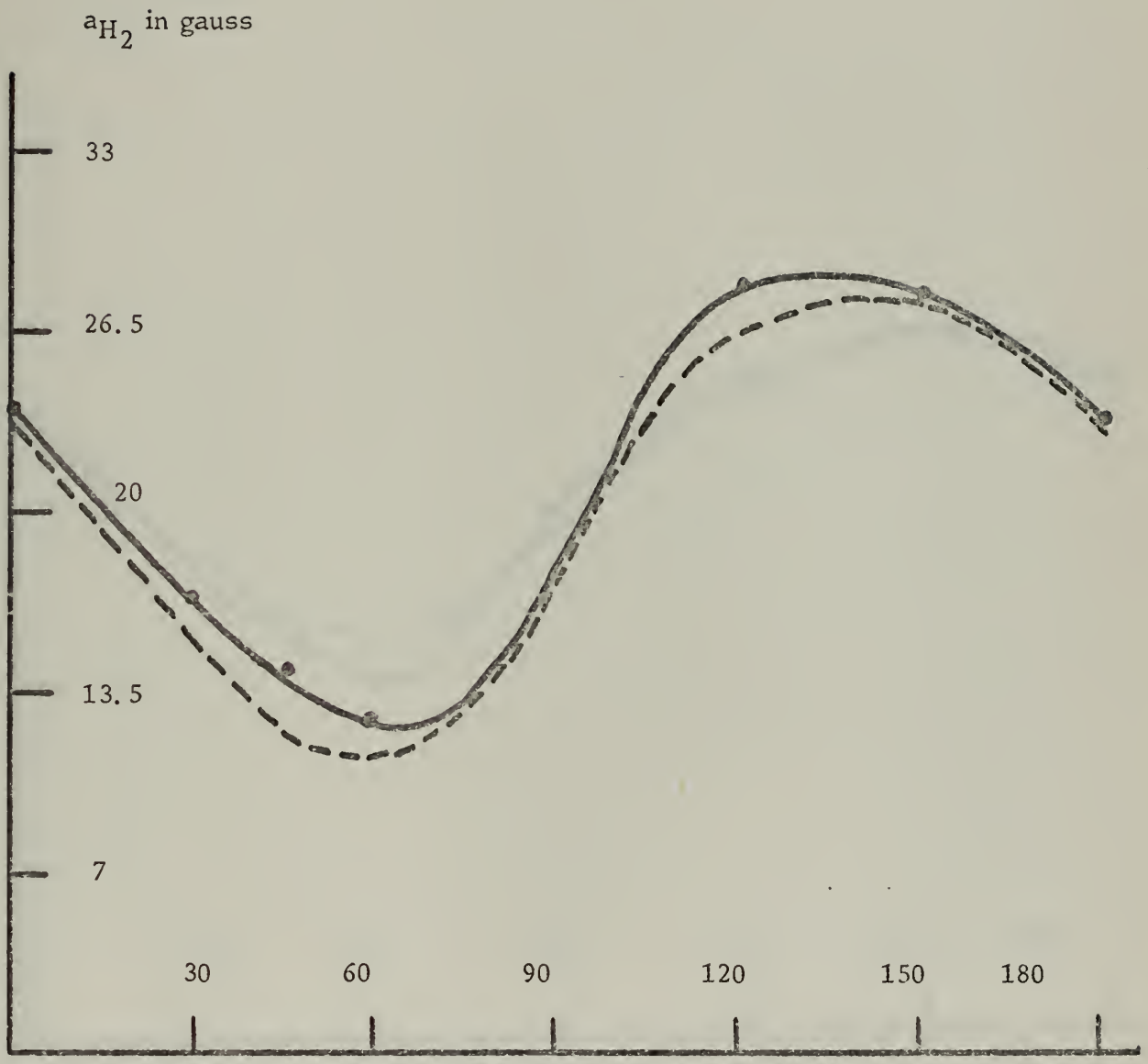

Figure 13I $\phi = 30$

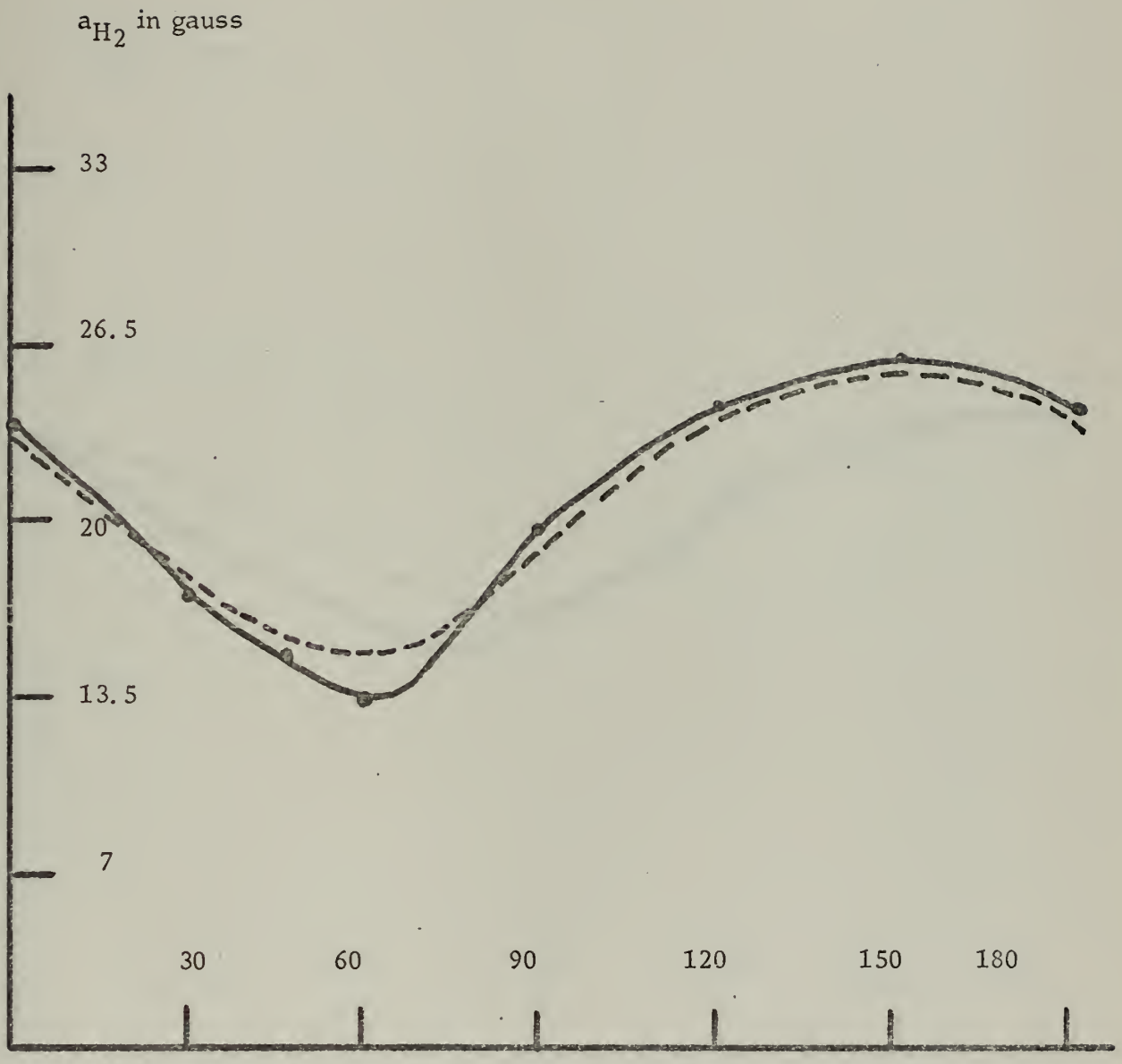

Figure 13J $\emptyset = 0$

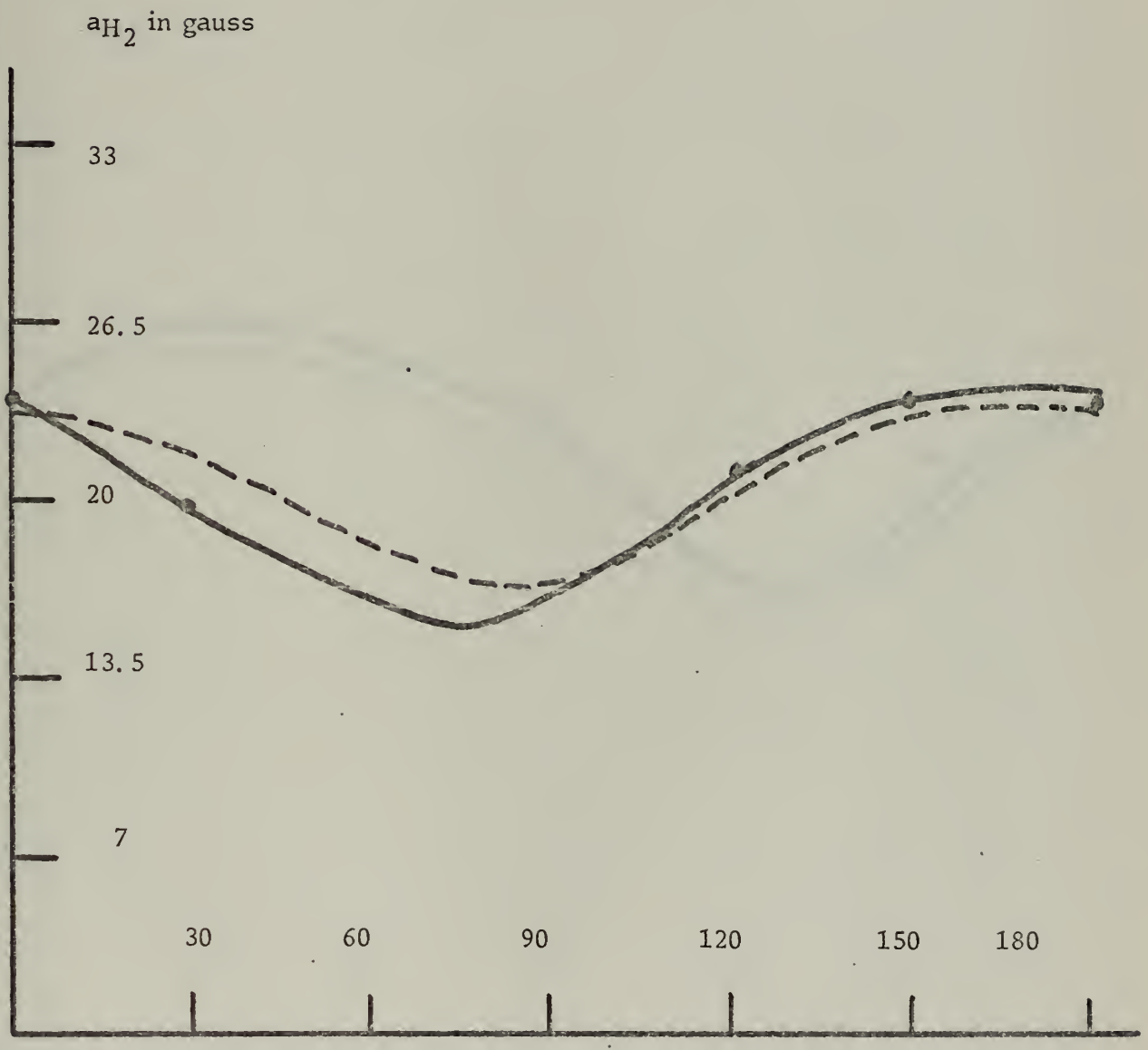

Figure 13K $\emptyset = -30$

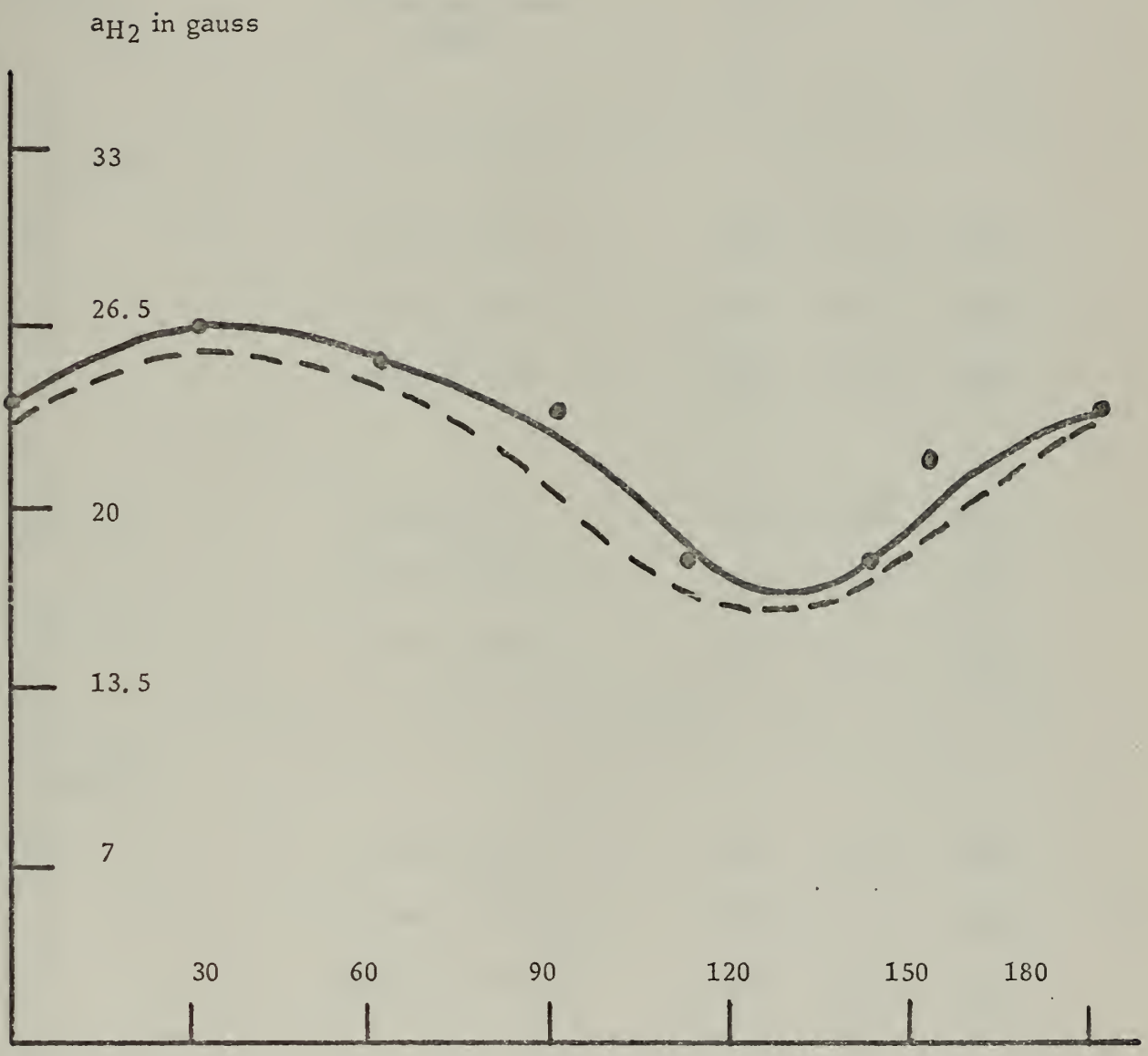

Figure 13L Ø= -60

TABLE III

Species	Principal Values (MHZ)	Direction Cosine X	Y	Z
$\cdot CH_2CO_2^-$				
H_1	-57.24 ± 2.72	.9552	-.1937	-.2238
	-92.92 ± 1.10	-.1142	.4563	-.8825
	-36.85 ± 1.78	.2730	.8685	.4137
H_2	-59.79 ± 1.96	.6515	-.6684	-.3589
	-90.52 ± 1.40	.6874	.3198	.6521
	-25.41 ± 2.24	-.3211	-.6715	.6678
$\cdot CH_2CO_2^-$				
H_1	-61.84 ± 2.55	.9765	.1328	-.1696
	-98.94 ± 1.40	.0869	.4771	.8745
	-43.38 ± 2.52	-.1971	.8687	-.4544
H_2	-54.79 ± 1.65	.8367	-.5457	-.0464
	$-81.43 + 2.21$	.3119	.5445	-.7786
	-24.30 ± 1.65	-.4501	-.6370	-.6258

Principal Values for the coupling constants for the $\cdot CH_2CO_2^-$ radicals in mercuric acetate. Observation temperature was -80°C.

Figure 14. Room temperature irradiation spectrum of mercuric acetate observed at room temperature. Top is at $(^{0}_{0})$ and bottom is at $(^{30}_{0})$

IV. CONCLUSIONS

A positive identification of the $\cdot CH_2CO_2^-$ radical in a liquid-nitrogen-temperature irradiated single crystal of lithium acetate dihydrate has been made. The orientation of the radical has been found with an HCH angle of $118.2^\circ \pm 2.^\circ 0$. The radical's configuration is planar. The principal values of the A and g tensors were found to be the same magnitude as tensors in other similar radicals in radiation damage studies. The crystalline structure of lithium acetate dihydrate reported by Galigne [23] was confirmed. No $\cdot CH_3$ radical was observed in lithium acetate dihydrate crystals in contrast to the previously reported results for zinc acetate dihydrate, strontium acetate hemihydrate, and sodium acetate trihydrate.

An unusual species in room temperature irradiated lithium acetate dihydrate has been observed. The identity of this radical could not be made. Initial attempts at interpreting the spectra as due to an interaction with a single hydrogen atom proved to be inconclusive. The unidentified species could be due to impurities and further study of this crystal is warranted.

The simple EPR spectrum for liquid nitrogen temperature irradiated single crystals of lithium acetate seem to indicate that this crystalline host could be suitable for further impurity studies. Oney [25] has recently conducted such studies in strontium acetate hemihydrate.

The study of liquid nitrogen temperature irradiated mercuric acetate showed the presence of two CO_2^- radical species at -170°C. The two CO_2^- species were found to decay rapidly when warmed above -80°C and when lowered again to -170°C the spectral lines were not so intense. Two additional species in mercuric acetate irradiated at liquid nitrogen temperature and observed at -80°C were found. Tentative identification of these species was made as two inequivalent $\cdot CH_2CO_2^-$ radicals. The HCH angles in both of these species were found to be $100.^\circ5 \pm 2.^\circ0$ and $113.^\circ7 \pm 2.^\circ0$.

Room temperature irradiated mercuric acetate showed a 1:2:1 spectrum at some orientations and more splittings at other positions of $\binom{\theta}{\phi}$. Upon lowering the observation temperature to -80°C the same spectrum was observed as that seen in liquid nitrogen temperature irradiated crystals observed at -80°C. This indicated that a reversible behavior was present.

Further study of liquid nitrogen temperature irradiated mercuric acetate is warranted. Either more data to obtain HCH angles of approximately 120° or an explanation for the large variance is needed. This requires the obtaining of the crystallographic location of the atoms in mercuric acetate.

```
C   THIS PROGRAM LEAST SQUARE FITS INPUT HYPERFINE COUPLING CONSTANTS AND OR
C   G TENSOR CONSTANTS IN THE PRINCIPAL AXIS SYSTEM AND THEN GIVES
C   THE PRINCIPAL VALUES AND DIRECTION COSINES OF RADICAL(S) RELATIVE TO
C   THE ASSIGNED CRYSTALLOGRAPHIC AXES.  DIFFERENCES BETWEEN THE CALCULATED
C   AND EXPERIMENTAL VALUES ARE GIVEN WITH ESTIMATES OF ERRORS FOR THE
C   PRINCIPAL VALUES.
C
C   WRITTEN BY WILLIAM M. TOLLES, DEPARTMENT OF CHEMISTRY, UNITED STATES
C   NAVAL POSTGRADUATE SCHOOL, MONTEREY, CALIFORNIA
C
C   WRITE FUNCTION SUBPROGRAM TO CALCULATE THE FUNCTION TO BE LEAST SQUARED.
C   THE DIMENSIONED ARRAYS HAVE THE FOLLOWING MEANINGS--
C
C   A(10) CONTAINS THE PARAMETERS WHICH ARE TO BE VARIED.
C
C   X(200) AND XB(200) CONTAIN THE INDEPENDENT PARAMETERS, THETA AND PHI
C
C   Z(200) CONTAINS THE OBSERVED VALUES OF THE FUNCTION - THE OBSERVED
C   DEPENDENDENT PARAMETERS.
C
C   FINCR(10) CONTAINS THE MAGNITUDE OF THE INCREMENTS FOR THE PARAMETERS SO
C   THAT THE PROGRAM MAY TAKE NUMERICAL DERIVATIVES WITH REASONABLE ACCURACY.
C
C   R(200) CONTAINS THE DIFFERENCES BETWEEN OBSERVED (Z(200)) AND CALCULATED.
C
C   E(10) CONTAINS THE ESTIMATES OF THE ERRORS OF THE PARAMETERS A(10) AFTER
C   ITERATION.
C
C   INPUT
C
C   FIRST CARD - WILL BE REPRODUCED ON OUTPUT AND CAN BE USED FOR LABELING OR
C   COMMENT.
C
C   SECOND CARD, IS, NOF, FNMR, AND EPSIL, WITH FORMAT (I3,I2,2F5.2)
C   IS= NUMBER OF POINTS
C   NOF= FUNCTION NUMBER
C   USE THE FOLLOWING FUNCTION NUMBERS FOR THIS PROGRAM--
C         25 = HYPERFINE COUPLING CONSTANT (A) NON SYMMETRICAL
C         26 = HYPERFINE COUPLING CONSTANT (A) AXIAL SYMMETRICAL
C         27 = NON SYMMETRICAL G TENSOR
C         28 = AXIAL SYMMETRICAL G TENSOR
C   FNMR = NMR FREQUENCY IN THE SAME ENERGY UNITS AS DATA (MHZ, GAUSS, ETC.)
C   EPSIL= CRITERION FOR CONVERGENCE.  IF THE RELATIVE VALUES OF THE RESIDUAL
C   CHANGE BY LESS THAN EPSIL IN TWO SUCCESSIVE ITERATIONS THEN CONVERGENCE
C   IS REACHED.
C
C   THIRD CARD(S) - FORMAT (6F5.2) - CONTAIN YOUR ESTIMATESS OF THE PARAMETERS
C   A(XX), A(YY), A(ZZ), THETA, PHI, AND PSI
```

```
C  STACKING OF JOBS IS PERMITTED - ONE BLANK CARD MUST BE INSERTED BETWEEN
C  CONSECUTIVE RUNS.
C  THE PROGRAM STOPS WHEN IT READS A ZERO (SECOND CARD INPUT), THUS SEVERAL
C  BLANK CARDS AFTER THE LAST JOB IS SUFFICIENT TO STOP THE ROUTINE.
CC
CC
C
      IMPLICIT REAL*8 (A-H,O-Z)
      DIMENSION A(10), X(200), XB(200), XC(200), Z(200), FINCR(10),
     1R(200), E(10), ECOS(3,3), T(3), P(3), COMENT(20)
    2 READ(5,106) (COMENT(I),I = 1,20)
      READ(5,100) IS,NOF,FNMR,EPSIL
      IF(IS) 200,200,10
   10 IC = NOF-(NOF/4)*4
      IC2 = (IC-(IC/2)*2)*2
      IR = 4+IC2
      NINP = 2
      IF(EPSIL.NE.(0.0)) GO TO 12
      EPSIL = .0001
   12 CONTINUE
      DO 13 I = 1,IR
   13 FINCR(I) = 0.1
      READ(5,102) ((X(I),XB(I),Z(I)), I = 1,IS)
    1 READ 101, (A(I), I = 1,IR)
      IF(DABS(A(1))) 2,2,20
   20 WRITE(6,130) (COMENT(I),I = 1,20)
      WRITE (6,109)
      WRITE (6,107)
      WRITE (6,108) (IR,IS,NOF,NINP,EPSIL)
      WRITE (6,128) FNMR
  128 FORMAT (/,' THE NMR FREQUENCY, FNMR, FED IN IS = ',F6.3)
      WRITE (6,109)
      WRITE (6,110)
      WRITE (6,109)
      WRITE (6,111) (A(I), I = 1,IR)
      WRITE (6,109)
      WRITE (6,112)
      WRITE (6,109)
      WRITE (6,111) (FINCR(I), I = 1,IR)
      WRITE (6,114) ((X(I),XB(I),Z(I)), I = 1,IS)
   30 CALL LEAST(IR,IS,A,X,XB,XC,Z,FINCR,EPSIL,NOITR,RRQ,NOF,R,E,FNMR)
      WRITE (6,109)
      WRITE (6,119)
      WRITE (6,109)
      WRITE (6,120) (A(I), I = 1,IR)
      WRITE (6,109)
      WRITE (6,124)
      WRITE (6,109)
```

```
      WRITE (6,120) (E(I), I = 1,IR)
      CAR = 3.1415926536/180.0
      TH = A(1)*CAR
      PH = -A(2)*CAR
      PS = A(3)*CAR
      STH = DSIN(TH)
      SPH = DSIN(PH)
      SPS = DSIN(PS)
      CTH = DCOS(TH)
      CPH = DCOS(PH)
      CPS = DCOS(PS)
      ECOS(1,1) = CPS*CPH
      ECOS(1,2) = SPS*CTH-CPS*SPH*STH
      ECOS(1,3) = SPS*STH+CPS*SPH*CTH
      ECOS(2,1) = -SPS*CPH
      ECOS(2,2) = CPS*CTH+SPS*SPH*STH
      ECOS(2,3) = CPS*STH-SPS*SPH*CTH
      ECOS(3,1) = -SPH
      ECOS(3,2) = -CPH*STH
      ECOS(3,3) = CPH*CTH
      WRITE (6,126) ECOS
  126 FORMAT (/' ROW VECTORS OF TENSOR AXES',//,(1X,3G18.10))
      DO 40 I = 1,3
      T(I) = (DARCOS(ECOS(3,I)))/CAR
      X1 = ECOS(2,I)
      X2 = ECOS(1,I)
   40 P(I) = (DATAN2(X1,X2))/CAR
      WRITE(6,127) ((T(I),P(I)), I = 1,3)
  127 FORMAT (/'     THETA         PHI    FOR PRINCIPAL AXES',//,(2F10.2))
      WRITE (6,109)
      WRITE (6,121) NOITR, RRQ
      WRITE (6,109)
      WRITE (6,122)
      WRITE (6,109)
      WRITE (6,123) (R(I), I = 1,IS)
  125 FORMAT (' OBSERVED MINUS CALCULATED',/,(1X,10G11.2))
      GO TO 1
  100 FORMAT (I3,I2,2F5.2)
  101 FORMAT (16F5.2)
  102 FORMAT (15F5.2)
  103 FORMAT (16F5.2)
  104 FORMAT (16F5.2)
  105 FORMAT (16F5.2)
  106 FORMAT (20A4)
  107 FORMAT(/99H NUMBER OF PARAMETERS      NUMBER OF POINTS      FUNCTION
     1 NUMBER     NUMBER OF INDEP PARAM      EPSILON)
  108 FORMAT (8X,I2,24X,I3,17X,I2,19X,I2,12X,E10.2)
  109 FORMAT (1H )
```

```
  110 FORMAT (26H THE PARAMETERS FED IN ARE)
  111 FORMAT (1H ,5G14.6)
  112 FORMAT (55H THE INCREMENTS FOR OBTAINING NUMERICAL DERIVATIVES ARE
     1)
  113 FORMAT (34H THE OBSERVED VALUES TO BE FIT ARE)
  114 FORMAT (/' THETA,PHI,Z FED IN',//,(5(3X,3F7.2)))
  115 FORMAT (31H THE INDEPENDENT PARAMETERS ARE)
  116 FORMAT (1H ,5G14.6)
  117 FORMAT (1H ,5G14.6)
  118 FORMAT (1H ,5G14.6)
  119 FORMAT (38H THE BEST VALUES OF THE PARAMETERS ARE)
  120 FORMAT (1H ,7G17.10)
  121 FORMAT (24H NUMBER OF ITERATIONS = ,I2,50H    THE SUM OF THE SQUAR
     1ES OF THE ERRORS IS NOW = ,G12.6)
  122 FORMAT (53H OBSERVED MINUS CALCULATED VALUES OF THE BEST FIT ARE)
  123 FORMAT (1H ,5F24.5)
  124 FORMAT (66H ESTIMATES OF THE ERROR IN EACH PARAMETER ARE (STANDARD
     1 DEVIATION))
  130 FORMAT(1H1,20A4)
  200 STOP
      END
C
C
      SUBROUTINE LEAST(IR,IS,A,X,XB,XC,Z,FINCR,EPSIL,NOITR,RRQ,NOF,R,E,
     1FNMR)
      IMPLICIT REAL*8 (A-H,O-Z)
C  IR = NO. OF PARAMETERS, IS = NO. OF POINTS, A IS ARRAY OF PARAMETERS,
C  X IS INDEPENDENT VARIABLE( Z DEPENDENT.  FINCR IS ARRAY OF INCREMENTS
C PARAMETERS.  EPSIL IS  -FRACTIONAL-  ERROR CRITERION.  NOITR IS NO. OF
C ITERATIONS REQUIRED (UP TO 10).  RRQ = SUM OF SQUARES OF RESIDUALS)
C NOF IS THE NUMBER OF THE FUNCTION USED IN -EQN-.
C  E IS THE ARRAY OF ESTIMATED ERRORS IN THE PARAMETERS
      DIMENSION A(10), X(200), XB(200), XC(200), Z(200), FINCR(10), R(20
     10), D(200,10), DT(10,200), DEL(10), DS(10), DPI(10,10), DP(10,10),
     2E(10)
      NOITR = 0
      DO 20 I = 1,IS
   20 R(I) = Z(I) - EQN(A,X(I),XB(I),FNMR,NOF)
      IF(NOF.GT.20) WRITE (6,995)(R(I), I = 1,IS)
   25 IF(NOITR-9) 130,130,102
  130 NOITR = NOITR + 1
      DO 220 J = 1, IR
      A(J) = A(J)+FINCR(J)
      DO 15 I = 1,IS
   15 D(I,J) = EQN(A,X(I),XB(I),FNMR,NOF)
      A(J) = A(J)-FINCR(J)
  220 CONTINUE
```

```
      DO 30 I = 1,IS
      CONST = EQN(A,X(I),XB(I),FNMR,NOF)
      DO 30 J = 1,IR
   30 D(I,J) = (D(I,J)-CONST)/FINCR(J)
      DO 35 I = 1,IS
      DO 35 J = 1,IR
   35 DT(J,I) = D(I,J)
      IF(NOF.GT.95) WRITE (6,991)((DT(I,J), J = 1,IS), I = 1,IR)
      DO 36 I = 1,IR
      DO 36 J = 1,IR
      DP(I,J) = 0.0
      DO 36 K = 1,IS
   36 DP(I,J) = DP(I,J)+DT(I,K)*D(K,J)
      IF(NOF.GT.92) WRITE (6,992) ((DP(I,J), J = 1,IR), I = 1,IR)
       CALL GAUSS3 (IR,1.00E-30,DP,DPI,KER)
      IF(NOF.GT.91) WRITE (6,993) ((DPI(I,J), J = 1,IR), I = 1,IR)
      IF(KER-1) 120,37,120
   37 DO 40 I = 1,IS
      DO 38 J = 1,IR
      DS(J) = 0.0
      DO 38 K = 1,IR
   38 DS(J) = DS(J)+DPI(J,K)*DT(K,I)
      DO 39 L = 1,IR
   39 DT(L,I) = DS(L)
   40 CONTINUE
      DO 110 I = 1, IR
      DEL(I) = 0.0
      DO 110 J = 1, IS
  110 DEL(I) = DEL(I)+DT(I,J)*R(J)
      DO 10 I = 1,IR
   10 A(I) = A(I)+DEL(I)
      IF(NOF.GT.15) WRITE (6,991) (A(I), I = 1,IR)
      DO320 I = 1,IS
  320 R(I) = Z(I) - EQN(A,X(I),XB(I),FNMR,NOF)
      IF(NOF.GT.30) WRITE (6,995) (R(I), I = 1,IS)
      RRQ = 0.0
      DO 50 I = 1,IS
   50 RRQ = RRQ+R(I)**2
      IF(NOF.GT.90) WRITE (6,994) RRQ
      CRES = DABS(RRQ-RRP) - EPSIL*RRP
      RRP = RRQ
      IF(CRES) 100,100,25
  102 CONTINUE
  101 FORMAT (20H CONVERGENCE FAILURE)
    4 WRITE (6,101)
      GO TO 100
  120 WRITE (6,1001)
  990 FORMAT (1H ,10F11.5)
```

```
  991 FORMAT (1H ,10F11.5)
  992 FORMAT (1H ,10D11.4)
  993 FORMAT (1H ,10F11.5)
  994 FORMAT (1H ,10F11.5)
  995 FORMAT (/(1H ,10G11.3))
 1001 FORMAT (///,' *** MATRIX IS SINGULAR ***',///)
  100 FIS1 = IS-1
      DO 150 I = 1,IR
  150 E(I) = DSQRT(RRQ*DPI(I,I)/FIS1)
      RETURN
      END
C
      SUBROUTINE   GAUSS3(N,EP,A,X,KER)
      IMPLICIT REAL*8 (A-H,O-Z)
      DIMENSION A(10,10), X(10,10)
      DO 1 I=1,N
      DO 1 J=1,N
    1 X(I,J)=0.0
      DO 2 K=1,N
    2 X(K,K)=1.0
   10 DO 34 L=1,N
      KP=0
      Z=0.0
      DO 12 K=L,N
      IF(Z-DABS(A(K,L)))11,12,12
   11 Z=DABS(A(K,L))
      KP=K
   12 CONTINUE
      IF(L-KP)13,20,20
   13 DO 14 J=L,N
      Z=A(L,J)
      A(L,J)=A(KP,J)
   14 A(KP,J)=Z
      DO 15 J=1,N
      Z=X(L,J)
      X(L,J)=X(KP,J)
   15 X(KP,J)=Z
   20 IF(DABS(A(L,L))-EP)50,50,30
   30 IF(L-N)31,34,34
   31 LP1=L+1
      DO 36 K=LP1,N
      IF(A(K,L))32,36,32
   32 RATIO=A(K,L)/A(L,L)
      DO 33 J=LP1,N
   33 A(K,J)=A(K,J)-RATIO*A(L,J)
      DO 35 J=1,N
```

```
35 X(K,J)=X(K,J)-RATIO*X(L,J)
36 CONTINUE
34 CONTINUE
40 DO 43 I=1,N
   II=N+1-I
   DO 43 J=1,N
   S=0.0
   IF(II-N)41,43,43
41 IIP1=II+1
   DO 42 K=IIP1,N
42 S=S+A(II,K)*X(K,J)
43 X(II,J)=(X(II,J)-S)/A(II,II)
   KER=1
   RETURN
50 KER=2
   RETURN
   END
   REAL FUNCTION EQN*8(A,X,XB,XC,NOF)
   IMPLICIT REAL*8(A-H,O-Z)
   DIMENSION A(10), ECOS(10,3,3), AC(10,3), UH(3), DE(1000), FINT(100
  10)
   CAR = 3.1415926536/180.0
   FNMR = XC
   THETA = X*CAR
   PHI = XB*CAR
   TH = A(1)*CAR
   PH = -A(2)*CAR
   STHE = DSIN(THETA)
   SPHI = DSIN(PHI)
   CTHE = DCOS(THETA)
   CPHI = DCOS(PHI)
   UH(1) = STHE*CPHI
   UH(2) = STHE*SPHI
   UH(3) = CTHE
   IF((NOF/2)*2-NOF)55,56,56
55 PS = A(3)*CAR
   AC(1,1) = A(4)
   AC(1,2) = A(5)
   AC(1,3) = A(6)
   STH = DSIN(TH)
   SPH = DSIN(PH)
   SPS = DSIN(PS)
   CTH = DCOS(TH)
   CPH = DCOS(PH)
   CPS = DCOS(PS)
   ECOS(1,1,1) = CPS*CPH
   ECOS(1,1,2) = SPS*CTH-CPS*SPH*STH
   ECOS(1,1,3) = SPS*STH+CPS*SPH*CTH
```

```
      ECOS(1,2,1) = -SPS*CPH
      ECOS(1,2,2) = CPS*CTH+SPS*SPH*STH
      ECOS(1,2,3) = CPS*STH-SPS*SPH*CTH
      ECOS(1,3,1) = -SPH
      ECOS(1,3,2) = -CPH*STH
      ECOS(1,3,3) = CPH*CTH
      GO TO 57
   56 AC(1,1)=A(4)
      AC(1,2)=A(4)
      AC(1,3)=A(3)
      STH=DSIN(TH)
      SPH=DSIN(PH)
      CTH=DCOS(TH)
      CPH=DCOS(PH)
      ECOS(1,1,1)=CPH
      ECOS(1,1,2)=-SPH*STH
      ECOS(1,1,3)=SPH*CTH
      ECOS(1,2,1)=0.
      ECOS(1,2,2)=CTH
      ECOS(1,2,3)=STH
      ECOS(1,3,1)=-SPH
      ECOS(1,3,2)=-CPH*STH
      ECOS(1,3,3)=CPH*CTH
   57 IC = NOF
C TRANSPOSE TO OBTAIN ROW VECTORS AS THAT IS WHAT SSESR USES
      DO 58 I = 1,3
      DO 58 J = I,3
      TEMP = ECOS(1,I,J)
      ECOS(1,I,J) = ECOS(1,J,I)
   58 ECOS(1,J,I) = TEMP
      CALL SSESR(1,ECOS,AC,UH,FNMR,DE,FINT,IC)
      IF(FINT(1).GT.0.5) GO TO 65
      EQN = DE(2)-DE(3)
      GO TO 66
   65 EQN = DE(1)-DE(4)
   66 IF(NOF.EQ.99) WRITE (6,100) EQN
  100 FORMAT (7H EQN =     ,1D15.8)
      RETURN
      END


      SUBROUTINE SSESR(NN,ECOS,A,UH,H,DE,FINT,IC)
      IMPLICIT REAL*8(A-H,O-Z)
C   NM IS THE NUMBER OF NUCLEI WITH SPIN V .5
C   ECOS IS THE DIRECTION COSINE MATRIX. ELEMENT I,J,K RELATES THE COMPO
C   FOR ATOM I OF THE J-TH PRINCIPAL AXIS ALONG THE K-TH CRYSTAL AXIS.
C   A(I,J) IS THE J-TH PRINCIPAL VALUE FOR THE I-TH ATOM
C   UH(I) IS THE I-TH COMPONENT OF THE UNIT VECTOR POINTING ALONG THE
```

```
C   DIRECTION OF THE MAGNETIC FIELD
C   DE IS THE ARRAY OF TRANSITION FREQUENCIES CALCULATED
C   FINT IS THE CORRESPONDING ARRAY OF INTENSITIES
C   IC IS THE NUMBER OF TRANSITIONS CALCULATED
      DIMENSION ECOS(10,3,3), A(10,3),UH(3),DE(1000),FINT(1000),
     1HV(10,3),HVP(10,2,3),CE(10),HCOS(10,3),ABH(10,2),S(2),IQ(20)
      IF(IC.NE.85) GO TO 5
      WRITE (6,101) (((ECOS(I,J,K), K = 1,3), J = 1,3))
      WRITE (6,102) (A(I,I), I = 1,6)
      WRITE (6,103) (UH(I), I = 1,3)
  101 FORMAT (' ECOS'/,(3G12.5))
  102 FORMAT (' A',6G12.5)
  103 FORMAT (' UH',3G12.5)
    5 S(1) = 1.0
      S(2) = -1.0
      DO 10 I = 1,NN
      DO 10 J = 1,3
      HCOS(I,J) = 0.0
      DO 10 K = 1,3
   10 HCOS(I,J) = HCOS(I,J)+UH(K)*ECOS(I,J,K)
      IF(IC.EQ.99) WRITE (6,100) ((HCOS(I,J), J = 1,3), I = 1,NN)
       IF((((NOF+1)/2)/2)*2-(NOF+1)/2).EQ.0) GO TO 80
      DO 15 I = 1,NN
      DO 15 J = 1,3
   15 HV(I,J) = 0.0
      DO 20 I = 1,NN
      DO 20 J = 1,3
      CAS = HCOS(I,J)*A(I,J)
      DO 20 K = 1,3
   20 HV(I,K) = HV(I,K) + CAS*ECOS(I,J,K)
      IF(IC.EQ.99) WRITE (6,100) ((HV(I,J), J = 1,3), I = 1,NN)
      DO 30 I = 1,NN
      DO 30 J = 1,2
      DO 30 K = 1,3
   30 HVP(I,J,K) = H*UH(K)-0.5*S(J)*HV(I,K)
      IF(IC.EQ.99) WRITE(6,100) (((HVP(I,J,K), K = 1,3), J = 1,2), I = 1
     1,NN)
      DO 40 I = 1,NN
      DO 40 J = 1,2
      ABH(I,J) = 0.0
      DO 35 K = 1,3
   35 ABH(I,J) = ABH(I,J) + HVP(I,J,K)**2
   40 ABH(I,J) = DSQRT(ABH(I,J))
      IF(IC.EQ.99) WRITE (6,100) ((ABH(I,J), J = 1,2), I = 1,NN)
      DO 50 I = 1,NN
      CE(I) = 0.0
      DO 45 J = 1,3
   45 CE(I) = CE(I) + HVP(I,1,J)*HVP(I,2,J)
```

```
   50 CE(I) = CE(I)/(ABH(I,1)*ABH(I,2))
      IF(IC.EQ.99) WRITE (6,100) (CE(I), I = 1,NN)
      NN2 = 2*NN
      NNTT = 2**(2*NN)
      HNNT = 2**NN
      DO 55 I = 1,NN2
   55 IQ(I) = 1
      IC = 0
      DO 70 I = 1,NNTT
      IC = IC+1
      DE(IC) = 0.0
      FINT(IC) = 1.0
      DO 60 J = 1,NN
      J1 = IQ(J)
      J2 = IQ(NN+J)
      FINT(IC) = FINT(IC)*(1.0-S(J1)*S(J2)*CE(J))
   60 DE(IC) = DE(IC) + S(J1)*ABH(J,1) + S(J2)*ABH(J,2)
      DE(IC) = 0.5*DE(IC)
      FINT(IC) = FINT(IC)/HNNT
      J = 1
   64 IF(IQ(J)-2) 66,65,66
   65 IQ(J) = 1
      J = J+1
      GO TO 64
   66 IQ(J) = 2
   70 CONTINUE
  100 FORMAT (1H ,10F11.5)
      RETURN
   80 DE(3) = 0.0
      DE(4) = 0.0
      DE(1) = DSQRT(A(1,1)**2*HCOS(1,1)**2+A(1,2)**2*HCOS(1,2)**2+A(1,3)
     1**2*HCOS(1,3)**2)
      DE(2) = DE(1)
      RETURN
      END
```

BIBLIOGRAPHY

1. Ghosh, D.K., and Whiffen, D.H., Mol. Phys., 2, 285 (1959)

2. Gisch, R.G., Electron Paramagnetic Resonance Study of Copper Halide Tetrazole Complexes and the Free Radicals in Irradiated Strontium Acetate Hemihydrate, (Thesis) USNPS, (1969)

3. Box, H.C., Freund, H.G., and Budzinski, E.E., J. Chem. Phys., 46, 4470 (1967)

4. Shields, H.W., Marsh, William, and Hamrick, P.J., J. Chem. Phys., 52, 6437 (1970)

5. Hoff, A.J., and Koningsberger, D.C., Int. J. Radiat. Biol., 17, 459 (1970)

6. Alexander, C., and Franklin, C.E., J. Chem. Phys., 54, 1909 (1971)

7. Sharma, V.K., J. Chem. Phys., 54, 496 (1971)

8. Rogers, Max T., and Kispert, L.K., J. Chem. Phys., 46, 221 (1967)

9. Tolles, W.M., Crawford, L.P., and Valenti, J.L., J. Chem. Phys., 49, 4745 (1968)

10. Tolles, W.M., Sanders, R.A., and Gisch, R.G., J. Chem. Phys., 54, 1532 (1971)

11. Apaydin, F., and Clough, S., Proc. Phy. Soc. (London), Solid State Phys. Ser., 2, 1536 (1969)

12. Morton-Blake, D.A., J. Phys. Chem., 73, 2964 (1969)

13. Morton-Blake, D.A., J. Phys. Chem., 74, 1508 (1970)

14. Carrington, A., and McLacklan, A.D., Introduction to Magnetic Resonance; Harper and Row, Inc., (1967)

15. Poole, C.P., Electron Spin Resonance; John Wiley and Sons, (1967)

16. Slichter, C.P., Principles of Magnetic Resonance; Harper and Row, Inc., (1963)

17. Segal, B.G., Kaplan, M., and Fraenkel, G.K., J. Chem. Phys., 43, 4191 (1965)

18. Morton, J.R., J. Chem Rev., 64, 453 (1964)

19. Crawford, L.P., Electron Paramagnetic Resonance of the $CH_2C0_2^-$ Radical in Irradiated Zinc Acetate Dihydrate, (Thesis), USNPS (1967)

20. Valenti, J.L. Electron Spin Resonance Study of Free Radical Formation in Irradiated Zinc Acetate Dihydrate, (Thesis), USNPS (1967)

21. Tolles, W.M., Determination of Tensor Parameters, unpublished

22. Tolles, W.M., A Computer Program for Calculating the Least Square Fit and Obtaining Principal Values

23. Galigne, J.L., Mouvet, M., and Falgueirettes, J., Acta. Cryst., B26, 368 (1970)

24. Amirthalingam, V., and Padmanabhan, V.M., Acta Cryst., 11, 896 (1958)

25. Oney W.E., Electron Paramagnetic Resonance Investigation of Isobutyrate and n-Butyrate Doped Strontium Acetate Hemihydrate Single Crystals, (Thesis), USNPS (1971)

INITIAL DISTRIBUTION LIST

		No. Copies
1.	Defense Documentation Center Cameron Station Alexandria, Virginia 22314	2
2.	Library, Code 0212 Naval Postgraduate School Monterey, California 93940	2
3.	Associate Professor William H. Tolles, Code 54 Dk (thesis advisor) Department of Material Science and Chemistry Naval Postgraduate School Monterey, California 93940	1
4.	LT Clinton James Coneway, USN (student) 104 Rio Vista Drive Hereford, Texas 79045	1

Security Classification

DOCUMENT CONTROL DATA - R & D

(Security classification of title, body of abstract and indexing annotation must be entered when the overall report is classified)

1 ORIGINATING ACTIVITY (Corporate author)

Naval Postgraduate School
Monterey, California 93940

2a. REPORT SECURITY CLASSIFICATION

Unclassified

2b. GROUP

3 REPORT TITLE

Electron Paramagnetic Resonance Investigation of Irradiated Lithium Acetate Dihydrate and Mercuric Acetate Single Crystals

4 DESCRIPTIVE NOTES (Type of report and inclusive dates)

Master's Thesis; (June 1971)

5. AUTHOR(S) (First name, middle initial, last name)

Clinton James Coneway

6 REPORT DATE	7a. TOTAL NO. OF PAGES	7b. NO. OF REFS
June 1971	94	25

8a. CONTRACT OR GRANT NO.	9a. ORIGINATOR'S REPORT NUMBER(S)
b. PROJECT NO.	
c.	9b. OTHER REPORT NO(S) (Any other numbers that may be assigned this report)
d.	

10. DISTRIBUTION STATEMENT

Approved for public release; distribution unlimited.

11. SUPPLEMENTARY NOTES	12. SPONSORING MILITARY ACTIVITY
	Naval Postgraduate School Monterey, California 93940

13. ABSTRACT

An electron paramagnetic resonance study of x-ray irradiated single crystals of lithium acetate dihydrate and mercuric acetate has been made. The $\cdot CH_2CO_2^-$ radical has been identified in lithium acetate dihydrate irradiated at liquid nitrogen temperature. The HCH angle was found to be $118.^{\circ}2 \pm 2.0^{\circ}$. The principal elements of the hyperfine tensor and the g tensor were calculated. Mercuric acetate irradiated at liquid nitrogen temperature showed the presence of two CO_2^- species. Spectra at -80°C showed the presence of two $\cdot CH_2CO_2^-$ radicals. The principal values of the hyperfine tensor for the two magnetically distinct sites were obtained.

DD FORM 1 NOV 65 1473 (PAGE 1)

S/N 0101-807-6811

Security Classification

A-31409

KEY WORDS	LINK A		LINK B		LINK C	
	ROLE	WT	ROLE	WT	ROLE	WT
ithium Acetate Dihydrate						
Iercuric Acetate						
PR						
SR						
radiated Single Crystals						
adical						

128360

Thesis
C702
c.1

Coneway
Electron paramagnetic resonance investigation of irradiated lithium acetate dihydrate and mercuric acetate single crystals.